European air quality maps for 2017

PM_{10}, $PM_{2.5}$, Ozone, NO_2 and NO_x spatial estimates and their uncertainties

August 2020

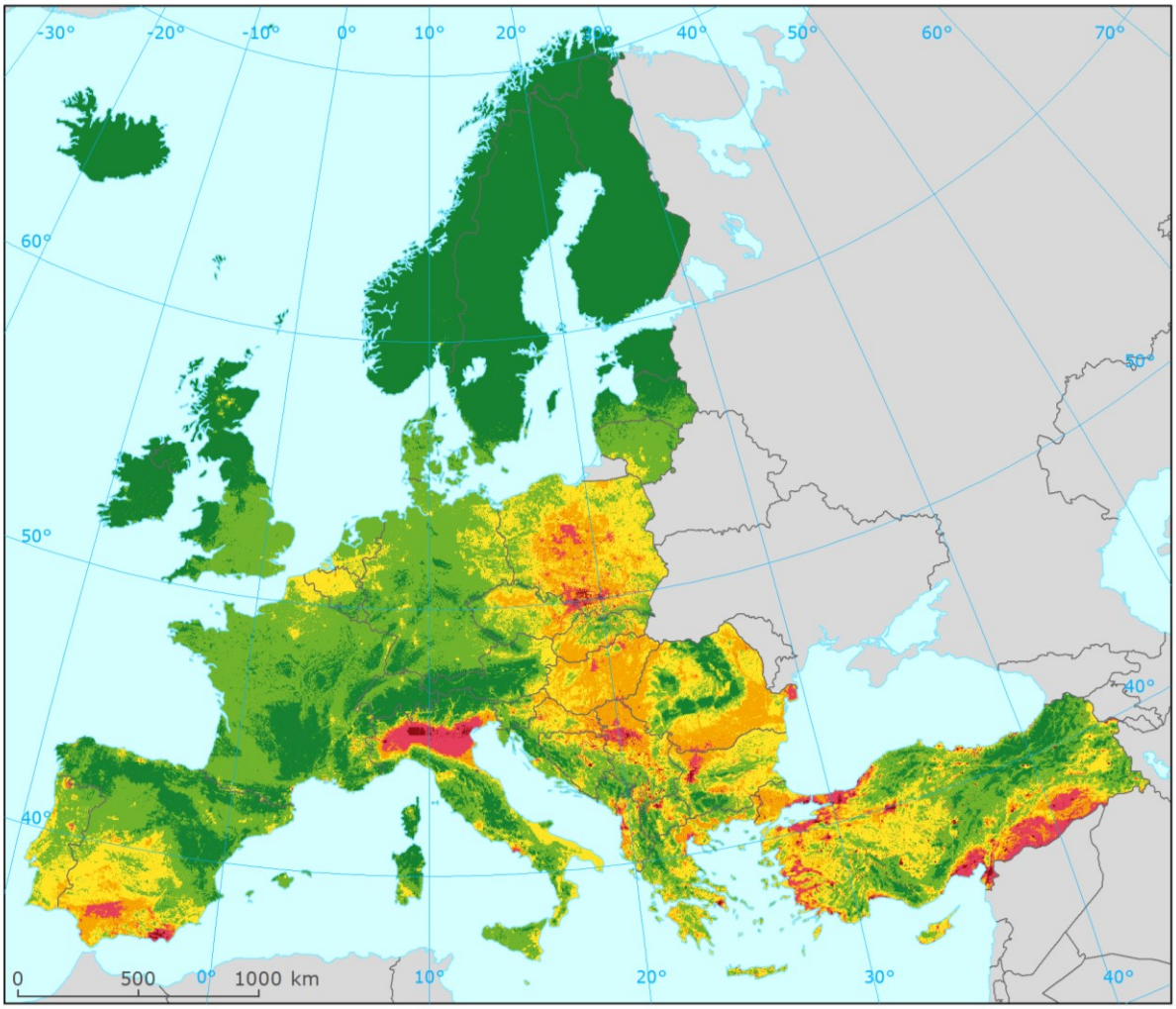

Authors:
Jan Horálek (CHMI), Markéta Schreiberová (CHMI), Philipp Schneider (NILU), Pavel Kurfürst (CHMI), Jana Schovánková (CHMI), Jana Ďoubalová (CHMI)

ETC/ATNI consortium partners:
NILU – Norwegian Institute for Air Research, Aether Limited, Czech Hydrometeorological Institute (CHMI), EMISIA SA, Institut National de l'Environnement Industriel et des risques (INERIS), Universitat Autònoma de Barcelona (UAB), Umweltbundesamt GmbH (UBA-V), 4sfera Innova, Transport & Mobility Leuven NV (TML)

European Environment Agency
European Topic Centre on Air pollution, transport, noise and industrial pollution

Cover picture – *Concentration map of PM_{10} indicator 90.4 percentile of daily means for the year 2017. Spatially interpolated concentration field. Units: $\mu g \cdot m^{-3}$. (Map 2.2 of this report.)*

The withdrawal of the United Kingdom from the European Union did not affect the production of the report.
Data reported by the United Kingdom are included in all analyses and assessments contained herein, unless otherwise indicated.

Author(s)
Jan Horálek, Markéta Schreiberová, Pavel Kurfürst, Jana Schovánková, Jana Ďoubalová: Czech Hydrometeorological Institute (CHMI, CZ), Philipp Schneider: NILU Norwegian Institute for Air Research (NILU, NO)

ETC/ATNI c/o NILU
ISBN 978-82-93752-14-1

European Topic Centre on Air pollution,
transport, noise and industrial pollution
c/o NILU – Norwegian Institute for Air Research
P.O. Box 100, NO-2027 Kjeller, Norway
Tel.: +47 63 89 80 00
Email: etc.atni@nilu.no
Web : https://www.eionet.europa.eu/etcs/etc-atni

Contents

Summary

European air quality concentrations maps have been prepared for the year 2017. The maps are based on air quality data as reported under the air quality directive by EEA member and cooperating countries and voluntary reporting countries. Concentration maps have been produced to assess the situation with respect to the most stringent air quality limit values and the indicators most relevant for the assessment of impacts on human health and vegetation.

The mapping method follows the methodology developed earlier (Horálek et al, 2019a, 2019b, and reference cited therein); it combines the monitoring data with supplementary data (such as the results from a chemical transport model, land cover, meteorological and geographical data). The method ('Regression – Interpolation – Merging Mapping') is based on a linear regression model followed by kriging of residuals produced from that model (residual kriging). This methodology has been applied systematically during the past 13 years, which enables the evaluation of changes in exposure over time.

Population exposure

Concentrations of particulate matter continued to exceed the EU and WHO standards in large parts of Europe. Seven percent of the European population is exposed to levels above the EU $PM_{2.5}$ limit value of 25 µg·m^{-3}; 74 % of the European population is exposed to levels above the WHO $PM_{2.5}$ Air Quality Guideline of 10 µg·m^{-3} (Table 3.1). Table 2.2 shows that in ten (eastern European) countries more than 50 % of the population is exposed to concentrations above the PM_{10} daily limit value. Figure ES.1 shows that the countries with the highest values of annual average PM_{10} are located in the eastern parts of Europe as well. The concentrations of $PM_{2.5}$ and PM_{10} are often highly correlated, with the highest $PM_{2.5}$ exposures also found in the eastern parts.

Figure ES.1 PM_{10} concentrations to which the population per country was exposed in 2017, in relation to the annual limit value (40 µg·m^{-3}). The box plots show for each country, the concentration to which 2, 25, 75 and 98% of the population was exposed. The black marker corresponds to the concentration to which 50% of the population was exposed.

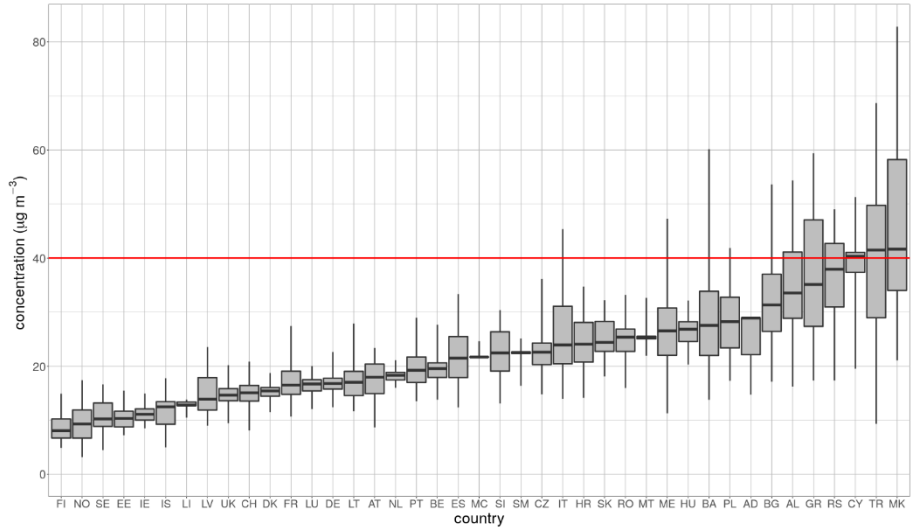

The NO_2 annual mean concentration map shows a different spatial distribution than the PM maps. Table 5.1 indicates that in 17 countries a limited fraction of the population (5 % in total) is exposed to concentrations above the annual limit value of 40 µg·m^{-3}. Figure ES.2 shows that in all countries, the majority of population lived well below the limit value in 2017, according to the presented assessment. High exposures are observed in the larger urban areas (e.g. greater London, the Benelux-Ruhr area, Po valley, Naples, Paris, Madrid, and Istanbul).

Figure ES.2 NO_2 concentrations to which the population per country was exposed in 2017, in relation to the annual limit value (40 µg·m^{-3}). The box plots show for each country, the concentration to which 2, 25, 75 and 98% of the population was exposed. The black marker corresponds to the concentration to which 50% of the population was exposed.

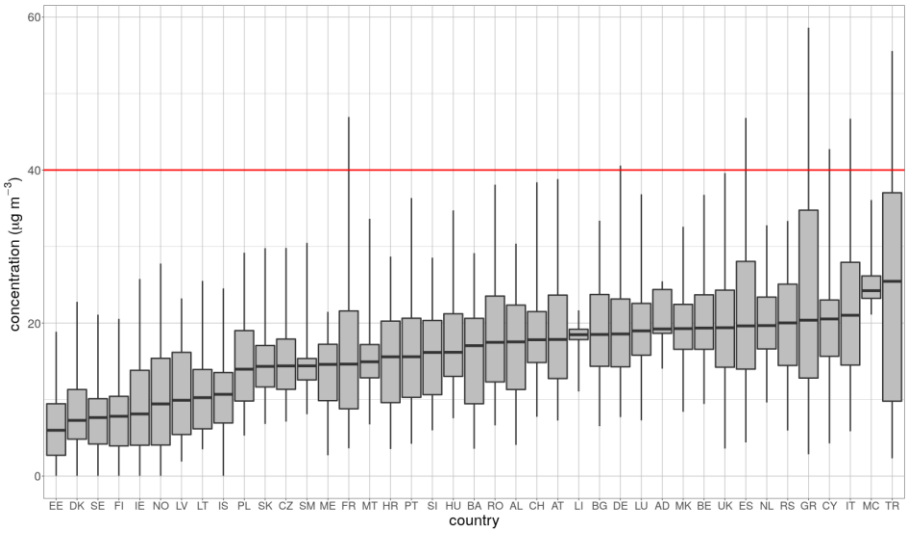

Exposure to ozone concentrations above the EU target value threshold (a maximum daily 8-hour average value of 120 µg·m^{-3} not to be exceeded on more than 25 days per year) occurs in large parts of southern Europe. 13 % of the Europeans live in areas where the ozone target value is exceeded (Table 4.1). Figure ES.3 shows that the countries with the highest values of SOMO35 are located in the southern parts of Europe.

Figure ES.3 Ozone concentrations to which the population per country was exposed in relation to the indicator SOMO35 in 2017. The box plots show for each country, the concentration to which 2, 25, 75 and 98% of the population was exposed. The black marker corresponds to the concentration to which 50% of the population was exposed.

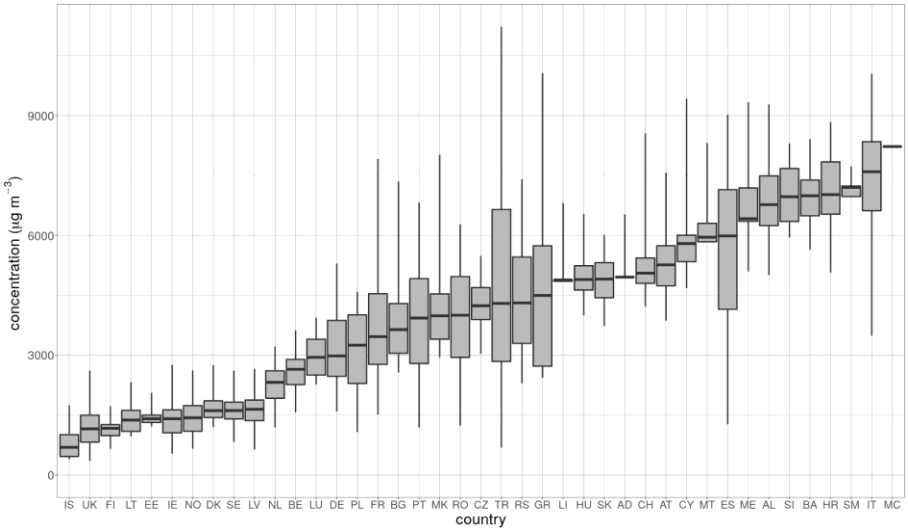

Accumulated risks

Although the spatial distributions of PM, NO_2 and ozone concentrations differ widely, the possibility of an accumulation of risk resulting from high exposures to all three pollutants cannot be excluded. Combining the maps of the three most frequently exceeded standards (PM_{10} daily limit value, NO_2 annual limit value and ozone target value) shows that out of the total population of 619 million in the model area, 8.2% (50.6

million) lived in areas where two or three air quality standards were exceeded; 2.8 million people lived in areas where all three standards were exceeded. The worst situation was observed in Italy (in particular the Po valley): 4.5% lived in areas where the three standards were breached.

Vegetation exposure

Standards for the protection of vegetation have been set, among others, for NO_x and ozone. In a limited number of cases, the NO_x critical level has been exceeded, though this is relevant only if there is vegetation in those areas. A larger impact on vegetation can be expected from the direct exposure to ozone. The target value for the protection of vegetation (AOT40) is exceeded in about 28 % of the agricultural areas. The long-term objective is exceeded in 77 % of the agricultural areas.

Changes over time

Since 2005 (resp. since 2007 in the case of $PM_{2.5}$), the maps have been prepared in an overall consistent way, although the mapping methodology has been subject to continuous improvement. This enables an analysis of changes in exposure over time. In the case of the of PM_{10} and $PM_{2.5}$ maps, major methodology change has been applied for 2017, these maps have been constructed based on the updated methodology as developed and tested in Horálek et al. (2019b). For comparability reasons, also the maps based on the old methodology have been constructed and used in the trend analysis. The PM concentrations show a steady decrease of about 0.7 $\mu g \cdot m^{-3}$ per year (PM_{10} annual average) resp. 0.4 $\mu g \cdot m^{-3}$ per year ($PM_{2.5}$ annual average). For the ozone concentration (expressed as SOMO35) a small decreasing trend is observed, in spite of the year-to-year variability. For changes in population-weighted concentrations, see Figure ES.4. The population-weighted concentration is calculated for the area of all countries considered in the report, except Turkey, for comparability reasons, because the area of Turkey has not been mapped until 2016.

Figure ES.4 Changes in population-weighted concentrations of PM_{10} (annual mean), $PM_{2.5}$ (annual mean), ozone (SOMO35), and NO_2 (annual mean). For PM_{10} and $PM_{2.5}$, results based on both the old (blue dots) and the updated (red dots) mapping methodology are presented, where available.

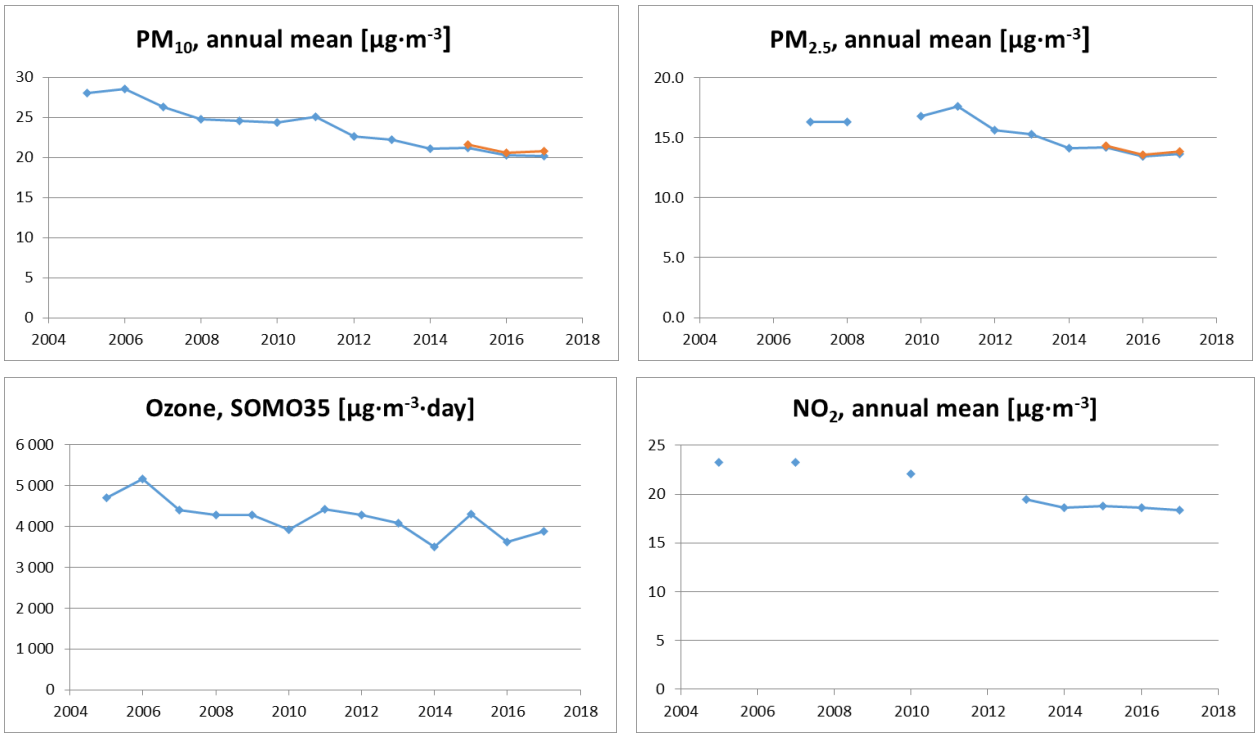

The agricultural-weighted concentration tends to decrease by about 408 $\mu g \cdot m^{-3} \cdot h$ per year over the period 2005–2017, in terms of AOT40 for vegetation. For changes in agricultural-weighted concentrations, see

Figure ES.5. Again, the agricultural-weighted concentration is calculated for the area of all countries considered in the report, except Turkey.

Figure ES.5Changes in agricultural-weighted concentrations of ozone indicator AOT40 for vegetation.

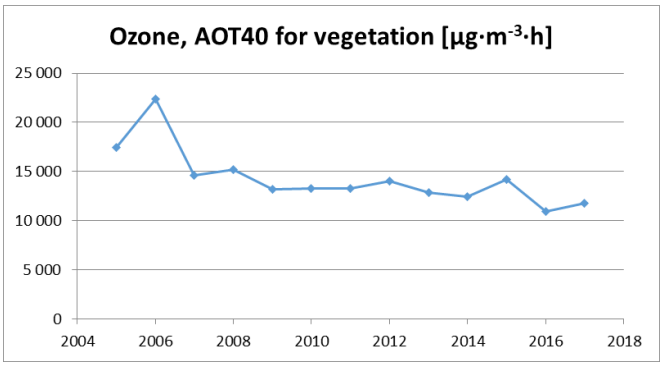

1 Introduction

This report provides an update of European air quality concentration maps, population exposure and vegetation exposure estimates for 2017. It builds on the previous reports (Horálek et al., 2019a, and references cited therein). The analysis is based on interpolation of annual statistics of validated monitoring data from 2017, reported by the EEA member and cooperating countries (and the voluntary reporting country of Andorra) in 2018. The paper presents mapping results and includes an uncertainty analysis of the interpolated maps, adopting the latest methodological developments, see Horálek et al. (2019a, 2019b) and reference cited therein. The mapping area covers all of Europe apart from Belarus, Moldova, Ukraine and the European parts of Russia and Kazakhstan. Turkey is included in the mapping area for all pollutants except $PM_{2.5}$, due to the lack of rural stations in Turkey for $PM_{2.5}$ for 2017 in the AQ e-reporting database (EEA, 2019a).

We consider in this report PM_{10}, $PM_{2.5}$, ozone, NO_2 and NO_x for 2017, being the most relevant pollutants for annual updating due to their potential impacts on health or ecosystems. The analysis method applied is similar to that of previous years. Another potentially relevant pollutant, benzo[a]pyrene (BaP), is not presented, as the station coverage is not dense enough for enabling the regular mapping. The current status of mapping the BaP concentrations in Europe was discussed by Guerreiro et al. (2016) and Horálek et al. (2017a).

The mapping is based primarily on air quality measurements. It combines monitoring data, chemical transport model results and other supplementary data (such as altitude and meteorology). The method is a linear regression model followed by kriging of the residuals produced from that model ('residual kriging'). It should be noted that this methodology does not allow for formal compliance checking with limit or target values as set by the air quality directive.

The maps of health-related indicators of ozone are created for the rural and urban (including suburban) background areas separately on a grid at 10x10 km^2 resolution. Subsequently, the rural and urban background maps are merged into one final combined air quality indicator map using a 1x1 km^2 population density grid, following a weighting criterion applied per grid cell. This fine resolution takes into account the smaller settlements in Europe that are not resolved at the 10x10 km^2 grid resolution. The maps of health related indicators of PM_{10}, $PM_{2.5}$, and NO_2 are constructed by improved methodology developed in Horálek et al. (2017c, 2019b): next to the rural and urban background map layers, the urban traffic map layer is constructed and incorporated into the final merged map using the road data. All individual map layers are created at 1x1 km^2 resolution and land cover and road data are included in the mapping process as supplementary data. The maps of ozone and NO_x vegetation-related indicators are at a grid resolution of 2x2 km^2 and based on rural background measurements; in the case of ozone they serve as input to the EEA's core set indicator CSI005 (EEA, 2018d).

Next to the annual indicator maps, we present in tables the population exposure to PM_{10}, $PM_{2.5}$, ozone, and NO_2, and the exposure of vegetation to ozone. Tables of population exposure are prepared using the final combined maps and the population density map of 1x1 km^2 grid resolution. For PM_{10}, $PM_{2.5}$ and NO_2, the population exposure in each grid cell is calculated separately for urban areas directly influenced by traffic and for the background (both rural and urban) areas, in order to better reflect the population exposed to traffic emissions. The tables of the vegetation exposure are prepared with a 2x2 km^2 grid resolution based on the Corine Land Cover 2012 dataset.

Chapters 2, 3, 4 and 5 present the concentration maps and exposure estimates for PM_{10}, $PM_{2.5}$, ozone and NO_2, respectively. Chapter 5 presents the concentration map for NO_x; exceedances of the critical level for the protection of vegetation occur in very limited areas and, as such, it is considered not to provide relevant information from the European scale perspective. Chapter 6 summarizes the trends in exposure estimates in the period 2005 – 2017.

Annex 1 describes briefly the different methodological aspects. Annex 2 documents the input data applied in the 2017 mapping and exposure analysis. Annex 3 presents the technical details of the maps and their uncertainty analysis including the cross-validation results. Annex 4 shows the inter-annual changes including the inter-annual difference maps between 2016 and 2017 and the variations in population exposure in the period 2005 – 2017. Annex 5 presents the concentration maps including the station points, in order to provide more complete information of the air quality in 2017 across Europe.

2 PM_{10}

The Ambient Air Quality Directive (EU, 2008) sets limit values for long-term and for short-term PM_{10} concentrations. The long-term annual PM_{10} limit value is set at 40 $\mu g \cdot m^{-3}$. The Air Quality Guideline recommended by the World Health Organization (WHO, 2005) for the PM_{10} annual average is 20 $\mu g \cdot m^{-3}$. The short-term limit value indicates that the daily average PM_{10} concentration should not exceed 50 $\mu g \cdot m^{-3}$ during more than 35 days per year. It corresponds to the 90.4 percentile of daily PM_{10} concentrations in one year. This daily limit value is the most frequently exceeded air quality limit value in Europe.

This chapter presents the 2017 updates of two PM_{10} indicators: the annual average and the 90.4 percentile of the daily averages. The latter is a more relevant indicator in the context of the AQ Directive (EU, 2008) than the formerly used 36th highest daily mean (Horálek et al., 2016b).

The maps of PM_{10} are based on an improved mapping methodology developed and tested in Horálek et al. (2019b). The map layers are created for the rural, urban background and urban traffic areas separately on a grid at 1x1 km^2 resolution. Subsequently, the urban background and urban traffic map layers are merged together using the gridded road data into one urban map layer. This urban map layer is further combined with the rural map layer into the final PM_{10} map using a population density grid at 1x1 km^2 resolution. For both PM_{10} indicators, we present this final combined map in this 1x1 km^2 grid resolution.

The population exposure tables are calculated based on these maps, according to the methodology described in Horálek et al. (2019b), i.e. they are calculated separately for urban areas directly influenced by traffic and for the background (both rural and urban) areas, in order to better reflect the population exposed to traffic. For details, see Annex I, Equation A1.6.

2.1 PM_{10} annual average

2.1.1 Concentration map

Map 2.1 presents the final combined concentration map for the 2017 PM_{10} annual average as the result of interpolation and merging of the separate maps as described in Annex 1 (for a more detailed description see Horálek et al., 2007, 2019b). Red and purple areas indicate exceedances of the limit value (LV) of 40 $\mu g \cdot m^{-3}$.

The final combined concentration map presented in Map 2.1 is constructed on a 1x1 km^2 grid resolution (Annex 1). The station points are not presented in the map, in order to better visualise the urban areas. However, concentration values from measurements at the station points used in the kriging interpolation methodology (Annex 3) are considered to provide relevant information. In Map A5.1 of Annex 5 these point values are presented on top of Map 2.1 and illustrate the smoothing effect the interpolation methodology can have on the gridded concentration fields.

Map 2.1 shows LV exceedances in southern Spain near Almeria, in northern Italy near Milan, in Greece in Athens, in southern Poland in areas around Katowice, in some urban areas of Bulgaria with high concentrations at Sofia, in urban areas of North Macedonia, Serbia and Turkey. The extent of the exceeded area near Almeria is smaller in 2017 compared to 2016. Concerning the estimated exceedances in the Almeria area and in Athens, it should be noted that they are primarily based on high concentration values indicated in this area by the chemical transport modelling, and not on measurements (which are not available in this area with the minimum data coverage required to be taken into account, Almeria, or at the deadline set for their inclusion, Athens).

The uncertainty of the concentration map can be expressed in relative terms of the absolute Root Mean Square Error (RMSE) uncertainty related to the mean air pollution indicator value for all stations (see Annex 1). This *relative mean uncertainty* (RRMSE) of the final combined map of PM_{10} annual average is

18 % for rural areas and 20 % for urban background areas without Turkish stations (i.e. quite similar to the last years), resp. 20 % for rural areas and 29 % for urban background areas including Turkish stations (Annex 3). The main reason for presenting the results without Turkish stations is to enable the comparison with previous years.

Map 2.1 Concentration map of PM_{10} annual average, 2017

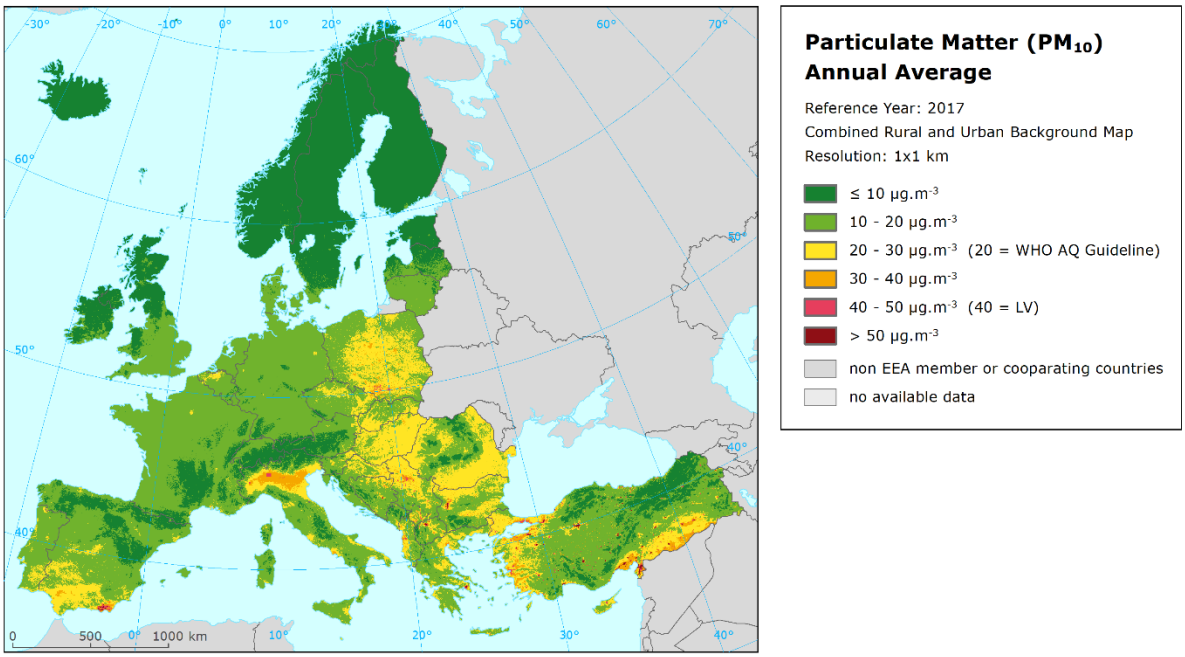

2.1.2 Population exposure

Table 2.1 gives the population frequency distribution for a limited number of exposure classes, as well as the population-weighted concentration for individual countries and for Europe as a whole according to Equation A1.7.

The human exposure to PM_{10} has been calculated based on the improved methodology as developed in Horálek et al. (2019b), i.e. similarly as for NO_2. The population exposure is calculated according to Equation A1.6 of Annex I, i.e. it is calculated separately for urban areas directly influenced by traffic and for the background (both rural and urban) areas, in order to better reflect the population exposed to traffic. Based on this, the different concentration levels in urban background and traffic areas inside the 1x1 km^2 grid cells are taken into account.

About 47 % of the European population and 41 % of the EU-28 population has been exposed to annual average concentrations above the Air Quality Guideline of 20 $\mu g \cdot m^{-3}$ recommended by the World Health Organization (WHO, 2005). CSI004 (EEA, 2019c) estimates that about 44 % of the population in urban agglomerations in the EU-28 was exposed in 2017 to levels above the WHO guideline. The latter estimate accounts for the urban population of the EU-28. It therefore represents areas where, in general, somewhat higher PM_{10} concentrations occur. The estimates in Table 2.1 account for the total European and EU-28 population, *including* the population in rural areas, smaller cities and villages that are in general exposed to lower levels of PM_{10}. Next to this, it should be mentioned that CSI004 refers to the population in cities for which PM_{10} data is available.

Table 2.1 Population exposure and population-weighted concentration, PM_{10} annual average, 2017

Country		Population	PM_{10} annual average, exposed population [%]						Population weighted conc. [µg.m^{-3}]
			< LV				> LV		
		[inhbs . 1000]	< 10 µg.m^{-3}	10 - 20 µg.m^{-3}	20 - 30 µg.m^{-3}	30 - 40 µg.m^{-3}	40 - 45 µg.m^{-3}	> 45 µg.m^{-3}	
Albania	AL	2 877	0.2	6.5	24.8	37.6	28.1	3.0	34.3
Andorra	AD	73	0.2	13.3	86.5				25.7
Austria	AT	8 773	4.3	64.8	30.9				17.3
Belgium	BE	11 352	0.0	57.4	42.6				19.5
Bosnia & Herzegovina	BA	3 510	0.0	16.0	41.6	30.1	5.2	7.1	29.6
Bulgaria	BG	7 102	0.0	4.8	40.2	44.2	7.7	3.1	32.3
Croatia	HR	4 154	0.0	19.8	69.1	11.1	0.0		24.2
Cyprus	CY	1 201		2.5	13.4	29.6	51.9	2.5	37.6
Czechia	CZ	10 579	0.0	22.5	69.3	8.0	0.1		22.8
Denmark	DK	5 749	0.4	98.8	0.8				15.1
Estonia	EE	1 316	45.1	54.9					10.5
Finland	FI	5 503	73.6	26.4					8.6
France (metropolitan)	FR	64 629	1.3	80.3	17.2	1.1	0.0		17.2
Germany	DE	82 522	0.3	91.4	8.3				16.9
Greece	GR	10 768	0.0	4.5	28.4	28.1	27.7	11.2	36.5
Hungary	HU	9 798		1.6	93.0	5.4			26.4
Iceland	IS	338	26.9	72.8	0.3				11.6
Ireland	IE	4 784	24.5	75.5					11.2
Italy	IT	60 589	0.3	21.0	50.6	22.3	5.7		26.1
Latvia	LV	1 950	7.1	77.4	14.6	1.0			15.2
Liechtenstein	LI	38	1.7	98.3					12.8
Lithuania	LT	2 848	0.1	79.7	18.4	1.8			17.2
Luxembourg	LU	591	0.0	98	2.4				16.4
Malta	MT	460		0.9	89	10			25.9
Monaco	MC	38			100				22.3
Montenegro	ME	622	0.7	16.6	51.0	28.5	3.1		26.0
Netherlands	NL	17 082		94.6	5.4				18.2
North Macedonia	MK	2 074	0.0	1.6	7.7	36.3	21.5	32.9	47.3
Norway	NO	5 258	56.1	43.9	0.0				9.6
Poland	PL	37 973	0.0	8.2	53.4	31.6	6.7	0.0	28.5
Portugal (excl. Az., Mad.)	PT	9 809	0.0	57.4	41.7	0.9	0.0		19.7
Romania	RO	19 644	0.0	9.8	83.7	6.4	0.0		24.9
San Marino	SM	33		12.1	87.9				22.0
Serbia (incl. Kosovo*)	RS	8 824	0.0	3.9	18.2	40.7	36.3	0.8	36.7
Slovakia	SK	5 435	0.0	4.4	86.0	9.5	0.0		25.2
Slovenia	SI	2 066	0.0	30.4	63.7	5.9			22.6
Spain (excl. Canarias)	ES	44 373	0.4	38.8	54.7	5.5	0.3	0.2	21.8
Sweden	SE	9 995	45.1	54.9	0.0				10.7
Switzerland	CH	8 420	5.8	91.6	2.6				14.8
Turkey	TR	79 815	2.7	13.8	9.5	19.1	30.4	24.5	40.2
United Kingdom (& dep.)	UK	65 844	2.7	95.1	2.1				14.6
Total		**618 808**	**3.1**	**49.7**	**27.8**	**9.9**	**6.1**	**3.4**	**23.1**
			52.8				**9.5**		
Total without Turkey		**538 993**	**3.2**	**54.5**	**30.3**	**8.7**	**2.8**	**0.5**	**20.8**
			57.7				**3.3**		
EU-28		**506 888**	**2.7**	**55.8**	**31.3**	**7.8**	**2.0**	**0.3**	**20.4**
			58.5				**2.4**		
Kosovo*	KS	1 784	0.0	4.7	16.2	33.7	45.3	0.0	37.2
Serbia (excl. Kosovo*)	RS	7 040	0.0	3.7	18.7	42.5	34.1	1.0	36.6

(*) under the UN Security Council Resolution 1244/99

Note: The percentage value "0.0" indicates that an exposed population exists, but it is small and estimated to be less than 0.05 %. Empty cells mean no population in exposure.

Approximately 9% of population of the European area (including Turkey) has been exposed to concentrations exceeding the EU annual limit value (ALV) of 40 µg·m^{-3}; the same is the case for about 3 % for the European population excluding Turkey and for 2 % of the EU-28 population. In Albania, Cyprus, Greece, North Macedonia, Serbia including Kosovo[1] and Turkey, more than 30 % of the population is exposed to concentrations above the ALV. A limited fraction of the population (3 – 15 %) is exposed to concentrations above the ALV in Bosnia & Herzegovina, Bulgaria, Italy, Montenegro and Poland. However, as the current mapping methodology tends to underestimate high values (see Annex 3, Section A3.1), the exceedance percentage will most likely be underestimated. Additional population exposure above the ALV could therefore be expected in countries like Bulgaria, Serbia or Albania where a relatively large fraction of the population lives in areas with concentration levels above 30 µg·m^{-3}.

The European-wide population-weighted concentration of the annual average for 2017 is estimated to be about 23 µg·m^{-3} including Turkey, 21 µg·m^{-3} without Turkey, and 20 µg·m^{-3} for the EU-28 only.

Figure 2.1 shows, for the whole mapped area (that is, all Europe including Turkey), the population frequency distribution for exposure classes of 1 µg·m^{-3}. One can see the highest population frequency for classes between 14 and 18 µg·m^{-3}. And quite continuous decline of population frequency for classes between 20 and 35 µg·m^{-3} and beyond 40 µg·m^{-3}.

Figure 2.1 Population frequency distribution, PM_{10} annual average, 2017

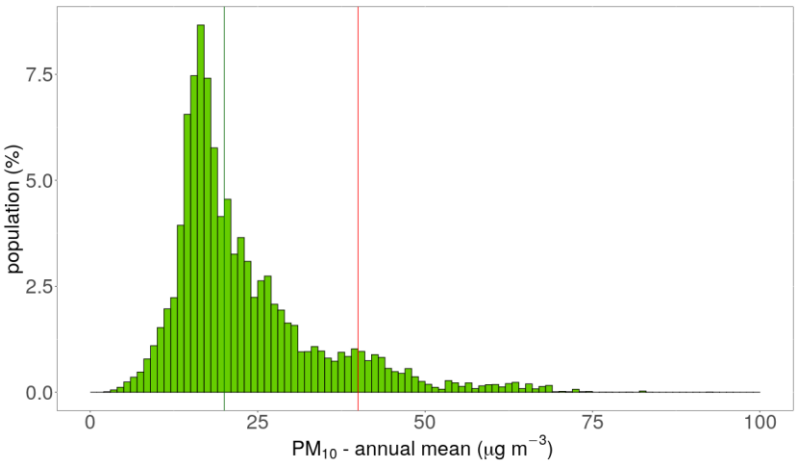

Note: Apart from the population distribution shown in the graph, it was estimated that 0.07 % of population lived in areas with PM_{10} annual average concentration in between 100 and 270 µg.m^{-3}.

2.2 PM_{10} – 90.4 percentile of daily means

The AQ Directive (EU, 2008) describes the PM_{10} daily limit value (DLV) as "a daily average of 50 µg·m^{-3} not to be exceeded more than 35 times a calendar year". This requirement can be evaluated by the indicator 36th highest daily mean, which is in principle equivalent to the indicator 90.4 percentile of daily means. However, for measurement data these two indicators are equivalent only if no data is missing, which is in general not the case. As shown in de Leeuw (2012), the additional uncertainty related to incomplete time series is substantially smaller when using percentile values instead of the x-th highest value. Furthermore, the AQ Directive requires the use of the 90.4 percentile when random measurements are used to assess

[1] In this paper, references to Kosovo shall be understood to be in the context of UN Security Council Resolution 1244/99.

the requirements of the PM_{10} DLV. As in the previous reports since the maps for 2014, we express the PM_{10} daily means as the 90.4 percentile instead of the formerly used 36th highest daily mean.

2.2.1 Concentration map

Map 2.2 presents the final combined map, where red and purple marked areas indicate exceedances of the DLV of 50 µg·m^{-3} on more than 35 measurement days. The similar mapping procedure as in the case of the annual average is used. The mapping details and the uncertainty analysis are presented in Annex 3. Large areas above the DLV are observed in northern Italy (i.e. the Po Valley) with elevated values in the region around Milan, in the region with the agglomerations Ostrava – Katowice - Krakow, the Almeria region in Spain, parts of Serbia and Bulgaria, and western parts of Turkey. Urban areas with concentrations above the DLV are observed in Poland, southern and eastern Romania, Bulgaria, Turkey, Croatia, Slovenia, Bosnia & Herzegovina, Greece, Albania, North Macedonia, and Serbia including Kosovo. In general, the central and the eastern parts of Europe appear with higher concentrations than the western and the northern parts. As for the PM_{10} annual averages, the estimated exceedances in the Almeria area and in Greece are based on the chemical transport modelling, not on measurements.

The relative mean uncertainty (relative RMSE) of the final combined map of the 90.4 percentile of PM_{10} daily means is 21 % for rural areas and 24 % for urban background areas without Turkish stations, resp. 24 % for rural areas and 31 % for urban background areas including Turkish stations (Annex 3).

The final combined map *including* the indicator 90.4 percentile of daily means based on the actual measurement data at station points is presented in Map A5.2 of Annex 5.

Map 2.2 Concentration map of PM_{10} indicator 90.4 percentile of daily means, 2017

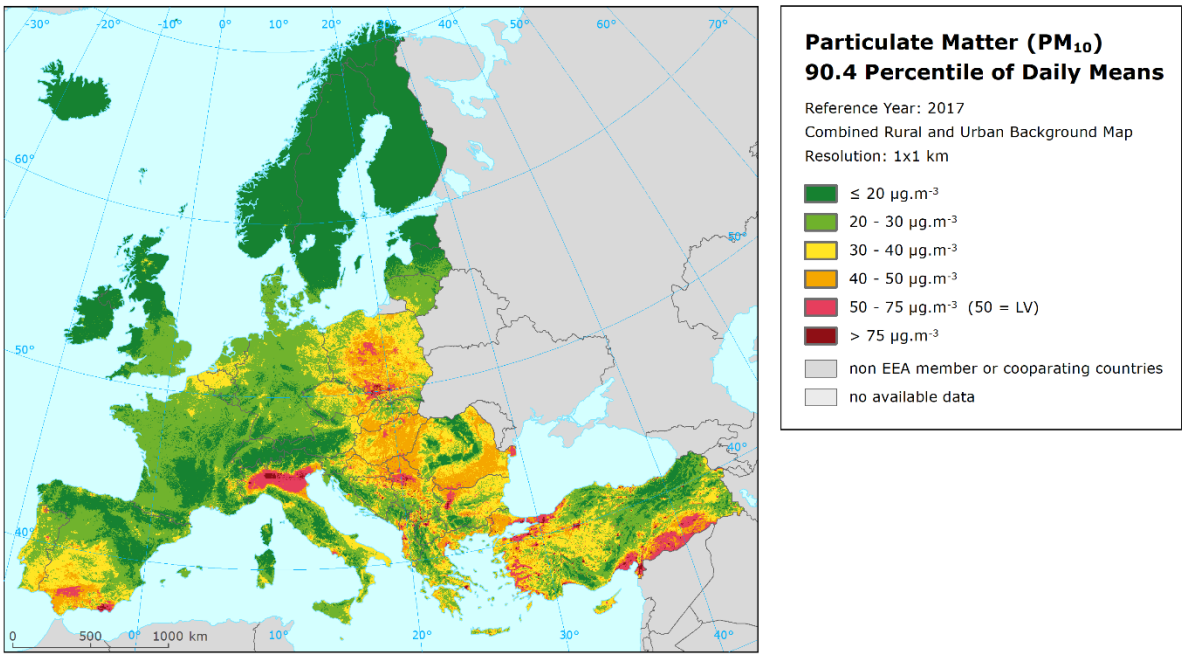

2.2.2 Population exposure

Table 2.2 gives the population frequency distribution for a limited number of exposure classes calculated at 1x1 km^2 grid resolution, as well as the population-weighted concentration for individual countries and for Europe as a whole. Annex 4 shows details on the twelve years evolution of population exposure.

Table 2.2 Population exposure and population-weighted concentrations, PM10 indicator 90.4 percentile of daily means, 2017

Country		Population	PM_{10}, 90.4 percentile of daily means, exposed population [%]						Pop. weighted conc.
			< LV				> LV		
			< 20	20 - 30	30 - 40	40 - 50	50 - 75	> 75	
		[inhbs . 1000]	µg.m^{-3}	µg.m^{-3}	µg.m^{-3}	µg.m^{-3}	µg.m^{-3}	µg.m^{-3}	[µg.m^{-3}]
Albania	AL	2 877	0.1	2.8	7.6	12.4	53.7	23.3	62.1
Andorra	AD	73	0.2	10.0	10.9	5.0	73.9		49.8
Austria	AT	8 773	6.8	35.5	49.9	7.7	0.1		31.4
Belgium	BE	11 352	0.0	9.6	83.6	6.8			34.0
Bosnia & Herzegovina	BA	3 510	0.1	4.7	16.6	18.7	37.5	22.4	60.6
Bulgaria	BG	7 102	0.0	1.4	8.3	21.9	53.7	14.8	61.4
Croatia	HR	4 154	0.2	5.7	27.0	24.7	42.2	0.2	47.3
Cyprus	CY	1 201	0.0	0.6	8.6	11.7	75.9	3.2	55.8
Czechia	CZ	10 579	0.1	5.2	26.7	47.5	19.3	1.2	44.1
Denmark	DK	5 749	1.2	92.5	6.3	0.0			26.3
Estonia	EE	1 316	84.8	15.2	0.0				18.1
Finland	FI	5 503	88.6	10.9	0.5				15.2
France (metropolitan)	FR	64 629	3.1	57.1	37.0	2.4	0.4	0.0	29.0
Germany	DE	82 522	0.7	67.7	30.8	0.9			29.2
Greece	GR	10 768	0.0	1.4	6.5	17.8	39.8	34.4	65.6
Hungary	HU	9 798		0.0	6.2	53.7	39.9	0.3	48.5
Iceland	IS	338	47.0	47.4	5.7				19.7
Ireland	IE	4 784	52.6	47.4	0.0				19.9
Italy	IT	60 589	0.7	13.0	34.7	14.7	25.7	11.2	47.6
Latvia	LV	1 950	11.6	57.5	28.7	1.3	1.0		27.0
Liechtenstein	LI	38	2.1	97.9					24.1
Lithuania	LT	2 848	0.1	46.1	48.2	5.0	0.6		30.8
Luxembourg	LU	591	0.1	89.5	10.4				27.8
Malta	MT	460		1.1	70.6	28			39.4
Monaco	MC	38			100				33.8
Montenegro	ME	622	0.9	9.3	15.0	25.8	45.7	3.2	49.5
Netherlands	NL	17 082	0.0	56.8	43.2				29.8
North Macedonia	MK	2 074	0.0	0.7	1.7	2.1	32.2	63.2	100.3
Norway	NO	5 258	72.2	20.1	7.7	0.0			18.0
Poland	PL	37 973	0.0	1.1	19.3	23.6	43.3	12.6	53.2
Portugal (excl. Az., Mad.)	PT	9 809	0.0	24.0	60.7	13.8	1.5	0.0	34.3
Romania	RO	19 644	0.1	3.9	26.3	58.6	11.1		42.2
San Marino	SM	33		2.8	16.6	81			40.4
Serbia (incl. Kosovo*)	RS	8 824	0.0	1.4	4.2	7.5	34.2	52.7	72.3
Slovakia	SK	5 435	0.0	0.8	11.2	52.5	34.6	0.9	48.2
Slovenia	SI	2 066	0.1	9.3	31.7	37.9	20.9		42.2
Spain (excl. Canarias)	ES	44 373	1.0	28.0	37.1	22.3	11.3	0.4	37.2
Sweden	SE	9 995	60.2	37.6	2.2	0.0			19.2
Switzerland	CH	8 420	9.1	72.1	16.6	2.1	0.0		26.3
Turkey	TR	79 815	1.5	7.2	8.0	5.5	27.6	50.2	75.8
United Kingdom (& dep.)	UK	65 844	8.7	85.9	5.4	0.0			25.1
Total		**618 808**	**4.9**	**34.9**	**24.4**	**11.5**	**14.2**	**10.0**	**41.6**
			75.8				**24.2**		
Total without Turkey		**538 993**	**5.3**	**38.7**	**26.6**	**12.4**	**12.4**	**4.6**	**37.0**
			83.0				**17.0**		
EU-28		**506 888**	**4.8**	**39.7**	**27.7**	**12.7**	**11.8**	**3.3**	**36.1**
			84.9				**15.1**		
Kosovo*	KS	1 784	0.0	1.5	6.4	7.0	21.0	64.1	75.5
Serbia (excl. Kosovo*)	RS	7 040	0.0	1.4	3.7	7.6	37.4	50.0	71.5

(*) under the UN Security Council Resolution 1244/99

Note: The percentage value "0.0" indicates that an exposed population exists, but it is small and estimated to be less than 0.05 %. Empty cells mean no population in exposure.

We estimate that in 2017 about 24 % of the European population lived in areas where the 90.4 percentile of the PM_{10} daily means exceeded the EU limit value of 50 µg·m^{-3}. In Albania, Bosnia & Herzegovina, Bulgaria, Cyprus, Greece, North Macedonia, Poland, Serbia (including Kosovo) and Turkey more than half of the population was exposed to concentrations exceeding the DLV. In Croatia, Hungary, Italy, Montenegro, and Slovakia the portion of the population living in areas with concentrations above the DLV was between 25 and 50 percent.

For the EU-28 around 15 % of the total population lived in areas where the 90.4 percentile of the PM_{10} daily mean exceeded the EU limit value of 50 µg·m^{-3}. According to CSI004 (EEA, 2019c), in 2017 about 17 % of the urban population in the EU-28 was exposed to PM_{10} above this limit value. The slight difference between the two estimates is influenced by the fact that the EEA accounts for the urban population only, while Table 2.2 provides estimates also including inhabitants in rural areas, smaller cities and villages.

The European-wide population-weighted concentration of the 90.4 percentile of PM_{10} daily means is estimated for 2017 at about 42 µg·m^{-3} (including Turkey), resp. 37 µg·m^{-3} (without Turkey), and 36 µg·m^{-3} for the EU-28.

Figure 2.2 shows, for the whole mapped area, the population frequency distribution for exposure classes of 2 µg·m^{-3}. One can see the highest population frequency for classes between cc. 22 and 30 µg·m^{-3}, continuous decline of population frequency for classes between cc. 30 and 50 µg·m^{-3} and continuous mild decline of population frequency for classes between cc. 50 and 100 µg·m^{-3}.

As in previous years, the daily limit value was more widely exceeded than the annual limit value in 2017.

Figure 2.2 Population frequency distribution, PM_{10} indicator 90.4 percentile of daily means, 2017

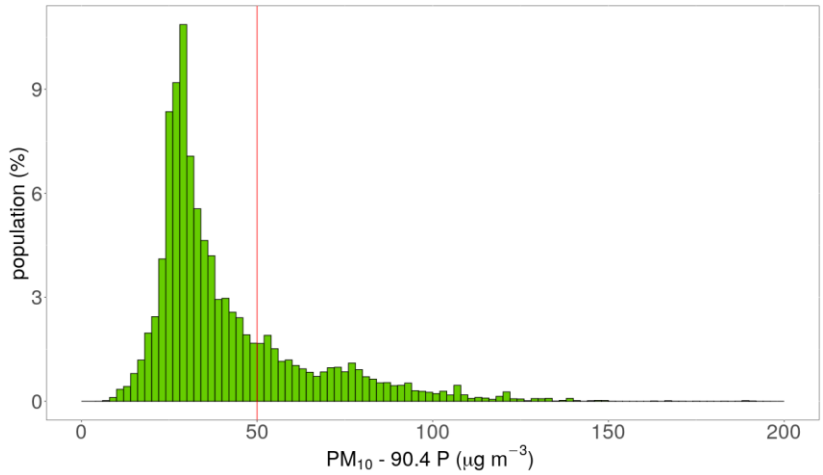

Note: Apart from the population distribution shown in graph, it was estimated that 0.07 % of population lived in areas with values of PM_{10} indicator 90.4 percentile of daily means in between 200 and 680 µg.m^{-3}.

3 $PM_{2.5}$

In the Ambient Air Quality Directive (EU, 2008), the limit value (LV) for the annual average $PM_{2.5}$ concentrations was set at 25 µg·m^{-3}. In the AQ directive there is also an indicative LV of 20 µg·m^{-3} defined as Stage 2 that could potentially become in place in 2020. The Air Quality Guideline recommended by the World Health Organization (WHO, 2005) for the $PM_{2.5}$ annual average is 10 µg·m^{-3}.

The current number of $PM_{2.5}$ measurement stations is still somewhat limited and its spatial distribution is irregular over Europe. Deriving a reasonably reliable European wide spatially interpolated $PM_{2.5}$ annual average map on the basis of these $PM_{2.5}$ measurement data alone is not feasible. The resulting map would not be suitable for being used in population exposure assessments.

Therefore, in this paper the mapping of the health-related indicator $PM_{2.5}$ annual average is based on a mapping methodology developed in Denby et al. (2011a, 2011b). This methodology derives additional *pseudo* $PM_{2.5}$ annual mean concentrations from PM_{10} annual mean measurement concentrations. As such, it increases the number and spatial coverage of $PM_{2.5}$ 'data points' and these data are used to derive a European wide map of annual mean $PM_{2.5}$. Pseudo $PM_{2.5}$ stations data are estimated using PM_{10} measurement data, surface solar radiation, latitude and longitude.

Like for PM_{10}, the map of $PM_{2.5}$ is based on an improved mapping methodology developed in Horálek et al. (2019b). The map layers are created for the rural, urban background and urban traffic areas separately on a grid at 1x1 km^2 resolution. Subsequently, the urban background and urban traffic map layers are merged together using the gridded road data into one urban map layer. This urban map layer is further combined with the rural map layer into the final PM_{10} map using a population density grid at 1x1 km^2 resolution. We present this final combined map at this 1x1 km^2 grid resolution.

Annex 3 provides details on the regression and kriging parameters applied for deriving the $PM_{2.5}$ annual average map, as well as the uncertainty analysis of the map. Annex 4 discusses briefly the inter-annual changes observed in the concentration maps and the relevant population exposure.

3.1 $PM_{2.5}$ annual average

3.1.1 Concentration map

Map 3.1 presents the final combined map for the 2017 $PM_{2.5}$ annual average as a result of the interpolation and merging of the separate rural and urban map layers. The dark red areas exceed the ALV of 25 µg·m^{-3}. Red areas show exceedances of the indicative LV of 20 µg·m^{-3} defined as Stage 2 (LV_{2020}).

Due to the lack of rural $PM_{2.5}$ stations in Turkey, no proper interpolation results could be estimated for this country in a rural map. Therefore, we do not present the estimated $PM_{2.5}$ values for Turkey in the final map.

According to Map 3.1, the areas with the highest $PM_{2.5}$ concentrations appear to be the Po Valley in Northern Italy, the areas around the Balkan cities of Sofia, Tirana, Skopje and Belgrade and the Krakow – Katowice (PL) – Ostrava (CZ) industrial region. Different other cities in Bulgaria, Greece[2], Serbia, Kosovo, North Macedonia, Bosnia & Herzegovina and Poland also show elevated $PM_{2.5}$ annual average concentrations. Like in the case of PM_{10}, the central and the eastern parts of Europe show higher concentrations than the western and the northern parts.

[2] As for PM_{10}, based only on the modelling and distant measurements in other countries, since measurement data from the Greek stations were reported later than the deadline to may take them into account.

The relative mean uncertainty of the 2017 map of $PM_{2.5}$ annual average is 23 % for rural areas and 18 % for urban background areas and determined exclusively on the actual $PM_{2.5}$ measurement data points, i.e. not on the pseudo stations (Annex 3).

Map 3.1 Concentration map of $PM_{2.5}$ annual average, 2017

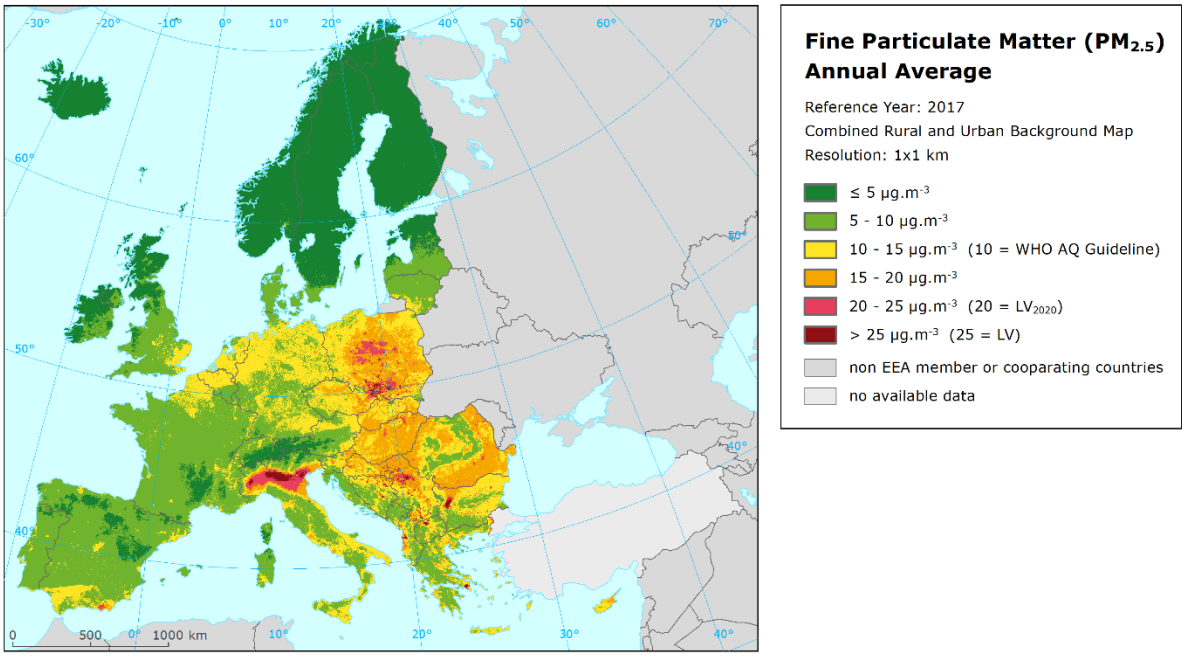

In order to provide more complete information of the air quality across Europe, the final combined map including the measurement data at station points is presented in Map A5.3 of Annex 5.

3.1.2 Population exposure

Table 3.1 gives the population frequency distribution for a limited number of exposure classes calculated on a grid of 1x1 km^2 resolution, as well as the population-weighted concentration for individual countries and for Europe as a whole according to Equation A1.7 of Annex 1. Annex 4 shows details on the ten year evolution of population exposure.

The population exposure is calculated according to Equation A1.6 of Annex I, i.e. it is calculated separately for urban areas directly influenced by traffic and for the background (both rural and urban) areas, in order to better reflect the population exposed to traffic.

In 2017, 74 % of the European and the EU-28 population has been exposed to $PM_{2.5}$ annual mean concentrations above the Air Quality Guideline of 10 $\mu g \cdot m^{-3}$ as defined by the World Health Organization (WHO, 2005). The European wide, resp. EU-28, population exposure exceeding the EU limit value (LV) of 25 $\mu g \cdot m^{-3}$ is about 7 %, resp. 6 %. In Albania, Bosnia & Herzegovina, Bulgaria, Greece, North Macedonia, and Serbia (including Kosovo) more than 25 % of the population suffers from exposures above this limit value; in Croatia, Italy, Montenegro and Poland it is between 5 to 25 %. The indicative Stage 2 limit value LV_{2020} of 20 $\mu g \cdot m^{-3}$ is exceeded for about 15 % (European wide) resp. 13 % (EU-28) of the population. In Albania, Bosnia & Herzegovina, Bulgaria, Croatia, Greece, Hungary, Italy, Montenegro, North Macedonia, Poland, Serbia and Slovakia, a quarter or more of the population is exposed to concentrations above the LV_{2020}. As the current mapping methodology tends to underestimate high values (Annex 3), the exceedance percentages and/or the number of countries with population exposed to concentrations above both the current ALV and the indicative LV_{2020} will most likely be higher.

Table 3.1 Population exposure and population-weighted concentration, $PM_{2.5}$ annual average 2017

Country		Population	$PM_{2.5}$ annual average, exposed population [%]						Population weighted conc. [µg.m^{-3}]
			< LV_{2020}				> LV_{2020}		
			< LV					> LV	
		[inhbs . 1000]	< 5 µg.m^{-3}	5 - 10 µg.m^{-3}	10 - 15 µg.m^{-3}	15 - 20 µg.m^{-3}	20 - 25 µg.m^{-3}	> 25 µg.m^{-3}	
Albania	AL	2 877		2.3	12.2	15.0	37.2	33.3	23.1
Andorra	AD	73		10.5	89.5				12.5
Austria	AT	8 773	0.7	19.1	73.1	7.0			12.3
Belgium	BE	11 352		8.0	84.8	7.2			12.5
Bosnia & Herzegovina	BA	3 510		2.1	20.9	22.2	15.4	39.3	22.6
Bulgaria	BG	7 102		1.4	10.6	22.6	34.3	31.1	22.4
Croatia	HR	4 154		4.7	33.3	23.3	30.0	8.7	17.6
Cyprus	CY	1 201		0.0	21.3	76.1	2.5		15.7
Czechia	CZ	10 579		1.0	22.1	60.9	11.2	4.8	17.1
Denmark	DK	5 749	0.9	95.9	3.2				8.5
Estonia	EE	1 316	36.3	63.7					5.4
Finland	FI	5 503	75.1	24.9					4.4
France (metropolitan)	FR	64 629	0.3	41.2	57.9	0.7			10.6
Germany	DE	82 522	0.0	8.1	88.0	3.9			11.8
Greece	GR	10 768		1.8	8.7	10.2	16.7	62.6	30.0
Hungary	HU	9 798		0.0	4.6	64.5	30.4	0.5	18.8
Iceland	IS	338	50.2	46.2	3.6				5.1
Ireland	IE	4 784	18.5	81.5					6.2
Italy	IT	60 589	0.1	6.5	42.8	22.7	13.4	14.6	17.0
Latvia	LV	1 950	0.5	68.7	19.4	11.5			9.5
Liechtenstein	LI	38	0.1	78.2	21.7				9.4
Lithuania	LT	2 848		44.4	53.7	1.8			10.3
Luxembourg	LU	591		42.6	57.4				10.0
Malta	MT	460		0.3	99.7				11.8
Monaco	MC	38			100.0				13.2
Montenegro	ME	622		8.8	19.7	30.3	34.1	7.1	18.6
Netherlands	NL	17 082		2.3	97.7				11.3
North Macedonia	MK	2 074		0.5	2.4	2.3	12.7	82.1	36.3
Norway	NO	5 258	48.8	46.0	5.3				5.2
Poland	PL	37 973		0.1	9.9	30.9	37.0	22.2	21.4
Portugal (excl. Az., Mad.)	PT	9 809	1.5	70.8	21.8	6.0			9.1
Romania	RO	19 644		0.7	11.8	71.6	14.4	1.5	17.9
San Marino	SM	33		1.4	93.2	5			14.2
Serbia (incl. Kosovo*)	RS	8 824		0.6	5.1	9.0	15.2	70.1	28.3
Slovakia	SK	5 435		0.0	8.3	57.0	32.8	1.9	18.8
Slovenia	SI	2 066		3.0	37.1	41.8	18.1		16.2
Spain (excl. Canarias)	ES	44 373	0.2	26.2	58.1	15.3	0.2	0.0	12.0
Sweden	SE	9 995	59.6	40.4					5.0
Switzerland	CH	8 420	1.1	48.6	49.7	0.6			9.9
United Kingdom (& dep.)	UK	65 844	1.3	60.3	38.3				9.3
Total		**538 993**	**2.8**	**22.9**	**45.1**	**14.3**	**7.7**	**7.2**	**13.8**
			25.8		**59.4**		**14.8**		
EU-28		**506 888**	**2.5**	**23.0**	**46.7**	**14.8**	**7.4**	**5.5**	**13.5**
			25.5		**61.5**		**13.0**		
Kosovo*	KS	1 784		0.2	6.4	9.4	9.9	74.0	28.6
Serbia (excl. Kosovo*)	RS	7 040		0.6	4.8	8.9	16.5	69.1	28.2

(*) under the UN Security Council Resolution 1244/99

Note 1: Turkey not included due to the lack of the rural stations.

Note 2: The percentage value "0.0" indicates that an exposed population exists, but it is small and estimated to be less than 0.05 %. Empty cells mean no population in exposure.

According to EEA CSI004 (EEA, 2019c), about 8 % of the urban population in the EU-28 was exposed to $PM_{2.5}$ concentrations above the LV in 2017. The difference with the estimated 5.5 % in Table 3.1 is because the EEA accounts for the urban population only. Whereas, Table 3.1 provides estimates for the total population, including the population in rural areas, smaller cities and villages. When it comes to the WHO AQ guideline, the EU-28 urban population exposed to concentrations above its recommended value (10 $\mu g \cdot m^{-3}$) in 2017 was estimated at 77 % by CSI004, which is somewhat higher than the total population estimation of 74 % as presented in Table 3.1.

The European-wide population-weighted concentration of the $PM_{2.5}$ annual means is estimated for 2017 at about 14 $\mu g \cdot m^{-3}$ for both Europe as a whole and the EU-28.

Figure 3.1 shows, for the whole mapped area, the population frequency distribution for exposure classes of 1 $\mu g \cdot m^{-3}$. The highest population frequency is found for classes between 10 and 12 $\mu g \cdot m^{-3}$.

Figure 3.1 Population frequency distribution, $PM_{2.5}$ annual average, 2017

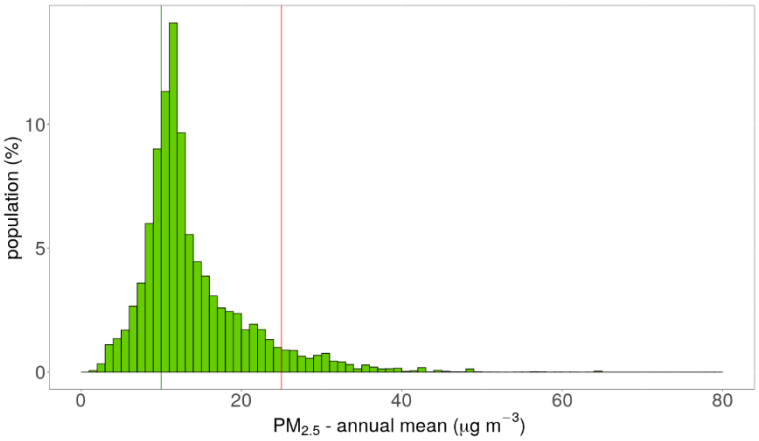

Note: Next to the population distribution shown in graph, it was estimated that 0.005 % of population lived in areas with $PM_{2.5}$ annual average concentration in between 80 and 220 $\mu g.m^{-3}$.

4 Ozone

For ozone, the three health-related indicators *93.2 percentile of maximum daily 8-hour means* (see below), *SOMO35* and *SOMO10*, and the two vegetation-related indicators *AOT40 for vegetation* and *AOT40 for forests* are considered. For the definition of the SOMO35, SOMO10 and AOT40 indicators, see following sections and Annex 2.

The separate rural and urban background health-related indicator fields are calculated at a resolution of 10x10 km^2. Subsequently, the final health-related indicator maps are created by combining rural and urban areas based on the 1x1 km^2 gridded population density map. We present these maps on this 1x1 km^2 grid resolution. The population exposure tables are calculated on the basis of these health-related indicator maps.

The vegetation-related indicator maps are calculated from observations at rural background stations and are representative for rural areas only (assuming urban areas do not cover vegetation). The maps have a resolution of 2x2 km^2. This resolution serves the needs of the EEA Core Set Indicator 005 (EEA, 2019d) on ecosystem exposure to ozone.

Annex 3 provides details on the regression and kriging parameters applied for deriving the maps of the ozone indicators, as well as the uncertainty analysis of the maps. Annex 4 discusses briefly the inter-annual changes observed in the concentration maps and the relevant population and vegetation exposure.

4.1 Ozone – 93.2 percentile of maximum daily 8-hour means

The AQ Directive (EU, 2008) describes the ozone target value (TV) for the protection of human health as "a maximum daily 8-hour mean of 120 $\mu g \cdot m^{-3}$ not to be exceeded on more than 25 times a calendar year, averaged over three years". On an annual basis, it can be evaluated by the indicator 26th highest maximum daily 8-hour mean, which is in principle equivalent to the indicator 93.2 percentile of maximum daily 8-hour means. However, for measurement data these two indicators are equivalent only if no data is missing, which is in general not the case. As shown in de Leeuw (2012), the additional uncertainty related to incomplete time series is substantially smaller when using percentile values instead of the x-th highest value. As in the previous ETC/ACM Technical Papers 2016/6 and 2017/7, we express this ozone indicator as the 93.2 percentile of maximum daily 8-hour means instead of the formerly used 26th highest maximum daily 8-hour mean.

4.1.1 Concentration map

Map 4.1 presents the final combined map for 93.2 percentile of the maximum daily 8-hour means as a result of combining the separate rural and urban interpolated maps following the procedures as described in Annex 1 (for a more detailed description, see Horálek et al., 2007, 2010). The supplementary data used are EMEP model output, altitude and surface solar radiation for rural areas and EMEP model output, wind speed and surface solar radiation for urban areas (Annex 3).

In the final combined map the red and dark red areas show values above the TV threshold of 120 $\mu g \cdot m^{-3}$ on more than 25 days in 2017. Note that in the AQ Directive (EU, 2008) the target value is actually defined as 120 $\mu g \cdot m^{-3}$ not to be exceeded on more than 25 days per calendar year *averaged over three years*. Here only 2017 data are presented, and no three-year average is calculated.

The map shows that in 2017 values above 120 $\mu g \cdot m^{-3}$ on more than 25 days occur mainly in the Alps, most of Italy, southern France, central and south-eastern Spain, most of Greece, all the coastal area

around the Adriatic sea, southern Turkey and parts of Cyprus. In general, the southern parts of Europe show higher ozone concentrations than the northern parts, which is caused mainly by higher solar radiation and temperature in these areas. An exception is north-eastern Romania where comparatively low values are observed. Furthermore, in general, higher levels of ozone do also occur more frequently in mountainous areas than in lowlands.

The relative mean uncertainty of the 2017 map of the 93.2 percentile of maximum daily 8-h ozone means is about 9 % for both rural and urban areas (Annex 3).

In order to provide more complete information of the air quality across Europe, the final combined map including the measurement data at station points is presented in Map A5.4 of Annex 5.

Map 4.1 Concentration map of ozone indicator 93.2 percentile of maximum daily 8-hour means, 2017

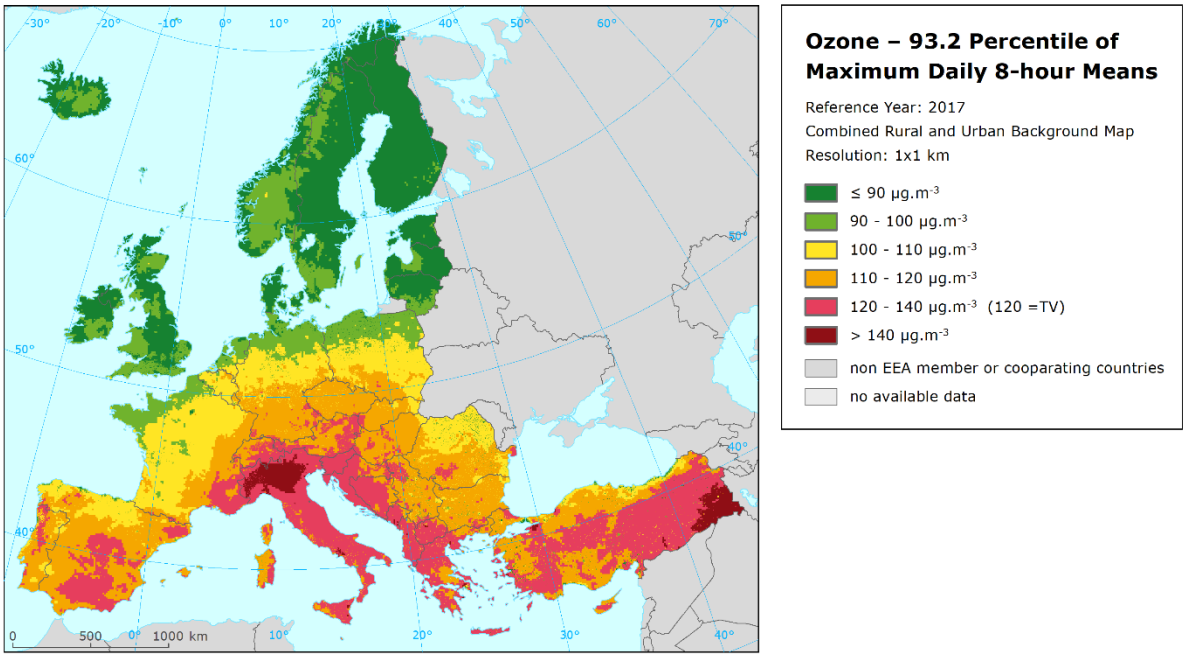

4.1.2 Population exposure

Table 4.1 gives, for the 93.2 percentile of maximum daily 8-hour means, the population frequency distribution for a limited number of exposure classes, as well as the population-weighted concentration for individual countries and for Europe as a whole. Annex 4 presents the twelve-years evolution of population exposure.

It has been estimated that in 2017 about 13 % of both the European population (either including or without Turkey) and the EU-28 lived in areas where the ozone concentration exceeded the health related target value threshold (TV of 120 µg·m^{-3}). According to CSI004 (EEA, 2019c), about 14 % of the urban population in the EU-28 was exposed to ozone above the target value threshold in 2017. It should be mentioned that the CSI004 refers only to the population in cities for which ozone measurement data is available and does not take into account population in rural areas, where ozone concentrations tend to be higher.

Table 4.1 Population exposure and population-weighted concentrations, ozone indicator 93.2 percentile of maximum daily 8-hour means, 2017

Country		Population	Ozone, 93.2 percentile of max. daily 8-h means, exposed population [%]						Population-weighted conc.
			< TV				> TV		
		[inhbs . 1000]	< 90 µg.m^{-3}	90 - 100 µg.m^{-3}	100 - 110 µg.m^{-3}	110 - 120 µg.m^{-3}	120 - 140 µg.m^{-3}	> 140 µg.m^{-3}	[µg.m^{-3}]
Albania	AL	2 877		0.3	12.2	57.6	29.8	0.0	116.9
Andorra	AD	73			76.8	22.1	1.1		111.2
Austria	AT	8 773			5.4	63.7	30.9		117.3
Belgium	BE	11 352	0.2	26.7	66.4	6.7			102.6
Bosnia & Herzegovina	BA	3 510			0.0	30.3	69.7		122.1
Bulgaria	BG	7 102	2.1	46.4	38.8	12.3	0.5		102.2
Croatia	HR	4 154			0.0	32.5	67.1	0.3	123.2
Cyprus	CY	1 201		28.6	54.7	12.1	4.6		103.7
Czechia	CZ	10 579			26.3	72.9	0.8		112.0
Denmark	DK	5 749	88.9	10.9	0.1				87.2
Estonia	EE	1 316	95.6	4.4	0.0				84.8
Finland	FI	5 503	99.4	0.6					83.0
France (metropolitan)	FR	64 629	8.8	22.7	39.9	23.1	5.4	0.0	104.4
Germany	DE	82 522	3.7	19.7	48.8	27.4	0.4		105.3
Greece	GR	10 768	5.6	33.5	41.0	10.4	9.4	0.1	103.7
Hungary	HU	9 798			6.8	91.0	2.2		114.8
Iceland	IS	338	100	0.3					80.4
Ireland	IE	4 784	83	16.8	0.0				87.0
Italy	IT	60 589	0.0	2.3	8.2	23.1	38.3	28.1	129.2
Latvia	LV	1 950	64.0	34.0	2.0				87.4
Liechtenstein	LI	38				80.3	19.7		119.9
Lithuania	LT	2 848	92.0	8.0	0.0				84.5
Luxembourg	LU	591		23.7	67.1	9.2			104.4
Malta	MT	460			94.1	4.3	1.6		104.3
Monaco	MC	38					100		120.2
Montenegro	ME	622			12.3	40.2	47.0	0.4	118.3
Netherlands	NL	17 082	10.9	61.3	27.5	0.2			96.3
North Macedonia	MK	2 074		24.9	67.4	4.2	3.5	0.1	102.6
Norway	NO	5 258	78.7	21.2	0.0				86.6
Poland	PL	37 973	10.9	22.8	42.1	21.7	2.5		103.2
Portugal (excl. Az., Mad.)	PT	9 809	4.7	15.2	48.9	27.6	3.6		105.8
Romania	RO	19 644	11.1	25.4	41.2	21.2	1.1		102.6
San Marino	SM	33					100.0		128.1
Serbia (incl. Kosovo*)	RS	8 824	3.1	46.8	24.1	24.3	1.7		102.3
Slovakia	SK	5 435			25.1	65.2	9.6		113.5
Slovenia	SI	2 066				5.4	94.5	0.1	125.5
Spain (excl. Canarias)	ES	44 373	5.6	13.5	17.6	43.2	20.1		110.9
Sweden	SE	9 995	87.0	13.0	0.1				86.1
Switzerland	CH	8 420			2.0	83.1	11.8	3.1	117.1
Turkey	TR	79 815	33.7	15.9	16.8	17.4	14.6	1.6	100.8
United Kingdom (& dep.)	UK	65 844	89.9	9.8	0.2	0.0			84.5
Total		**618 808**	**22.3**	**16.7**	**24.6**	**23.1**	**10.3**	**3.0**	**104.5**
			38.9		**47.8**		**13.3**		
Total without Turkey		**538 993**	**20.7**	**16.8**	**25.7**	**23.9**	**9.7**	**3.2**	**105.0**
			37.5		**49.6**		**12.9**		
EU-28		**506 888**	**21.1**	**16.7**	**26.5**	**23.1**	**9.3**	**3.4**	**104.8**
			37.8		**49.6**		**12.7**		
Kosovo*	KS	1 784		44.6	35.4	18.0	2.1		103.1
Serbia (excl. Kosovo*)	RS	7 040	3.9	47.4	21.3	25.8	1.6		102.0

(*) under the UN Security Council Resolution 1244/99

Note: The percentage value "0.0" indicates that an exposed population exists, but it is small and estimated to be less than 0.05 %. Empty cells mean no population in exposure.

In the following countries at least 25 % of the population suffered exposures above the TV threshold: Albania, Austria, Bosnia & Herzegovina, Croatia, Italy, Montenegro and Slovenia. As the current mapping methodology tends to underestimate high values due to interpolation smoothing (Annex 3), the exceedance percentage is most likely somewhat underestimated; additional population exposure above the TV threshold might be expected in additional countries: Czechia, Hungary, Slovakia, Spain and Switzerland. The reason is that in these countries the estimated percentage population exposed to the concentrations above 110 µg·m^{-3} is considerable.

The overall European and EU-28 population-weighted ozone concentrations in terms of the 93.2 percentile of maximum daily 8-hour means were estimated for 2017 as being 105 µg·m^{-3}, which is the second lowest of the thirteen-years period 2005 – 2017 (Table 6.3), together with the year 2016.

Figure 4.1 shows, for the whole mapped area, the population frequency distribution for exposure classes of 2 µg·m^{-3}. The highest population frequency is found for classes between 100 and 118 µg·m^{-3}.

Figure 4.1 Population frequency distribution, O_3 indicator 93.2 percentile of maximum daily 8-hour means, 2017

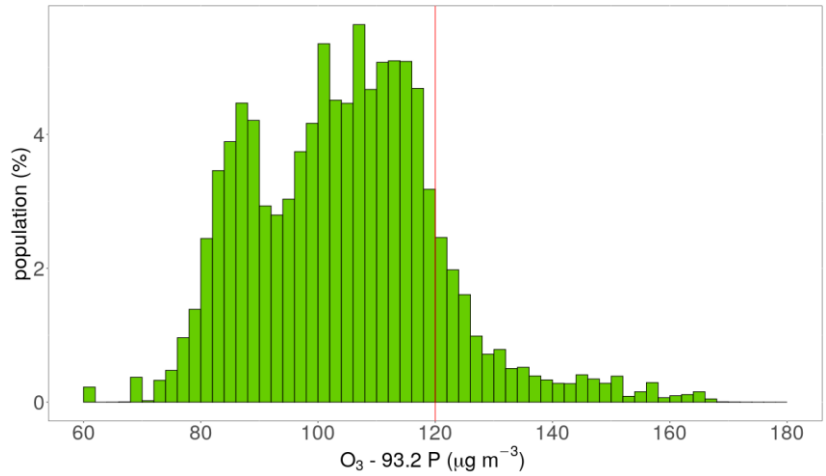

4.2 Ozone – SOMO35 and SOMO10

SOMO35 is the annually accumulated ozone maximum daily 8-hourly means in excess of 35 ppb (i.e. 70 µg·m^{-3}). It is not subject to any of the EU air quality directives and there are no limit or target values defined. Comparing the 93.2 percentile of maximum daily 8-hour means versus the SOMO35 for all background stations shows no simple relationship between the two indicators. However, it seems that the target value of the 93.2 percentile of maximum daily 8-hour means (being 120 µg·m^{-3}) is related approximately with a SOMO35 value in the range of 6 000 – 8 000 µg·m^{-3}·d. This comparison motivates a somewhat arbitrarily chosen threshold of 6 000 µg·m^{-3}·d, in order to facilitate the discussion of the observed distributions of SOMO35 levels in their spatial and temporal context. This threshold is used in this and previous papers (Horálek et al. 2017b, and the references cited therein) when dealing with the population exposure estimates.

SOMO10 is the annually accumulated ozone maximum daily 8-hourly means in excess of 10 ppb (i.e. 20 µg·m^{-3}). We introduce this indicator for the first time, due to its link to the health impact assessment. Be it noted that the WHO recommends to use the SOMO10 as an alternative to the SOMO35 when estimating the health impact of ozone (WHO, 2013).

4.2.1 Concentration maps

Map 4.2 presents the final combined map for SOMO35 as a result of combining the separate rural and urban interpolated maps following the same procedure as for 93.2 percentile of the maximum daily 8-hour means. The mapping details and the uncertainty analysis are presented in Annex 3. In the final combined map the red and dark red areas show values above 8 000 µg·m^{-3}·d, while the orange areas show values above 6 000 µg·m^{-3}·d.

Like in the case of the 93.2 percentile of the maximum daily 8-hour means, the southern parts of Europe show higher ozone SOMO35 concentrations than the northern parts. Higher levels of ozone do also occur more frequently in mountainous areas south of 50 degrees latitude than in lowlands. The relative mean uncertainty of the 2017 map of the SOMO35 is about 30 % for both rural and urban areas (see Annex 3).

Map 4.2 Concentration map of ozone indicator SOMO35, 2017

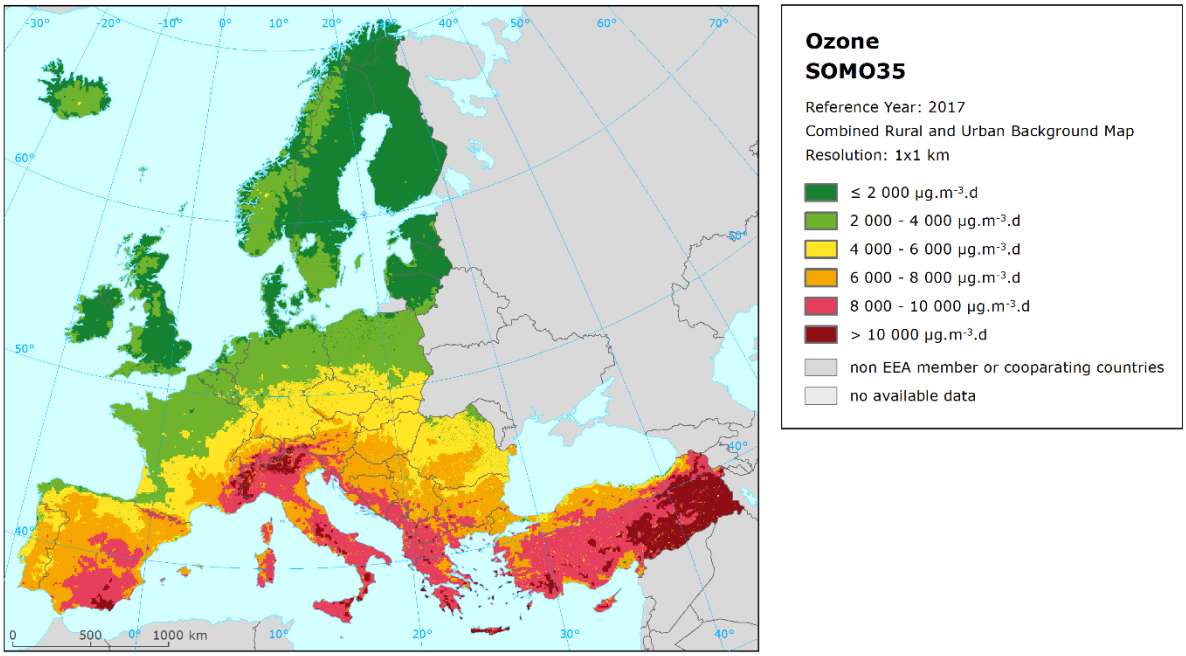

Map 4.3 presents the final combined map for SOMO10, as a results of the similar mapping procedure as in the cases of other ozone health-related indicators. The boundaries of concentration classes have been chosen quite arbitrary, in order to reflect the concentration distribution of this indicator. In the final combined map the red and dark red areas show values above 24 000 µg·m^{-3}·d.

The spatial distribution of the SOMO10 concentrations are quite similar like on the case of the SOMO35, i.e. higher values in the southern parts of Europe compared to its southern parts, and also in the mountainous areas compared to the lowlands. The relative mean uncertainty of the 2017 map of the SOMO10 is about 11 % for rural areas and about 13 % for urban areas (see Annex 3).

In order to provide more complete information of the air quality across Europe, the final combined maps including the ozone indicators SOMO35 and SOMO10 values at station points, based on the measurement data are presented in Maps A5.5 and A5.6, respectively, of Annex 5.

Map 4.3 Concentration map of ozone indicator SOMO10, 2017

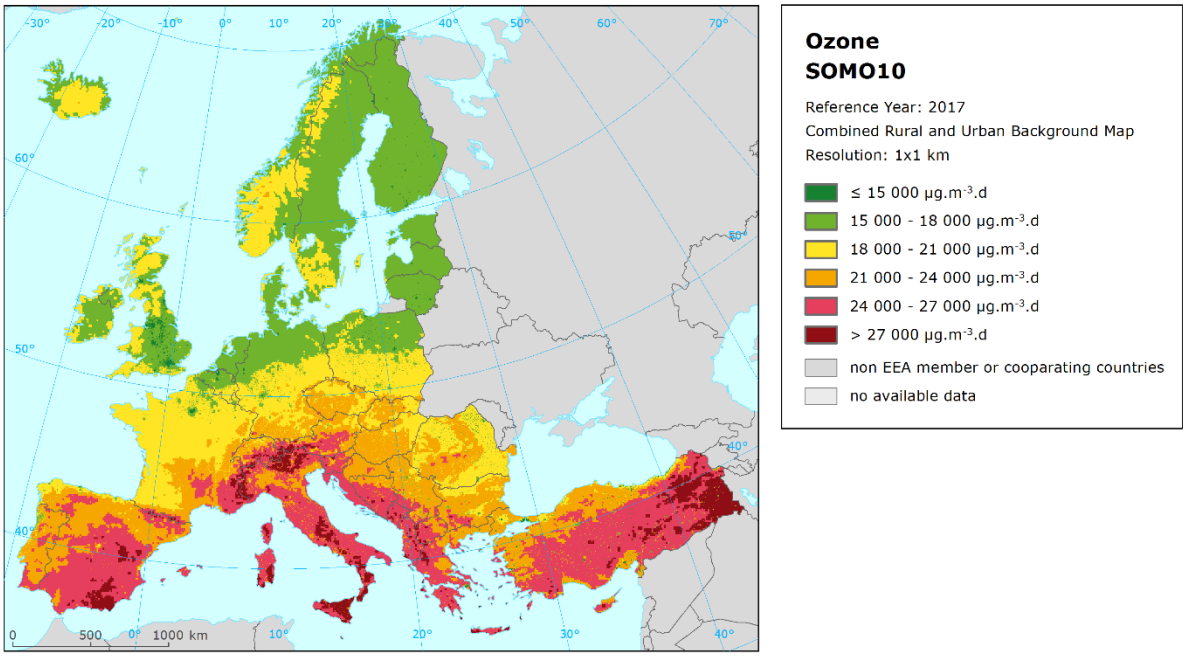

4.2.2 Population exposure

Table 4.2 gives for SOMO35 the population frequency distribution for a limited number of exposure classes, as well as the population-weighted concentration for individual countries and for Europe as a whole. Annex 4 shows details on the twelve-year evolution of population exposure.

Table 4.3 presents the same table for SOMO10.

It has been estimated that in 2017 about 20 % of the European population (including Turkey), resp. about 19 % of both European population without Turkey and the EU-28 population, lived in areas with SOMO35 values above 6 000 µg·m^{-3}·d (see above on the motivation of this criterion).

In 2017, like in the previous several years, the northern and north-western European countries do not have inhabitants exposed to SOMO35 concentrations above 6 000 µg·m^{-3}·d, and almost no inhabitants above 4 000 µg·m^{-3}·d. Most of the countries in southern and south-eastern Europe show exposures above or well above 6 000 µg·m^{-3}·d, most notably (at least 20 % of population) Albania, Bosnia-Herzegovina, Croatia, Cyprus, Greece, Italy, Malta, Montenegro, Slovenia, Spain, and Turkey. This can also be observed in Map 4.2.

In 2017, the total European, resp. the EU-28, population-weighted ozone concentrations, in terms of SOMO35, were estimated to be around 4 000 µg·m^{-3}·d, resp. 3 800 µg·m^{-3}·d. For Europe without Turkey, it was 3 900 µg·m^{-3}·d, which is the third lowest in the thirteen years period 2005 – 2017 (Table 6.3).

The total European, resp. the EU-28, population-weighted ozone concentrations, in terms of SOMO10, were estimated to be about 18 400 µg·m^{-3}·d, resp. 18 500 µg·m^{-3}·d.

Table 4.2 Population exposure and population-weighted concentrations, ozone indicator SOMO35, 2017

Country		Population	Ozone, SOMO35, exposed population [%]						Population-weighted conc.
			< 2000	2000 - 4000	4000 - 6000	6000 - 8000	8000 - 10000	> 10000	
		[inhbs.1000]	µg.m^{-3}.d	µg.m^{-3}.d	µg.m^{-3}.d	µg.m^{-3}.d	µg.m^{-3}.d	µg.m^{-3}.d	[µg.m^{-3}.d]
Albania	AL	2 877			16.3	66.3	17.2	0.2	6 898
Andorra	AD	73			96.7	2.5	0.8		5 182
Austria	AT	8 773		6.6	76.2	16.5	0.7	0.0	5 311
Belgium	BE	11 352	18.5	81.4	0.1				2 553
Bosnia & Herzegovina	BA	3 510			6.4	89.2	4.3		6 967
Bulgaria	BG	7 102	0.3	64.0	26.3	8.9	0.5	0.0	3 938
Croatia	HR	4 154			13.2	65.5	21.0	0.3	7 110
Cyprus	CY	1 201			70.9	16.6	12.0	0.5	6 029
Czechia	CZ	10 579		32.1	67.7	0.2			4 307
Denmark	DK	5 749	81.4	18.5	0.0				1 711
Estonia	EE	1 316	94.6	5.4					1 462
Finland	FI	5 503	99.3	0.7					1 153
France (metropolitan)	FR	64 629	9.4	54.8	25.5	8.3	1.9	0.0	3 809
Germany	DE	82 522	8.2	70.2	21.3	0.3	0.0		3 182
Greece	GR	10 768		36.6	41.5	11.5	8.3	2.1	4 858
Hungary	HU	9 798		2.0	89.2	8.8			5 010
Iceland	IS	338	99.1	0.9					782
Ireland	IE	4 784	90.7	9.2	0.0				1 418
Italy	IT	60 589		2.4	13.2	45.2	37.0	2.2	7 405
Latvia	LV	1 950	85.5	14.5					1 557
Liechtenstein	LI	38			92.9	7.0	0.1		5 045
Lithuania	LT	2 848	93.7	6.3	0.0				1 417
Luxembourg	LU	591		99.3	0.7				3 001
Malta	MT	460			73.7	23.9	1.8	0.6	6 174
Monaco	MC	38					100.0		8 223
Montenegro	ME	622			15.7	68.3	16.0	0.0	6 787
Netherlands	NL	17 082	29.1	70.8	0.1				2 281
North Macedonia	MK	2 074		50.7	40.9	6.4	2.0	0.0	4 248
Norway	NO	5 258	89.6	10.4					1 448
Poland	PL	37 973	16.8	58.0	25.2	0.0			3 111
Portugal (excl. Az., Mad.)	PT	9 809	9.7	41.4	40.3	8.5	0.1		3 914
Romania	RO	19 644	10.8	39.0	46.3	3.9			3 885
San Marino	SM	33				100.0			7 192
Serbia (incl. Kosovo*)	RS	8 824	0.1	44.1	43.0	12.3	0.5	0.0	4 418
Slovakia	SK	5 435		6.9	90.9	2.2			4 861
Slovenia	SI	2 066			4.8	81.8	13.4		7 035
Spain (excl. Canarias)	ES	44 373	5.9	18.3	25.9	41.3	8.4	0.2	5 600
Sweden	SE	9 995	82.4	17.6	0.0				1 641
Switzerland	CH	8 420		1.8	85.1	9.8	3.1	0.1	5 281
Turkey	TR	79 815	14.8	28.5	28.9	9.8	11.5	6.5	4 864
United Kingdom (& dep.)	UK	65 844	92.4	7.5	0.1				1 218
Total		**618 808**	**22.1**	**33.8**	**23.9**	**12.7**	**6.4**	**1.1**	**4 006**
				79.9			**20.1**		
Total without Turkey		**538 993**	**23.1**	**34.5**	**23.3**	**13.0**	**5.7**	**0.3**	**3 890**
				80.9			**19.1**		
EU-28		**506 888**	**23.7**	**35.5**	**22.3**	**12.3**	**5.9**	**0.3**	**3 838**
				81.5			**18.5**		
Kosovo*	KS	1 784		21.7	58.1	19.2	1.1	0.0	4 930
Serbia (excl. Kosovo*)	RS	7 040	0.1	49.6	39.3	10.6	0.4		4 293

(*) under the UN Security Council Resolution 1244/99

Note: The percentage value "0.0" indicates that an exposed population exists, but it is small and estimated to be less than 0.05 %. Empty cells mean no population in exposure.

Table 4.3 Population exposure and population-weighted concentrations, ozone indicator SOMO10, 2017

Country		Population	Ozone, SOMO35, exposed population [%]						Population-weighted conc.
			< 15000	15000 - 18000	18000 - 21000	21000 - 24000	24000 - 27000	> 27000	
		[inhbs.1000]	µg.m^{-3}.d	µg.m^{-3}.d	µg.m^{-3}.d	µg.m^{-3}.d	µg.m^{-3}.d	µg.m^{-3}.d	[µg.m^{-3}.d]
Albania	AL	2 877			13.6	64.2	21.8	0.5	22 664
Andorra	AD	73				98.2	1.3	0.6	21 462
Austria	AT	8 773		13.5	64.3	18.4	3.7	0.1	20 021
Belgium	BE	11 352	19.6	76.7	3.7				16 020
Bosnia & Herzegovina	BA	3 510			20.0	70.1	9.8	0.1	22 177
Bulgaria	BG	7 102	2.7	66.2	23.7	7.1	0.3	0.0	17 468
Croatia	HR	4 154			12.2	57.7	30.0	0.1	22 768
Cyprus	CY	1 201		30.0	52.5	11.1	6.2	0.2	19 104
Czechia	CZ	10 579		1.9	90.8	7.3	0.0		19 314
Denmark	DK	5 749		91.0	9.0				17 148
Estonia	EE	1 316		99.4	0.6				15 963
Finland	FI	5 503	40.8	59.0	0.2				15 337
France (metropolitan)	FR	64 629	9.7	23.2	49.7	13.7	3.6	0.1	18 799
Germany	DE	82 522	1.7	61.4	35.2	1.7	0.0	0.0	17 546
Greece	GR	10 768	30.3	25.6	22.9	12.3	8.5	0.6	17 926
Hungary	HU	9 798		0.2	87.8	12.0			19 508
Iceland	IS	338	53.0	46.1	0.9				15 269
Ireland	IE	4 784	6.8	83.7	9.5	0.0			16 485
Italy	IT	60 589			5.7	71.4	21.8	1.2	23 201
Latvia	LV	1 950	18.7	79.9	1.4				16 017
Liechtenstein	LI	38			92.0	7.9	0.1		19 564
Lithuania	LT	2 848	45.3	54.4	0.3				15 430
Luxembourg	LU	591		86.4	12.9	0.6			17 017
Malta	MT	460				74.5	24.3	1.2	23 809
Monaco	MC	38					100.0		24 960
Montenegro	ME	622			15.1	62.6	21.9	0.4	22 442
Netherlands	NL	17 082	4.3	91.5	4.2	0.0			16 674
North Macedonia	MK	2 074		60.7	31.1	6.1	2.0	0.1	18 084
Norway	NO	5 258	11.4	79.7	8.9	0.0			16 315
Poland	PL	37 973	11.3	58.5	29.9	0.3	0.0		17 116
Portugal (excl. Az., Mad.)	PT	9 809		28.5	40.9	28.6	2.1		19 548
Romania	RO	19 644	10.8	40.4	43.9	4.9	0.0		17 849
San Marino	SM	33				100.0			23 209
Serbia (incl. Kosovo*)	RS	8 824	0.1	50.5	34.4	13.4	1.7	0.0	18 367
Slovakia	SK	5 435		0.4	92.8	6.7	0.0		19 665
Slovenia	SI	2 066			37.9	40.5	21.4	0.2	22 283
Spain (excl. Canarias)	ES	44 373	1.8	12.1	25.3	35.7	24.2	0.9	21 584
Sweden	SE	9 995	3.5	89.3	7.2				16 762
Switzerland	CH	8 420		1.8	82.0	13.6	2.4	0.1	19 973
Turkey	TR	79 815	35.5	33.9	5.0	9.9	12.9	2.7	17 435
United Kingdom (& dep.)	UK	65 844	57.4	39.0	3.4	0.1			14 875
Total		**618 808**	**14.7**	**36.6**	**25.5**	**16.0**	**6.7**	**0.5**	**18 417**
				76.8			**23.2**		
Total without Turkey		**538 993**	**11.9**	**37.0**	**28.3**	**16.8**	**5.8**	**0.2**	**18 551**
				77.1			**22.9**		
EU-28		**506 888**	**12.5**	**37.3**	**27.7**	**16.4**	**5.9**	**0.2**	**18 500**
				77.5			**22.5**		
Kosovo*	KS	1 784		30.6	47.3	18.3	3.9	0.0	19 388
Serbia (excl. Kosovo*)	RS	7 040	0.1	55.3	31.2	12.2	1.2		18 118

(*) under the UN Security Council Resolution 1244/99

Note: The percentage value "0.0" indicates that an exposed population exists, but it is small and estimated to be less than 0.05 %. Empty cells mean no population in exposure.

Figure 4.2 shows, for the whole mapped area, the frequency distribution of SOMO35 for population exposure classes of 250 µg·m^{-3}.d. The highest frequencies are found for classes between 1500 and 5000 µg·m^{-3}·d. For exposure classes above 5000 µg·m^{-3}.d a decline is seen.

Figure 4.2 Population frequency distribution, ozone indicator SOMO35, 2017

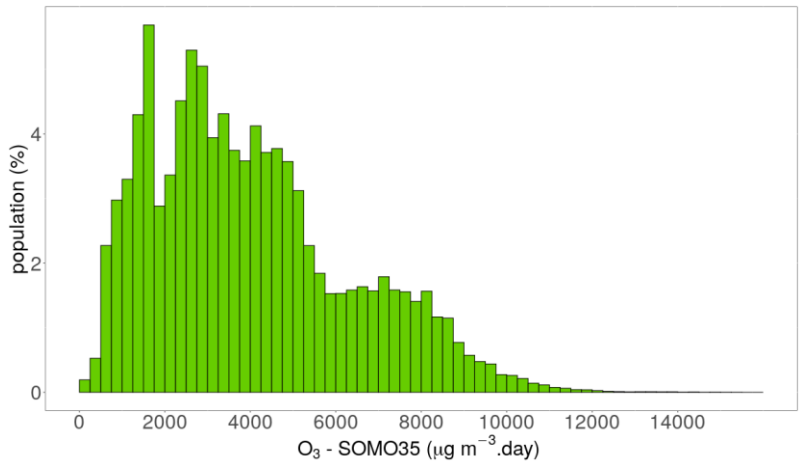

Figure 4.3 shows the population frequency distribution of SOMO10 for population exposure classes of 500 µg·m^{-3}.d. The graph shows the highest frequencies for classes between 15 000 and 20 000 µg·m^{-3}·d.

Figure 4.3 Population frequency distribution, ozone indicator SOMO10, 2017

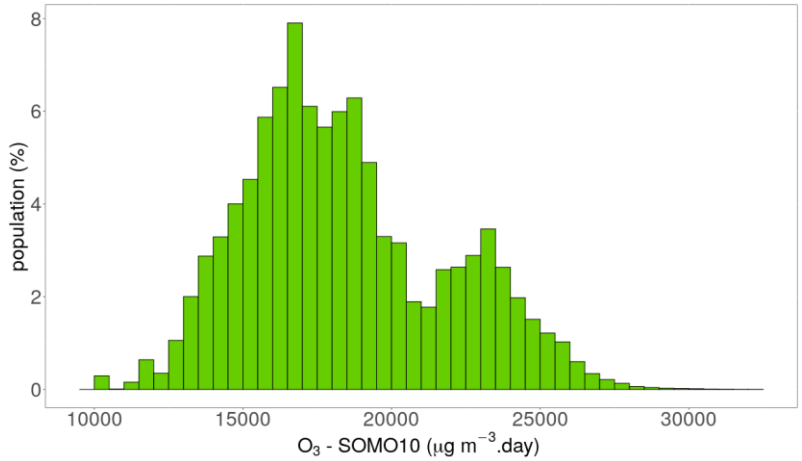

4.3 Ozone – AOT40 vegetation and AOT40 forests

In the Ambient Air Quality Directive (EU, 2008) a target value (TV) and a long-term objective (LTO) for the *protection of vegetation* from high ozone concentrations accumulated during the growing season have been defined. TV and LTO are specified using "accumulated ozone exposure over a threshold of 40 parts per billion" (AOT40). This is calculated as a sum of the difference between hourly concentrations greater than 80 µg·m^{-3} (i.e. 40 parts per billion) and 80 µg·m^{-3}, using only observations between 08:00 and 20:00 Central European Time (CET) each day, calculated over three months from 1 May to 31 July. The TV is 18 000 µg·m^{-3}·h (averaged over five years) and the LTO is 6 000 µg·m^{-3}·h.

Note that the term *vegetation* as used in the Air Quality Directive (EU, 2008) is not further defined. Nevertheless, the target value used in the directive is the same as the critical load used in the Mapping Manual (UNECE, 2004) for "agricultural crops", so we have interpreted the term *vegetation* in the AQ directive as primarily agricultural crops. Therefore, the exposure of *agricultural crops* has been evaluated here based on the AOT40 for vegetation as defined in the AQ directive and the agricultural

areas, defined as the CORINE Land Cover level-1 class *2 Agricultural areas* (encompassing the level-2 classes *2.1 Arable land, 2.2 Permanent crops, 2.3 Pastures* and *2.4 Heterogeneous agricultural areas)*, see Section 4.3.2. Note that in addition to these agricultural areas there are several other CLC classes that could be considered "vegetation", namely level-2 classes *1.4 Artificial, non-agricultural vegetated areas* (encompassing the level-3 classes *1.4.1 Green urban areas* and *1.4.2 Sport and leisure facilities*), *3.1 Forests* (see below) and 3.*2 Scrub and/or herbaceous vegetation associations*.

Next to the AOT40 for vegetation protection, the AQ Directive (EU, 2008) defines also the AOT40 for *forest protection*, which is calculated similarly as the AOT40 for vegetation, but is summed over six months from 1 April to 30 September. For AOT40 for forests there is no TV defined. However, there is a critical level (CL) established by UNECE (2004). This critical level is set at 10 000 $\mu g \cdot m^{-3} \cdot h$.

For the exposure of forests evaluation, the CLC level-2 class *3.1 Forests* has been used.

The ecosystem based accumulative ozone indicators described in this section are specifically prepared for calculation of the EEA Core Set Indicator 005 (EEA, 2019d). For the estimation of the vegetation and forested area exposure to accumulated ozone, the maps in this section are created on a grid of 2x2 km^2 resolution. The exposure frequency distribution outcomes are based on the overlay with the 100x100 m^2 grid resolution of the CLC2016 land cover classes.

4.3.1 Concentration maps

The interpolated maps of AOT40 for vegetation and AOT40 for forests are created for rural areas only, as urban areas are considered not to represent agricultural or forested areas. These maps are therefore applicable to rural areas only, and as such they are based on AOT40 data derived from rural background station observations only. These AOT40 monitoring data are combined in the mapping with the supplementary data sources EMEP model output, altitude and surface solar radiation. These supplementary data sources are the same as those selected at the human health related ozone indicators.

Map 4.4 presents the final map of AOT40 for *vegetation* in 2017. Note that in Directive 2008/50/EC the target value is actually defined as 18 000 $\mu g \cdot m^{-3} \cdot h$ *averaged over five years*. Here only 2017 data are presented, and no five-year average is calculated.

The areas in the map with concentrations above the target value (TV) threshold of 18 000 $\mu g \cdot m^{-3} \cdot h$, are marked in red and dark red. The areas below the long term objective (LTO) are marked in green. The high and very high AOT40 levels for vegetation do occur specifically in southern, south-western and south-eastern regions of Europe. The relative mean uncertainty of the 2017 map of the AOT40 for vegetation is about 34 % (Annex 3).

Map 4.5 presents the final map of AOT40 for *forests* in 2017. The areas in the map with concentrations above the critical level (CL) defined by UNECE (2004) are marked in yellow, orange, red and dark red. One can see large European forested areas exceeding this level.

Like for the AOT40 for vegetation indicator, the highest levels of the AOT40 for forests are found in the south-western, southern and south-eastern European region. Nevertheless, values above the CL are found everywhere in Europe except in most of the Atlantic areas, the Northern region and the rest of the coastal areas of the Baltic sea. The relative mean uncertainty of the 2017 map of the AOT40 for forests is about 35 % (Annex 3).

Map 4.4 Concentration map of O_3 indicator AOT40 for vegetation, rural map, 2017

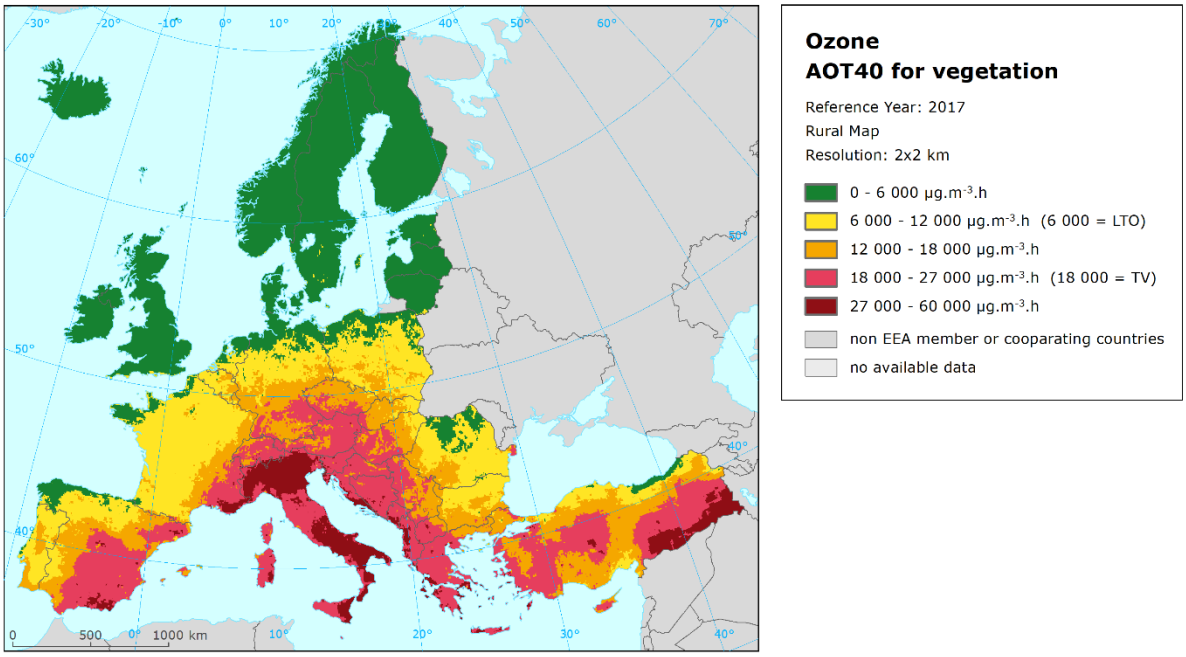

In order to provide more complete information of the air quality across Europe, the AOT40 maps including the AOT40 values based on the actual rural background measurement data at station points are presented in Maps A5.7 and A5.8 of Annex 5.

Map 4.5 Concentration map of ozone indicator AOT40 for forests, rural map, 2017

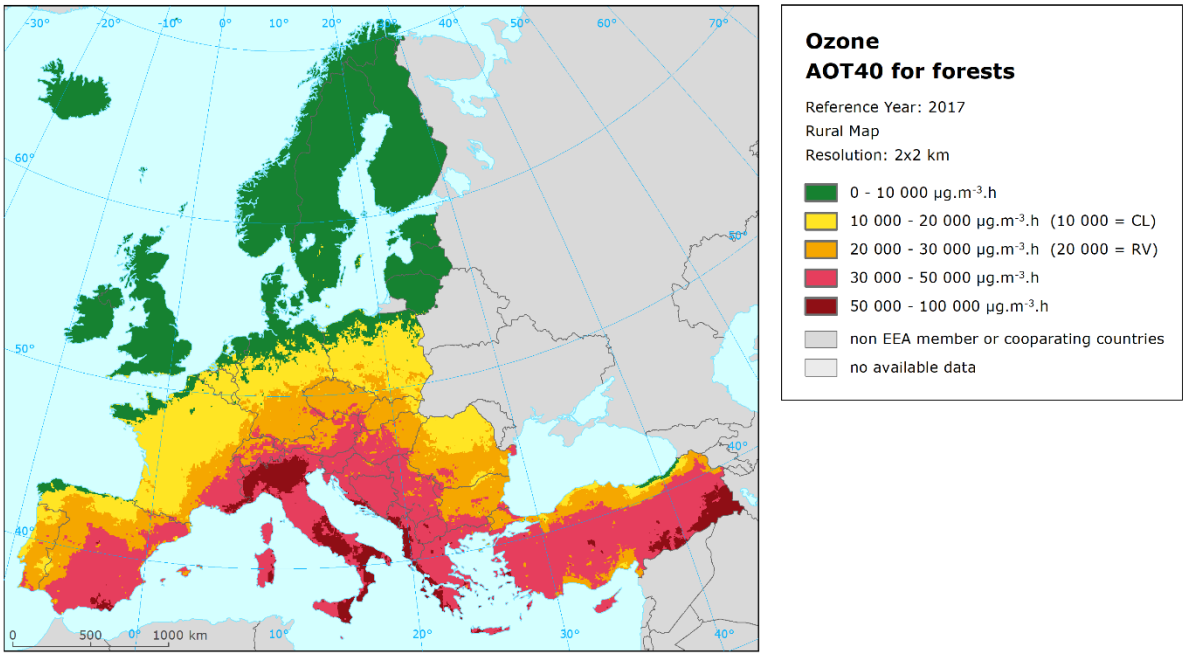

4.3.2 Vegetation exposure

Agricultural crops

The rural map with the ozone indicator AOT40 for vegetation has been combined with the land cover CLC2012 map. Following a similar procedure as described in Horálek et al. (2007), the exposure of agricultural areas (as defined above) has been calculated at the country-level.

Table 4.3 gives the absolute and relative agricultural area for each country and for four European regions where the ozone target value (TV) threshold and long-term objective (LTO) for protection of vegetation as defined in the AQ Directive (EU, 2008) are exceeded. The frequency distribution of the agricultural area over some exposure classes per country is presented as well. The table indicates the country grouping with corresponding colours of the region *Northern Europe*: Denmark, Estonia, Finland, Latvia, Lithuania, Norway, and Sweden. *North-western Europe*: Belgium, France north of 45 degrees latitude, Ireland, Iceland, Luxembourg, the Netherlands, and United Kingdom. *Central and Eastern Europe*: Austria, Bulgaria, Czechia, Germany, Hungary, Liechtenstein, Poland, Romania, Slovakia and Switzerland. *Southern Europe*: Albania, Bosnia-Herzegovina, Croatia, Cyprus, France south of 45 degrees latitude, Greece, Italy, Malta, Monaco, Montenegro, North Macedonia, Portugal, San Marino, Serbia (including Kosovo under the UN Security Council Resolution 1244/99), Slovenia, Spain and Turkey. Table 4.3 illustrates that in 2017, about 28 % of all European agricultural land was exposed to ozone exceeding the target value (TV) of 18 000 $\mu g \cdot m^{-3} \cdot h$. For the areas excluding Turkey, it was about 24 %, which is the fifth lowest percentage of the thirteen-year period 2005 – 2017, see Table 6.4.

Considering the long-term objective (LTO) of 6 000 $\mu g \cdot m^{-3} \cdot h$ the total European area in excess is about 77 %. For the areas excluding Turkey, it is 73 %, which is the lowest for this thirteen year period (Table 6.4). Iceland, together with Ireland, Finland and the most of Estonia, Lithuania and Norway are the areas with ozone levels not being in excess of the LTO. In Albania, Austria, Bosnia & Herzegovina, Croatia, Greece, Italy, Malta, Montenegro, North Macedonia, Slovenia, Switzerland and Turkey more than half of their agricultural area experienced exposures above the TV threshold in 2017.

Table 4.3 Agricultural area exposure and exceedance and agricultural-weighted concentrations, ozone indicator AOT40 for vegetation, 2017

Country	Agricultural Area, 2017					Percentage of agricultural area, 2017 [%]					Agricult. - weighted conc.
	Total area	> LTO (6 000 µg.m^{-3}.h)		> TV (18 000 µg.m^{-3}.h)		< 6 000	6 000 - 12 000	12 000 - 18 000	18 000 - 27 000	> 27 000	
	[km^2]	[km^2]	[%]	[km^2]	[%]	µg.m^{-3}.h	µg.m^{-3}.h	µg.m^{-3}.h	µg.m^{-3}.h	µg.m^{-3}.h	[µg.m^{-3}.h]
Albania	8041	8041	100	8020	100			0.3	72.9	26.8	25 124
Austria	26862	26862	100	23553	87.7			12.3	87.7	0.0	20 335
Belgium	17544	17413	99.2			0.8	80.6	18.6			10 386
Bosnia-Herzegovina	17830	17830	100	17492	98.1			1.9	96.1	2.0	21 525
Bulgaria	57550	57252	99.5	196	0.3	0.5	69.0	30.2	0.3		10 597
Croatia	22535	22535	100	20433	90.7			9.3	79.5	11.2	22 092
Cyprus	4304	4304	100	1842	43			57.2	42.2	0.6	17 882
Czechia	44966	44966	100	12545	27.9		2.6	69.5	27.9		16 596
Denmark (excl. Faroes)	31924	718	2.2			97.8	2.2	0.0			2 270
Estonia	14318	1	0.0			100.0	0.0				984
Finland	28370					100.0					348
France (metropolitan)	325895	298965	91.7	15399	4.7	8.3	77.2	9.8	4.1	0.6	9 548
Germany	204146	151217	74.1	21221	10.4	25.9	34.1	29.5	10.4	0.0	10 505
Greece	50469	50469	100	43367	85.9		0.1	13.9	72.1	13.8	22 758
Hungary	61298	61039	100	22399	36.5	0.4	15.8	47.2	36.5		16 143
Iceland	2456					100					5
Ireland	46761	6	0.0			100	0.0				875
Italy	156406	156406	100	155334	99.3		0.0	0.6	39.7	59.6	28 686
Latvia	26873	34	0.1			99.9	0.1				911
Liechtenstein	39	39	100	38.9	100				100.0		20 195
Lithuania	39018	84	0.2			99.8	0.2				1 673
Luxembourg	1376	1376	100				30	70.1			12 078
Malta	124	124	100	124	100				93.4	7	22 151
Monaco											
Montenegro	2231	2231	100	2197	98.5			1.5	82.3	16.2	22 879
Netherlands	23886	11652	48.8			51.2	48.1	0.7			6 069
North Macedonia	9237	9237	100	6435	69.7			30.3	68.5	1.2	19 633
Norway	15669	28	0.2			99.8	0.2				957
Poland	186164	136848	73.5			26.5	65.7	7.8			8 077
Portugal (excl. Az., Mad.)	41515	40378	97.3	39	0.1	2.7	79.8	17.4	0.1		9 647
Romania	135971	107441	79.0	435	0.3	21.0	61.1	17.6	0.3		8 569
San Marino	41	41	100	41	100					100	28 942
Serbia (incl. Kosovo*)	47350	47350	100	23029	48.6		0.3	51.1	48.6		17 943
Slovakia	23234	23205	99.9	2889	12.4	0.1	28.3	59.1	12.4		14 085
Slovenia	7070	7070	100	7049	99.7			0.3	94.8	4.9	23 687
Spain (excl. Canarias)	236224	224059	94.9	109137	46.2	5.1	20.6	28.1	44.9	1.3	16 541
Sweden	38581	661	1.7			98.3	1.7				2 096
Switzerland	11795	11795	100	8234	69.8		0.2	30.0	69.1	0.7	19 075
Turkey	338487	331851	98	172584	51.0	2.0	10.2	36.9	42.3	8.7	18 400
United Kingdom (& dep.)	137243	2812	2.0			98.0	2.0	0.0			2 476
Total	**2443805**	**1876339**	**76.8**	**674034**	**27.6**	**23.2**	**29.9**	**19.3**	**21.8**	**5.8**	**12 670**
Total without Turkey	**2105318**	**1544487**	**73.4**	**501449**	**23.8**	**26.6**	**33.1**	**16.5**	**18.5**	**5.3**	**11 676**
EU-28	**1990139**	**1447642**	**72.7**	**435962**	**21.9**	**27.3**	**35.0**	**15.9**	**16.5**	**5.4**	**11 468**
France over 45N	258413	66488	98.5	12482	18.5	1.5	68.3	11.7	15.5	3.0	8 804
France below 45N	67482	232477	90	2917	1.1	10.0	79.5	9.3	1.1	0.0	12 391
Kosovo*	4383	4383	100	1786	41			59.2	40.8		17 847
Serbia (excl. Kosovo*)	42967	42967	100	21242	49.4		0.3	50.2	49.4		17 953
Northern	194753	1525	0.8			99.2	0.8	0.0			1 448
North-western	296748	99746	33.6	12482	4.2	66.4	25.2	4.2	3.5	0.7	6 152
Central & Eastern	752027	620664	82.5	91513	12.2	17.5	44.2	26.2	12.2	0.0	10 981
Southern	1200277	1154403	96.2	570039	47.5	3.8	26.8	21.9	35.9	11.6	19 225

*) under the UN Security Council Resolution 1244/99

Note 1: Country not included due to the lack of land cover data: Andorra.

Note 2: The percentage value "0.0" indicates an exposed agricultural area exists, but is small and estimated less than 0.05 %. Empty cells mean no agricultural area in exposure.

Forests

The rural map with ozone indicator AOT40 for forests was combined with the land cover CLC2012 map. Following a similar procedure as described in Horálek et al. (2007), the exposure of forest areas (as defined above) has been calculated for each country, for the same four European regions as for crops and for Europe as a whole.

Table 4.4 gives the absolute and relative forest area where the Critical Level (CL) as defined in UNECE (2004) and the value 20 000 $\mu g \cdot m^{-3} \cdot h$ (which is equal to the earlier used Reporting Value, RV, as was defined in the repealed ozone directive 2002/3/EC) are exceeded. Next to the forest area in exceedance, the table presents the frequency distribution of the forest area over some exposure classes.

The Critical Level was exceeded in 2017 at about 58 % of all European forested area. For the areas excluding Turkey is was at about 55 %, which is the lowest exceedance observed for the twelve-year period 2005 – 2017 (Table 6.4). As in previous years, most countries continue to have in 2017 considerable forest areas in excess to the CL, with specifically almost all forest area in southern and central & eastern European countries.

In this context, it should be mentioned that the AOT40 indicator probably is not the best proxy for vegetation damage. For example, it does not take into account that the Mediterranean vegetation closes its stomata in the warmest and driest season protecting itself from the exposure to ozone. A flux approach – as done e.g. in the EMEP model – taking into account the reduced deposition when stomata are closed would be better. However, there is still a damage to Mediterranean forests – e.g. the Aleppo pine in southern France seems to be quite sensitive to ozone exposure and suffering damage, UNECE (2016).

Table 4.4 Forested area exposure and exceedance and forest-weighted concentrations, ozone indicator AOT40 for forests, 2017

Country	Forested area, 2017					Percentage of forested area, 2017 [%]					Forest - weighted conc.
	Total area	> CL (10 000 µg.m^{-3}.h)		> RV (20 000 µg.m^{-3}.h)		< 10 000	10 000 - 20 000	20 000 - 30 000	30 000 - 50 000	> 50 000	
	[km^2]	[km^2]	[%]	[km^2]	[%]	µg.m^{-3}.h	µg.m^{-3}.h	µg.m^{-3}.h	µg.m^{-3}.h	µg.m^{-3}.h	[µg.m^{-3}.h]
Albania	7572	7572	100	7572	100				68.9	31	47 859
Austria	36999	36999	100	36990	100		0.0	42.3	57.7		31 018
Belgium	6085	6045	99.3			0.7	99.3				16 037
Bosnia-Herzegovina	23469	23469	100	23469	100				99.7	0.3	38 578
Bulgaria	34798	34791	100	34551	99.3	0.0	0.7	54.8	44.5		29 179
Croatia	19868	19868	100	19868	100			1.5	91.2	7.3	39 708
Cyprus	1524	1524	100	1524	100			4.1	95.3	0.7	40 798
Czechia	26246	26246	100	26054	99		0.7	88.1	11.1		26 009
Denmark (excl. Faroes)	3671	235	6.4			93.6	6.4				5 352
Estonia	20952	51	0.2			99.8	0.2				2 578
Finland	205795					100.0					739
France (metropolitan)	141542	138366	97.8	57403	40.6	2.2	57.2	22.5	15.8	2.3	21 858
Germany	108509	95246	87.8	47985	44.2	12.2	43.6	40.4	3.9		18 783
Greece	24957	24957	100	24952	100		0.0	0.7	88.6	10.6	43 556
Hungary	17185	17185	100	16897	98.3		1.7	32.9	65.4		30 569
Iceland	424					100					43
Ireland	3691					100.0					2 347
Italy	79208	79208	100.0	79207	100.0		0.0	0.1	52.4	47.5	50 584
Latvia	24041	187	0.8			99.2	0.8				2 881
Liechtenstein	85	85	100	85	100				100.0		34 140
Lithuania	18871	310	1.6			98.4	1.6				4 868
Luxembourg	928	873	94	20	2.1	6.0	91.8	2.1			16 978
Malta	2	2	100	2	100				88.6	11	47 202
Monaco	0.44	0.44	100	0.44	100				72.7	27.3	27 768
Montenegro	5832	5832	100	5832	100				83.0	17	43 070
Netherlands	3099	1861	60.1	1	0.0	39.9	60.0	0.0			10 717
North Macedonia	8216	8216	100	8216	100			0.2	95.6	4	42 646
Norway	103616	53	0.1			99.9	0.1				1 942
Poland	96165	78561	81.7	17334	18.0	18.3	63.7	18.0			14 954
Portugal (excl. Az., Mad.)	20116	20112	100.0	15266	75.9	0.0	24.1	70.2	5.7		22 628
Romania	71842	71842	100	40646	56.6		43.4	51.4	5.2		21 389
San Marino	6	6	100	6	100				100.0		46 837
Serbia (incl. Kosovo)	27108	27108	100	27108	100			5.3	94.7		34 714
Slovakia	19964	19964	100	17621	88.3		11.7	81.1	7.2		24 458
Slovenia	11524	11524	100	11524	100			0.4	99.6	0.1	40 259
Spain (excl. Canarias)	110018	102996	93.6	81845	74.4	6.4	19.2	25.7	47.9	0.8	28 317
Sweden	261977	953	0.4			99.6	0.4				2 043
Switzerland	12401	12401	100	12362	100		0.3	50.9	46.3	2.5	31 268
Turkey	115599	111878	97	100276	87	3.2	10.0	32.3	52.9	1.5	30 301
United Kingd. (& dep.)	20434	199	1.0			99.0	1.0				3 430
Total	**1694337**	**986725**	**58.2**	**714614**	**42.2**	**41.8**	**16.1**	**17.6**	**21.6**	**3.1**	**17 717**
Total without Turkey	**1578738**	**874847**	**55.4**	**614338**	**38.9**	**44.6**	**16.5**	**16.5**	**19.3**	**3.2**	**17 126**
EU-28	**1389969**	**790098**	**56.8**	**529688**	**38.1**	**43.2**	**18.7**	**18.2**	**16.6**	**3.3**	**16 628**
France over 45N	89165	86035	96.5	23871	26.8	3.5	69.7	20.9	5.8	0.0	18 037
France below 45N	52377	52331	100	33531	64.0	0.1	35.9	25.2	32.6	6.2	28 422
Kosovo*	4304	4304	100	4304	100				100		37 193
Serbia (excl. Kosovo)*	22804	22804	100	22804	100			6.3	93.7		34 244
Northern	638922	1789	0.3			99.7	0.3				
North-western	123826	95013	76.7	23892	19.3	23.3	57.4	15.1	4.2	0.0	
Central & Eastern	424194	393320	93	250525	59.1	7.3	33.7	43.4	15.6	0.1	
Southern	507395	496603	97.9	440197	86.8	2.1	11.1	18.7	57.9	10.1	

*) under the UN Security Council Resolution 1244/99

Note 1: Country not included due to the lack of land cover data: Andorra.
Note 2: The percentage value "0.0" indicates an exposed forested area exists, but is small and estimated less than 0.05 %.
Empty cells mean: no forested area in exposure.

5 NO_2 and NO_x

Annual average maps for NO_2 (related to protection of human health) and for NO_x (related to protection of vegetation) have been produced and presented in the regular mapping report since the maps for year 2014 (Horálek et al., 2017b).

The methodology for creating the concentration maps follows the same principle as for the rest of pollutants: a linear regression model on the basis of European wide station measurement data, followed by kriging of the residuals produced from that regression model (residual kriging).

The map on NO_2 is based on an improved mapping methodology developed in Horálek et al. (2017c, 2018b). The map layers are created for the rural, urban background and urban traffic areas separately on a grid at 1x1 km^2 resolution. Subsequently, the urban background and urban traffic map layers are merged using the gridded road data into one urban map layer. This urban map layer is further combined with the rural map layer into the final NO_2 map using a population density grid at 1x1 km^2 resolution. We present this final combined map in this 1x1 km^2 grid resolution.

The map of the vegetation-related indicator NO_x annual average is created on a grid at 2x2 km^2 resolution, based on rural background measurements only, as vegetation is considered not to be extensively present at urban and suburban areas. Hence, this map is applicable to rural areas only. The resolution is chosen equally to the one of the vegetation indicator for ozone.

Annex 3 provides details on the regression and kriging parameters applied for deriving the maps, as well as the uncertainty analysis of the maps.

5.1 NO_2 – Annual mean

5.1.1 Concentration maps

The AQ Directive (EU, 2008) sets two limit values (LV) for NO_2 for the human health protection. The first one is an annual LV (ALV) at the level of 40 $\mu g \cdot m^{-3}$. This is the same concentration level as recommended by the World Health Organization for the NO_2 annual average as the Air Quality Guideline (WHO, 2005). The second one is an hourly LV (HLV, 200 $\mu g \cdot m^{-3}$ not to be exceeded on more than 18 hours per year). The HLV has been exceeded in 2017 at only 1.3 % of all the reporting stations, mostly at urban stations, in nine countries, with more than two stations exceeded in Turkey and Spain only (EEA, 2019b). In view of this low number of exceedances, the short-term LV has not been included in the mapping procedures.

Map 5.1 presents the final combined concentration 1x1 km^2 gridded map for the 2017 NO_2 annual average as the result of interpolation and merging of the separate maps as described in Annex 1.

Supplementary data used in the linear regression are in principle the same as described in Horálek et al. (2017c). For rural areas they consist of EMEP model output, altitude, OMI satellite data, wind speed, population density and land cover; for urban background areas these are EMEP model output, altitude, OMI satellite data, wind speed, population density and land cover; for traffic areas the EMEP model output, altitude, and OMI satellite data are used (Annex 3).

According to Map 5.1, the areas where the ALV of 40 $\mu g \cdot m^{-3}$ was exceeded include urbanized parts of some large cities, particularly Milan, Naples, Rome, Turin, Paris, Barcelona, Madrid, London, Athens, Ankara, Istanbul, and some other smaller cities in Turkey. Some other cities show NO_2 levels above 30 $\mu g \cdot m^{-3}$, e.g. in Germany, Italy, the Netherlands, Belgium, United Kingdom, Turkey. Most of the European area shows NO_2 levels below 20 $\mu g \cdot m^{-3}$, with most of the rural areas below 10 $\mu g \cdot m^{-3}$. Some larger areas above 20 $\mu g \cdot m^{-3}$ can be found in the Po valley, the Benelux, the German Ruhr region, in central and southern England, in the Île de France region and around Rome.

It should be noted that the interpolated map is created at 1x1 km^2 only and as such refers to the rural and urban *background* situations only, while the exceedances of the NO_2 limit values occur mostly at local *hotspots* such as dense traffic locations and densely urbanised and industrialised areas. Although the urban traffic map layer is used in the map creation, the traffic locations are smoothed in the 1x1 km^2 resolution. The relative mean uncertainty of the NO_2 annual average map is 30 % for rural and 27 % for urban background areas (Annex 3).

In order to provide more complete information of the air quality across Europe, the final combined map including the measurement data at station points is presented in Map A5.9 of Annex 5.

Map 5.1 Concentration map of NO_2 annual average, rural map, 2017

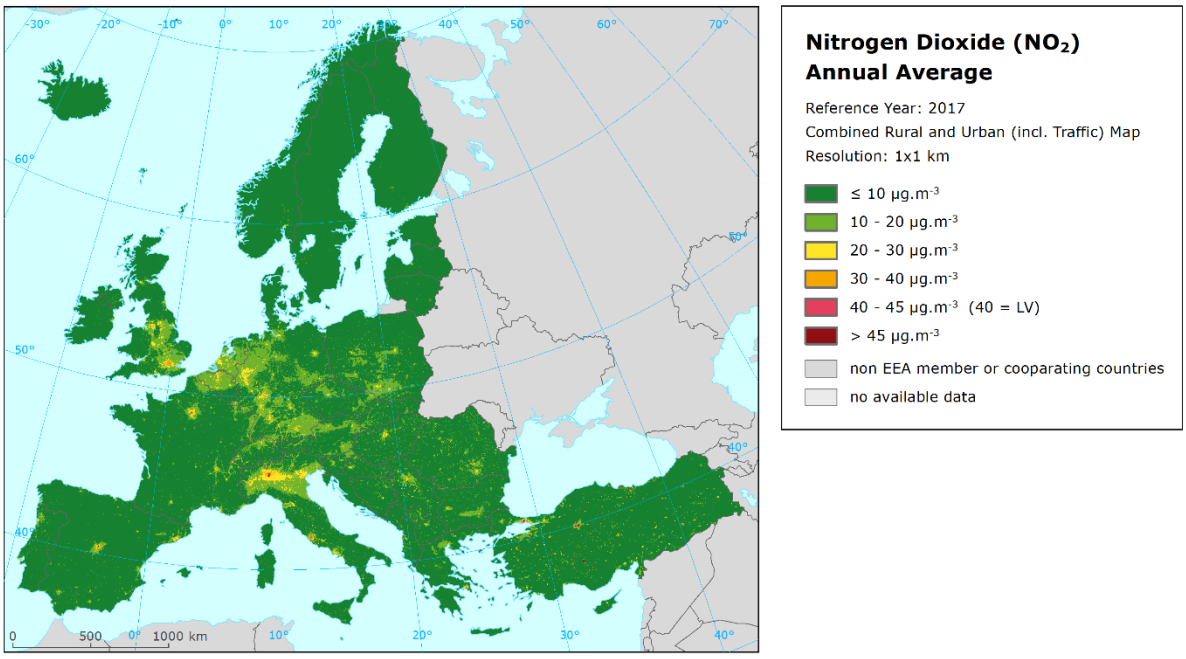

5.1.2 Population exposure

Table 5.1 gives the population frequency distribution for a limited number of exposure classes calculated on a grid of 1x1 km^2 resolution, as well as the population-weighted concentration for individual countries and for Europe as a whole according to Equation A1.7 of Annex 1.

The human exposure to NO_2 has been calculated based on the improved methodology as developed in Horálek et al. (2017c). The population exposure is calculated according to Equation A1.6 of Annex I, i.e. it is calculated separately for urban areas directly influenced by traffic and for the background (both rural and urban) areas, in order to better reflect the population exposed to traffic. Based on this, the different concentration levels in urban background and traffic areas inside the 1x1 km^2 grid cells are taken into account.

Table 5.1 Population exposure and population-weighted concentration, NO_2 annual average 2017

Country		Population [inhbs . 1000]	NO_2 annual average, exposed population [%]						Population weighted conc. [µg.m^{-3}]
			< LV				> LV		
			< 10 µg.m^{-3}	10 - 20 µg.m^{-3}	20 - 30 µg.m^{-3}	30 - 40 µg.m^{-3}	40 - 45 µg.m^{-3}	> 45 µg.m^{-3}	
Albania	AL	2 877	21.1	42.4	34.0	2.5			16.9
Andorra	AD	73	1.2	68.1	30.7				20.5
Austria	AT	8 773	11.0	49.0	29.9	8.6	1.5	0.1	18.9
Belgium	BE	11 352	2.5	52.7	31.8	11.6	0.9	0.5	20.9
Bosnia & Herzegovina	BA	3 510	26.5	45.1	27.7	0.7			15.7
Bulgaria	BG	7 102	11.7	47.5	30.5	10.3			19.2
Croatia	HR	4 154	26.8	47.3	24.7	1.3			15.6
Cyprus	CY	1 201	15.4	31.2	44.9	4.1	3.7	0.6	19.6
Czechia	CZ	10 579	16.5	67.3	14.3	1.9	0.0		15.2
Denmark	DK	5 749	69.0	24.5	6.1	0.4			8.8
Estonia	EE	1 316	81.1	18.2	0.7				6.3
Finland	FI	5 503	71.1	26.6	2.3				7.6
France (metropolitan)	FR	64 629	30.3	40.9	17.6	6.3	2.3	2.6	16.9
Germany	DE	82 522	7.1	51.7	34.0	5.0	1.4	0.8	19.4
Greece	GR	10 768	17.5	31.1	19.3	17.8	7.9	6.5	23.6
Hungary	HU	9 798	11.5	59.6	21.8	6.5	0.5	0.2	17.8
Iceland	IS	338	43.9	50.7	5.4				10.2
Ireland	IE	4 784	58.2	35.3	5.3	1.2			9.3
Italy	IT	60 589	9.4	36.7	34.7	13.1	3.6	2.5	22.1
Latvia	LV	1 950	50.7	36.7	12.4	0.3			11.1
Liechtenstein	LI	38	1.3	83.0	14.3	1.3			18.2
Lithuania	LT	2 848	47.9	47.4	4.4	0.4			10.8
Luxembourg	LU	591	7.2	50.1	35.9	6.9			19.5
Malta	MT	460	7.4	82.3	3.0	7			16.0
Monaco	MC	38			78	22			26.8
Montenegro	ME	622	25.2	67.7	7.1				13.5
Netherlands	NL	17 082	2.8	49.7	42.1	5.2	0.2		20.2
North Macedonia	MK	2 074	3.7	53.9	38.7	3.7			19.8
Norway	NO	5 258	52.8	35.2	10.6	1.4			10.4
Poland	PL	37 973	26.3	52.5	19.5	1.2	0.3	0.1	14.9
Portugal (excl. Az., Mad.)	PT	9 809	23.8	48.9	22.5	3.5	1.0	0.3	16.2
Romania	RO	19 644	15.4	46.7	25.5	11.2	0.5	0.7	18.8
San Marino	SM	33	6.1	89.3	0.6	4			14.5
Serbia (incl. Kosovo*)	RS	8 824	12.5	37.4	42.3	7.8			19.6
Slovakia	SK	5 435	14.8	76.8	6.6	1.9			14.7
Slovenia	SI	2 066	20.8	51.7	26.0	1.5			16.2
Spain (excl. Canarias)	ES	44 373	11.7	39.8	27.9	12.9	4.7	3.1	21.6
Sweden	SE	9 995	73.8	24.0	1.8	0.4			7.7
Switzerland	CH	8 420	6.1	61.2	25.9	5.5	1.4		18.8
Turkey	TR	79 815	25.3	13.9	21.4	19.4	6.9	13.1	25.3
United Kingdom (& dep.)	UK	65 844	11.0	42.4	34.9	9.8	0.8	1.1	19.8
Total		**618 808**	**18.8**	**41.2**	**26.2**	**8.8**	**2.3**	**2.7**	**19.2**
			95.0				**5.0**		
Total without Turkey		**538 993**	**17.9**	**44.9**	**26.9**	**7.3**	**1.7**	**1.3**	**18.4**
			97.0				**3.0**		
EU-28		**506 888**	**17.8**	**44.8**	**26.7**	**7.5**	**1.8**	**1.4**	**18.5**
			96.9				**3.1**		
Kosovo*	KS	1 784	15.8	63.9	20.3				15.6
Serbia (excl. Kosovo*)	RS	7 040	11.7	31.0	47.6	9.7			20.6

*) under the UN Security Council Resolution 1244/99

Note: The percentage value "0.0" indicates that an exposed population exists, but it is small and estimated to be less than 0.05 %. Empty cells mean no population in exposure.

Thus – like for PM_{10} and $PM_{2.5}$ – the population exposure refers not only to the rural and urban *background* areas, but to the urban *traffic* locations as well. However, it should be mentioned that only population density data at 1x1 km^2 resolution is used. This means that contrary to the concentration levels, the population density is constant within each 1x1 km^2 grid cell. This shortcoming can increase the uncertainty of the population exposure results.

It has been estimated that in 2017 about 5 % of the European population and about 3 % of both the total European population without Turkey and the EU-28 population lived in areas with NO_2 annual average concentrations above the EU limit value of 40 $\mu g \cdot m^{-3}$. CSI004 (EEA, 2019c) estimates that about 7 % of the population in urban agglomerations in the EU-28 was exposed in 2017 to levels above the EU limit value.

The European-wide and EU-28 only population-weighted concentration of the NO_2 annual average for 2017 is estimated to be about 19 $\mu g \cdot m^{-3}$, while for the total European population without Turkey it is about 18 $\mu g \cdot m^{-3}$.

Figure 5.1 shows, for the whole mapped area, the population frequency distribution for exposure classes of 1 $\mu g \cdot m^{-3}$. The frequency distribution is centred around 17-18 $\mu g \cdot m^{-3}$.

Figure 5.1 Population frequency distribution, NO_2 annual average, 2017

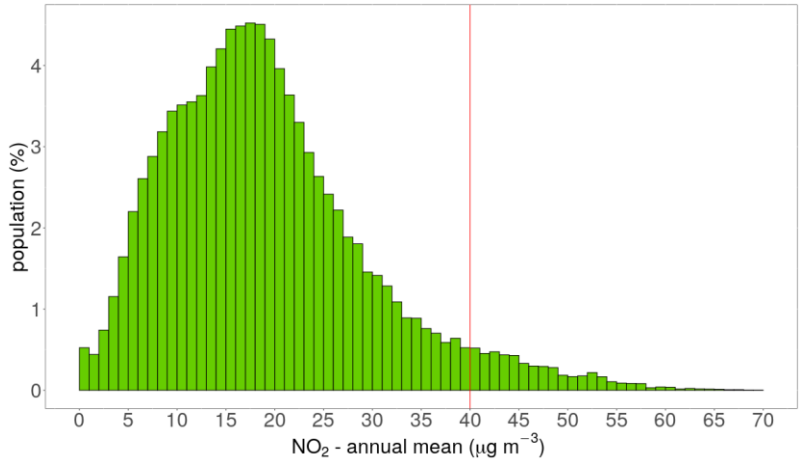

5.2 NO_x – Annual mean

5.2.1 Concentration maps

The AQ Directive (EU, 2008) sets a Critical Level (CL) for the protection of vegetation for the NO_x annual mean at 30 $\mu g \cdot m^{-3}$. According to this directive, the sampling points targeted at the protection of vegetation and natural ecosystems shall be in general sited more than 20 km away from agglomerations or more than 5 km away from other built-up areas. Thus, only the observations at rural background stations are used for the NO_x mapping and the resulting map is representative for rural areas only.

The number of NO_x measurement stations is limited. The mapping of the NO_x annual average is therefore performed on the basis of an approach presented in Horálek et al. (2007). This approach derives additional *pseudo* NO_x annual mean concentrations from NO_2 annual mean measurement concentrations and increases as such the number and spatial coverage of NO_x 'data points', and applies these data to the NO_x mapping. Section A1.1 of Annex 1 provides some details.

Map 5.2 presents the concentration map of NO_x annual average. It concerns rural areas only, representing an indicator for vegetation exposure to NO_x. The relative mean uncertainty of this rural map is 42 %.

Most of the European area shows NO_x levels below 20 $\mu g \cdot m^{-3}$. However, at the Po valley, southern part of the Netherlands, northern Belgium, the German Ruhr region and around some larger European cities (typically being the national capitals) elevated NO_x concentrations above the Critical Level (CL) are observed. Furthermore, around many larger European cities concentrations just below the CL are observed. These concentrations are expected to be the result of large emissions from transport in and around the cities, as well as energy production and industrial facilities taking place at these areas. However, this is relevant only if there is vegetation around those larger cities.

The NO_x annual average rural map including the data measured at rural background stations is presented in Map A5.10 of Annex 5. The map illustrates the lack of the NO_x rural stations in the Balkan area.

Map 5.2 Concentration map of NO_x annual average, rural map, 2017

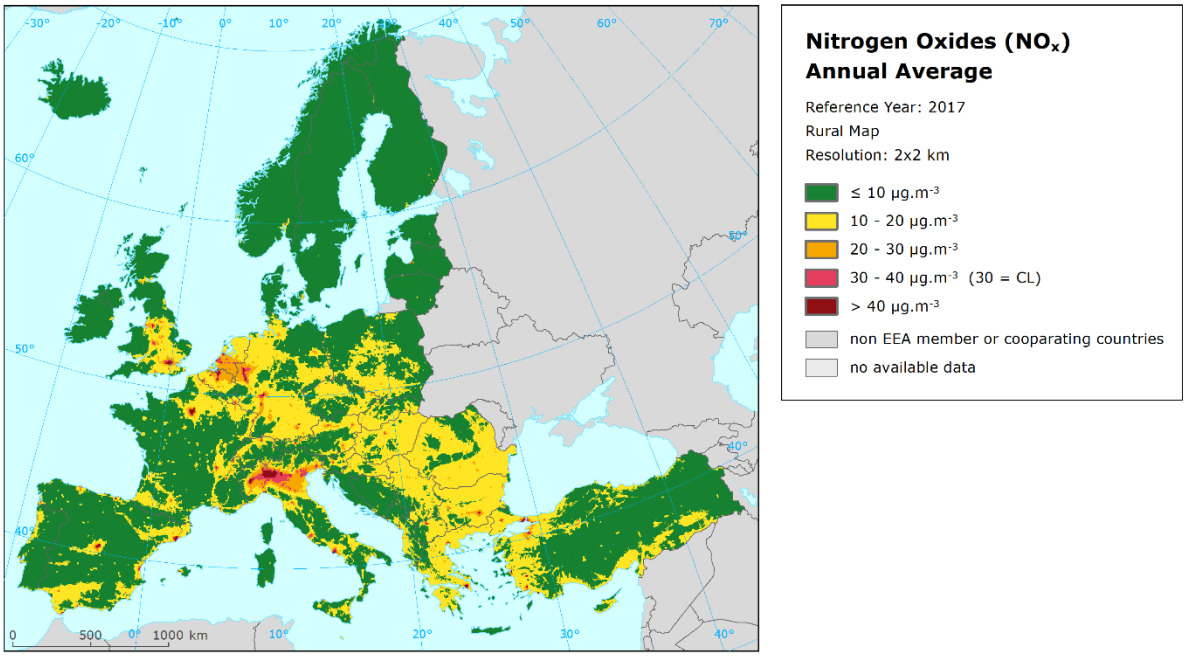

Vegetation exposure is not calculated for NO_x, as the critical level (CL) applies actually to vegetation only, which is by nature mostly allocated in rural areas where there is limited CL exceedance observed. Therefore, the vegetation exposure exceedance would occur in limited vegetation areas only and, as such, is considered not to provide essential information from the European scale perspective. Furthermore, contrary to vegetation exposure to high ozone concentrations in Europe that leads to considerable damage, vegetation exposure to NO_x pollution is of minor importance in terms of actual impacts. On the other hand, NO_x concentrations contribute in part to the total N-deposition, which leads to acidifying and eutrophying effects on vegetation. These effects, especially eutrophication, are still very important in Europe (e.g. EMEP, 2019). However, these effects on vegetation cannot be easily expressed by an exposure table.

Concerning the potential exposure estimate of vegetation and natural ecosystems to NO_x there is an additional dilemma: which receptor types should be selected to estimate the exposure and critical level exceedance of vegetation and natural ecosystems? An option would be the use of CLC classes (e.g. like in Horálek et al., 2008); nevertheless this classification is too general. Another option would be the NATURA2000 database. However, that data source contains a wide series of receptor types, species and classes. Serious additional efforts would be needed to conclude on the most relevant set of receptors from the NATURA 2000 geographical database.

6 Exposure trend estimates

This report has presented the interpolated maps for 2017 on the PM_{10}, $PM_{2.5}$, ozone and NO_2 *human health* related air pollution indicators (annual average and the 90.4 percentile of PM_{10} daily means, annual average for $PM_{2.5}$, the 93.2 percentile of maximum daily 8-hour means, SOMO35 and SOMO10 for ozone, and the annual average for NO_2), together with tables showing the frequency distribution of the estimated population exposures and exceedances per country and as European totals.

Furthermore, interpolated maps of ozone and NO_x *vegetation* related air pollution indicators have been produced. More specifically, these include a map of the ozone indicator AOT40 for vegetation and AOT40 for forests, and tables with the frequency distribution of estimated land area exposures and exceedances per country and the European totals. In addition, the map of the annual average for NO_x has been produced, but without exposure estimates.

A mapping approach similar to previous years (Horálek et al., 2019a and references therein) based primarily on observational data was used. With the interpolated air pollution maps and exposure estimates for the year 2017 completed, a thirteen-year (for PM_{10} and ozone, except SOMO10), resp. ten-year (for $PM_{2.5}$) and eight-year (for NO_2) overview of comparable exposure estimates has been obtained. In this chapter we provide these multi-annual overviews of exposure estimates for each of the indicators of PM_{10}, $PM_{2.5}$ and ozone (except SOMO10), including a trend analysis. Maps of the nitrogen related indicators were not produced on a multi-annual basis so far and therefore only a time series for NO_2 with eight annual averages can be given in this chapter.

For the previous years, mapping results as presented in Annex 4 of Horálek et al. (2019a) have been used, with the additions and changes as follows. PM_{10} and $PM_{2.5}$ results for 2011 have been recalculated, as the results for these pollutants presented in Horálek et al. (2019a) were mistakenly calculated based on maps in 10x10 km^2 aggregation. Next to this, PM_{10} and $PM_{2.5}$ results for 2015–2017 are presented in two variants, i.e. based on the old and the updated methodologies, for comparability reasons. For the old methodology, 2005–2016 results have been used based on in Horálek et al. (2019a), while 2017 results were calculated additionally. For the updated methodology, 2015 results have been used based on Horálek et al. (2019b), 2017 results are the main product of this paper and 2016 results have been calculated additionally.

For the human health indicators, we express the exposure estimates on the one hand as population-weighted concentration and on the other hand as percentage of population exposed to concentrations above the limit/target value. For the vegetation related indicators, the exposure estimates are expressed as the agricultural or forest areas exposed to concentrations above defined thresholds, as well as the agricultural- and forest- weighted concentrations.

It should be noted that the percentage of population resp. agricultural or forest area exposed is a less robust indicator compared to the population- resp. agricultural- or forest-weighted concentration, as a small concentration increase (or decrease) may lead to a major increase (or decrease) of population resp. agricultural or forest area exposed. This is not the case when taking the population-weighted concentration as indicator. Therefore, the trend analysis is done based on the population-weighted concentrations only.

When thinking about a trend, we should take into account (i) the meteorologically induced variations, (ii) the uncertainties involved in the interpolation (Annex 3), and (iii) the station densities and their spatial distributions over the European regions. In addition, we should be aware of the fact that different trends in various parts of Europe may occur. However, bearing in mind these limitations we provide here a trend analysis for the period 2005 – 2017 on the population-weighted concentrations for Europe as a whole.

For comparability reasons, we present in this chapter the results for Europe as a whole without Turkey, because 2016 was the first year for which the area of Turkey was mapped.

6.1 Human health PM_{10} indicators

Table 6.1 summarises the average concentration to which the European population has been exposed to over the thirteen year period 2005 – 2017 for both *human health PM_{10} indicators*, expressed as the population-weighted concentration, and the percentage of population exposed to PM_{10} concentrations above limit values (LV), i.e. the annual (ALV) and daily (DLV) limit value, respectively.

For the years 2012 and 2013 both the 36th highest value and the 90.4 percentile of daily mean(s) have been calculated. Their results demonstrate an underestimation of almost 1 µg·m^{-3} at the 36th highest daily mean. One may conclude that this underestimation is caused by the fact that when calculating the 36th highest daily mean value there is no correction for the missing values at incomplete time series. Whereas the 90.4 percentile of daily mean(s) adjusts for such missing data.

As the PM_{10} maps for 2017 (as presented in Chapter 2) have been constructed using the updated methodology as developed and tested in Horálek et al. (2019b), the table presents the results for 2017 (and 2015–2016) both based on the updated and the old methodologies, for comparability reasons.

Table 6.1 Population-weighted concentration and percentage of the European population (without Turkey) exposed to concentrations above the PM_{10} limit values (LV) for the protection of health for 2005 to 2017

PM_{10}		method	2005	2006	2007	2008	2009	2010	2011	2012	2013	2014	2015	2016	2017
Annual average															
Population-weighted concentration	[µg.m^{-3}]	old	28.0	28.5	26.2	24.8	24.6	24.3	25.0	22.7	22.2	21.1	21.2	20.2	20.2
		new											21.6	20.5	20.8
Population exposed > ALV (40 µg.m	[%]	old	13.3	10.3	6.8	5.8	6.0	5.2	7.0	3.4	2.6	2.0	0.6	1.7	2.9
		new											0.7	1.7	3.3
36th highest daily mean / 90.4 percentile of daily means															
Popul.-weighted conc. [µg.m^{-3}]	36th highest d. m.	old	46.8	47.8	44.1	41.3	41.2	41.9	44.6	39.7	38.6				
	90.4 perc. of d. m	old								40.6	39.4	37.1	36.9	35.7	36.1
	90.4 perc. of d. m	new											37.5	36.1	37.0
Popul. exposed > DLV (50 µg.m^{-3}) [%	36th highest d. m.	old	34.3	35.7	26.2	19.4	16.5	20.6	24.5	16.5	16.4				
	90.4 perc. of d. m	old								17.7	17.3	13.3	14.7	14.0	15.8
	90.4 perc. of d. m	new											16.2	14.6	17.0

In 2017 the population exposed to *annual mean* concentrations of PM_{10} above the limit value of 40 µg·m^{-3} is 3.3 % of the total population; using the old methodology, it would be 2.9 %, which is lower percentage compared to the years 2005–2012, but higher compared to the previous four years. Furthermore, it is estimated that European inhabitants are exposed on average to an annual mean PM_{10} concentration of 21 µg·m^{-3}; using the old methodology, it would be 20 µg·m^{-3}, the lowest value (together with the year 2016) in the thirteen years' time series. The comparison of results for 2015 and 2017 illustrates well that a clear decrease in the population-weighted concentrations does not lead necessarily to a similar decrease in the population exceedance exposure numbers.

In the thirteen-year time series, the number of people living in areas with concentrations above the annual LV is the lowest in the latest five years, 2013 – 2017. The overall picture of the population-weighted annual mean concentration of the European totals (i.e. totals of 40 European countries considered) demonstrates a downward trend approximately of -0.7 µg·m^{-3}.year^{-1} for the years 2005 – 2017 (for methodology, see Annex 1, Section A1.2). This trend is statistically significant (at the strongest level ***, i.e. 0.001) and expresses a mean decrease of 0.7 µg·m^{-3} per year.

In 2017 about 17 % of the European population lived in areas where the PM_{10} daily limit value (calculated using the *90.4 percentile*) was exceeded; using the old methodology, it would be 16 %, being somewhat higher than in the previous three years. The overall European population-weighted concentration of the 90.4 percentile of the PM_{10} daily means (formerly the 36th highest daily mean) for the background areas is estimated to be about 37 µg·m^{-3} in 2017; according to the old mapping methodology, it would be 36 µg·m^{-3}, which is the second lowest of the thirteen years considered. This is the case even though possible underestimated data have been used in the 2005 – 2011 calculations. The population-weighted concentration of the European total (i.e. total of 40 European countries considered) demonstrate a statistically significant (at the strongest level ***, i.e. 0.001) downward trend of -0.9 µg·m^{-3} per year for the years 2005 – 2017, for the daily LV related indicator 90.4 percentile of daily means (formerly the 36th highest daily mean).

6.2 Human health $PM_{2.5}$ indicators

Table 6.2 summarises for *human health $PM_{2.5}$ indicator* (annual average) the population-weighted concentration and the percentage of European population exposed to $PM_{2.5}$ concentrations above the EU LV for the years 2007 to 2017 (without 2009, for which neither a map nor a population exposure was prepared).

As in the case of PM_{10}, the $PM_{2.5}$ maps for 2017 (as presented in Chapter 3) has been constructed using the updated methodology. Due to this reason, the table presents the results for 2017 (and 2015–2016) both based on the updated and the old methodology, for comparability reasons.

Table 6.2 Population-weighted concentration and percentage of the European population (without Turkey) exposed to concentrations above the $PM_{2.5}$ limit value (LV) for the protection of health for 2007 to 2017

$PM_{2.5}$		method	2007	2008	2009	2010	2011	2012	2013	2014	2015	2016	2017
Annual average													
Population-weighted concentration	[µg.m^{-3}]	old	16.3	16.3	not mapped	16.8	17.6	15.6	15.3	14.1	14.2	13.4	13.6
		new									14.3	13.6	13.8
Population exposed > LV (25 µg.m^{-3})	[%]	old	7.8	7.6		8.3	13.0	9.0	5.8	4.2	6.3	5.4	7.0
		new									6.5	5.4	7.2

The percentage of population exposed in 2017 to annual mean concentrations of $PM_{2.5}$ above the LV of 25 µg·m^{-3} is about 7 %, which is a higher value compared to the previous four years. Furthermore, it is estimated that European inhabitants were exposed on average to an annual mean $PM_{2.5}$ concentration of about 14 µg·m^{-3} in 2017; also according the old methodology, being the second lowest value in the time series.

The trend analysis of the population-weighted concentrations across the period 2007 – 2017 for Europe as a whole has been executed. At European scale a statistical significant (at the level **, i.e. 0.01) downward trend can be observed, estimated to be -0.4 µg·m^{-3} per year.

6.3 Human health ozone indicators

Table 6.3 summarises for both *human health ozone indicators* the exposure levels of the European inhabitants in terms of population-weighted concentrations. Furthermore, it presents the percentage of European population exposed to concentrations above the target value (TV) and above a level of 6 000 µg·m^{-3}·d for the SOMO35 for the years 2005 to 2017.

Table 6.3 Population-weighted concentration and percentage of the European population (without Turkey) exposed to concentrations above the target value (TV) threshold for the protection of health and a SOMO35 threshold of 6 000 µg·m^{-3}·d for 2005 to 2017

Ozone		2005	2006	2007	2008	2009	2010	2011	2012	2013	2014	2015	2016	2017
26th highest daily max. 8-h mean / 93.2 percentile of daily max. 8-h means														
Pop.-weighted conc. [µg.m^{-3}]	26th highest d. max8h	####	####	####	####	####	####	####	####	####				
Pop.-weighted conc. [µg.m^{-3}]	93.2 perc. of d. max8h								####	####	####	####	####	####
Pop. exposed > TV (120 µg.m^{-3})	26th highest d. max8h	31.6	51.4	27.1	15.0	16.0	16.3	16.5	20.7	15.0				
Pop. exposed > TV (120 µg.m^{-3})	93.2 perc. of d. max8h								21.9	15.9	5.6	34.0	8.4	12.9
SOMO35														
Pop.-weighted concentration [µg.m^{-3}.d]		4706	5167	4411	4275	4275	3917	4414	4279	4088	3500	4312	3619	3890
Pop. exposed > 6000 µg.m^{-3}.d [%]		27.0	29.5	28.1	19.6	24.6	16.6	23.6	24.5	18.8	9.4	22.2	11.7	19.1

The table presents the results obtained with the 1x1 km^2 merging resolution as tested on the 2006 data in Horálek et al (2010), then recomputed for 2005 and 2007, and finally implemented fully on the 2008 data and onwards. For 2012 and 2013, both the 26th highest value and the 93.2nd percentile of maximum daily 8-hour mean(s) have been calculated. It demonstrates an underestimation of about 0.6 µg·m^{-3} at the 26th maximum daily 8-hour mean, which is caused by the fact that when calculating this indicator there is no correction for the missing values in the incomplete measurement time series.

Using the *93.2 percentile of ozone maximum daily 8-hour means* it is estimated that 13 % of the population lived in 2017 in areas where concentrations were above the ozone target value (TV) of 120 µg·m^{-3}, which is the third lowest number of the thirteen year period. The overall European population-weighted ozone concentration in terms of the 93.2 percentile maximum daily 8-hour means in the background areas is estimated at about 105 µg·m^{-3}, which is also the third lowest value of the whole thirteen year period (it should be noted that for 2005–2011 the 26th highest value of the maximum daily eight-hour mean was considered instead).

Examining the time series for 2005 – 2017, it can be concluded that 2006, but also 2005 and 2015 are exceptional years with high ozone concentrations, leading to increased exposure levels compared to the other ten years. The years 2014, 2016 and 2017 show the lowest exposure levels in the thirteen years' time series.

The trend analysis of the population-weighted concentrations for the 93.2 percentile of the maximum daily 8-hour means across the period 2005 – 2017 for Europe as a whole has been executed. The population-weighted concentration of the European totals (i.e. totals of 40 European countries considered) demonstrates a statistically significant (at the level *, i.e. 0.05) downward trend of -0.6 µg·m^{-3} per year.

A similar tendency is observed for *SOMO35*. In 2006 – 2007 almost one-third of the population lived in areas where a level of 6 000 µg·m^{-3}·d[3] was exceeded, with the highest level in 2006. In the period of 2008 – 2017, it fluctuates from about 17 % to 25 % of the population, except 2014 with about 9 % and 2016 with about 12 %.

The population-weighted SOMO35 concentrations show a quite similar pattern over time. Trend analysis on the population-weighted concentration of the European totals shows a slight downward trend of about -85 µg·m^{-3}·d per year, for the period 2005 – 2017, which is statistically significant (at the level *, i.e. 0.05).

[3] Note that the 6 000 µg·m^{-3}·d does not represent a health-related legally binding 'threshold'. In this and previous papers it represents a somewhat arbitrarily chosen threshold to facilitate the discussion of the observed distributions of SOMO35 levels in their spatial and temporal context. For motivation of this choice, see Section 4.2.

6.4 Vegetation related ozone indicators

Exposure indicators describing the *agricultural and forest areas exposed to accumulated ozone* concentrations above defined thresholds are summarised in Table 6.4. Those thresholds are the target value (TV) of 18 000 µg·m^{-3}·h and the long-term objective (LTO) of 6 000 µg·m^{-3}·h for the AOT40 for vegetation, and the former Reporting Value (RV) of 20 000 µg·m^{-3}·h and the Critical Level (CL) of 10 000 µg·m^{-3}·h for the AOT40 for forests.

Table 6.4 Percentages of the European agricultural and forest area (without Turkey) exposed to ozone concentrations above the target value (TV) and the long-term objective (LTO) for AOT40 for vegetation, and above Critical Level (CL) and Reporting Value (RV) for AOT40 for forests and agricultural- and forest-weighted concentrations for 2005 to 2017

Ozone	2005	2006	2007	2008	2009	2010	2011	2012	2013	2014	2015	2016	2017
AOT40 for vegetation													
Agricultural area % > TV (18 000 µg.m^{-3} [%]	48.5	69.1	35.7	37.8	26.0	21.3	19.2	30.0	22.1	17.8	31.4	14.7	23.8
Agricultural area % > LTO (6 000 µg.m^{-3}. [%]	88.8	97.6	77.5	95.5	81.0	85.4	87.9	86.4	81.0	85.5	79.7	74.1	73.4
Agricultural-weighted concentration (µg.m-3	17481	22344	14597	15214	13157	13310	13255	14041	12838	12427	14223	10942	11750
AOT40 for forests													
Forest area exposed > RV (20 000 µg.m^{-3} [%]	59.1	69.4	48.4	50.2	49.2	49.3	53.0	47.2	44.1	37.7	52.4	41.9	38.9
Forest area exposed > CL (10 000 µg.m^{-3} [%]	76.4	99.8	62.1	79.6	67.4	63.4	68.6	65.0	67.2	68.2	59.8	60.0	55.4
Forest-weighted concentration (µg.m-3.h)	25900	31154	23744	21951	23532	19625	21892	21580	21753	17124	21150	17573	16798

In 2017, some 24 % of all agricultural land (crops) was exposed to accumulated ozone concentrations (AOT40 for vegetation) exceeding the target value (TV) threshold, which is in the range of percentages in exceedance in the last eight years. About 73 % of all agricultural land was exposed to levels in excess of the long-term objective (LTO), which is the lowest of all thirteen years.

The trend analysis of the agricultural-weighted concentrations for the AOT40 for vegetation across the period 2005 – 2017 for Europe as a whole has been executed. The agricultural-weighted concentration of the European totals (i.e. totals of 40 European countries considered) demonstrates a statistically significant (at the level **, i.e. 0.01) downward trend of -408 µg·m^{-3}·h per year.

For the ozone indicator AOT40 for *forests* the level of 20 000 µg·m^{-3}·h (earlier used Reporting Value, RV) was exceeded in about 39 % of the European forest area in 2017, which is the second lowest of the whole time series. The forest area exceeding the Critical Level (CL) was in 2016 about 55 %, which is the lowest percentage of the thirteen years period.

The temporal pattern of the AOT40 for forests exceedances shows some similarity with those of the AOT40 for vegetation, despite their different definitions and receptors and their natural difference in area type characteristics and occurrence. Their annual variability is, however, heavily dependent on meteorological variability.

The trend analysis of the forest-weighted concentrations for the AOT40 for forests across the period 2005 – 2017 for Europe as a whole has been executed. The forest-weighted concentration of the European totals (i.e. totals of 40 European countries considered) demonstrates a statistically significant (at the strongest level ***, i.e. 0.001) downward trend of -726 µg·m^{-3}·h per year.

6.5 Human health NO_2 indicators

Table 6.5 summarises for the *human health NO_2 indicator* the exposure levels of the European inhabitants in terms of population-weighted concentrations. Furthermore, it presents the percentage of European population exposed to concentrations above the limit value (LV) of 40 µg·m^{-3} for the years

2005, 2010 and 2013 to 2017. The population-weighted concentration is presented additionally also for 2007, although based on different mapping methodology than the other years. This 2007 value is probably slightly underestimated; based on Horálek et al. (2017c), we can suppose the true value would be of about 1 % higher (i.e. it would be about 23.5 µg·m^{-3}).

Table 6.5 Population-weighted concentration and percentage of the European population (without Turkey) exposed to concentrations above the NO_2 limit value (LV) of 40 µg·m^{-3} for the protection of health for 2005 to 2017

NO_2	2005	2006	2007	2008	2009	2010	2011	2012	2013	2014	2015	2016	2017
Annual average													
Population-weighted concentration [µg.m^{-3}]	23.3	not mapped	23.3	not mapped		22.1	not mapped		19.4	18.6	18.8	18.6	18.4
Population exposed > LV (40 µg.m^{-3} [%]	7.9					4.9			3.2	2.8	3.2	2.8	3.0

In 2017 the population exposed to NO_2 annual mean concentrations above the limit value of 40 µg·m^{-3} is 3.0 % of the total population, which is slightly more than in 2014 and 2016 and slightly less than in 2013 and 2015. Furthermore, it is estimated that European inhabitants are exposed on average to an annual mean NO_2 concentration of 18 µg·m^{-3}, slightly less than in the four previous years.

References

Cressie, N., 1993, *Statistics for spatial data*, Wiley series, New York.

Danielson, J.J. and Gesch, D.B., 2011, *Global multi-resolution terrain elevation data 2010 (GMTED2010):* U.S. Geological Survey Open-File Report 2011–1073, https://lta.cr.usgs.gov/GMTED2010.

De Leeuw, F., 2012, *AirBase: a valuable tool in air quality assessments at a European and local level,* ETC/ACM Technical Paper 2012/4, http://www.eionet.europa.eu/etcs/etc-atni/products/etc-atni-reports/etcacm_tp_2012_4_airbase_aqassessment.

Denby, B., Schaap, M., Segers, A., Builtjes, P., Horálek, J., 2008, Comparison of two data assimilation methods for assessing PM_{10} exceedances on the European scale, *Atmos. Environ.* 42, 7122–7134.

Denby, B., et al., 2011a, *Calculation of pseudo $PM_{2.5}$ annual mean concentrations in Europe based on annual mean PM10 concentrations and other supplementary data*, ETC/ACC Technical Paper 2010/9, http://www.eionet.europa.eu/etcs/etc-atni/products/etc-atni-reports/etcacc_tp_2010_9_pseudo_pm2-5_stations.

Denby, B., et al., 2011b, *Mapping annual mean $PM_{2.5}$ concentrations in Europe: application of pseudo $PM_{2.5}$ station data*, ETC/ACM Technical Paper 2011/5, http://www.eionet.europa.eu/etcs/etc-atni/products/etc-atni-reports/etcacm_tp_2011_5_spatialpm2-5mapping.

De Smet, P., et al., 2011, *European air quality maps of ozone and PM_{10} for 2008 and their uncertainty analysis*, ETC/ACC Technical Paper 2010/10, http://www.eionet.europa.eu/etcs/etc-atni/products/etc-atni-reports/etcacc_tp_2010_10_spataqmaps_2008.

ECMWF, *Meteorological Archival and Retrieval System* (MARS), http://www.ecmwf.int/.

EEA, 2008, *ORNL Landscan 2008 Global Population Data conversion into EEA ETRS89-LAEA5210 1km grid* (eea_r_3035_1_km_landscan-eurmed_2008, by Hermann Peifer of EEA).

EEA, 2016, *Corine land cover 2012 (CLC2012) raster data,* 100x100m^2 gridded version 18 (09/2016).

EEA, 2018, *Guide for EEA map layout. EEA operational guidelines*, January 2015, version 5, https://www.eionet.europa.eu/gis/docs/GISguide_v5_EEA_Layout_for_map_production.pdf.

EEA, 2019a, *Air Quality e-Reporting. Air quality database*, https://www.eea.europa.eu/data-and-maps/data/aqereporting-8. Data extracted in March 2019.

EEA, 2019b, *Air quality in Europe – 2019 Report*, EEA Report 10/2019, https://www.eea.europa.eu/publications/air-quality-in-europe-2019.

EEA, 2019c, *Exceedance of air quality limit values in urban areas, CSI004 indicator assessment,* https://www.eea.europa.eu/data-and-maps/indicators/exceedance-of-air-quality-limit-3/assessment-5.

EEA, 2019d, *Exposure of ecosystems to acidification, eutrophication and ozone,* https://www.eea.europa.eu/data-and-maps/indicators/exposure-of-ecosystems-to-acidification-14/assessment-2.

EU, 2008, *Directive 2008/50/EC of the European Parliament and of the Council of 21 May 2008 on ambient air quality and cleaner air for Europe*, OJ L 152, 11.06.2008, 1-44. http://eur-lex.europa.eu/LexUriServ/LexUriServ.do?uri=OJ:L:2008:152:0001:0044:EN:PDF.

Eurostat, 2014, *GEOSTAT 2011 grid dataset, Population distribution dataset,* http://ec.europa.eu/eurostat/web/gisco/geodata/reference-data/population-distribution-demography.

Eurostat, 2019, *Total population for European states for 2017*, http://epp.eurostat.ec.europa.eu/tgm/table.do?tab=table&language=en&pcode=tps00001&tableSelection=1&footnotes=yes&labeling=labels&plugin=1.

EMEP, 2018, *Transboundary particular matter, photo-oxidants, acidifying and eutrophying components*, EMEP Report 1/2018, http://emep.int/publ/reports/2018/EMEP_Status_Report_1_2018.pdf.

Gilbert, R.O., 1987, *Statistical Methods for Environmental Pollution Monitoring*, Van Nostrand Reinhold, New York.

Guerreiro, C., et al., 2016, Benzo(a)pyrene in Europe: Ambient air concentrations, population exposure and health effects, *Environmental Pollution* 214, 657–667.

Horálek, J., et al., 2005, *Interpolation and assimilation methods for European scale air quality assessment and mapping, Part II: Development and testing new methodologies,* ETC/ACC Technical paper 2005/8, http://www.eionet.europa.eu/etcs/etc-atni/products/etc-atni-reports/etcacc_technpaper_2005_8_spatial_aq_dev_test_part_ii.

Horálek, J., et al., 2007, *Spatial mapping of air quality for European scale assessment*, ETC/ACC Technical paper 2006/6, http://www.eionet.europa.eu/etcs/etc-atni/products/etc-atni-reports/etcacc_technpaper_2006_6_spat_aq.

Horálek, J., et al., 2008, *European air quality maps for 2005 including uncertainty analysis*, ETC/ACC Technical paper 2007/7, http://www.eionet.europa.eu/etcs/etc-atni/products/etc-atni-reports/etcacc_tp_2007_7_spataqmaps_ann_interpol.

Horálek, J., et al., 2010, *Methodological improvements on interpolating European air quality maps,* ETC/ACC Technical Paper 2009/16, http://www.eionet.europa.eu/etcs/etc-atni/products/etc-atni-reports/etcacc_tp_2009_16_improv_spataqmapping.

Horálek, J., et al., 2014, *Additional 2011 European air quality maps*, ETC/ACM Technical Paper 2014/5, http://www.eionet.europa.eu/etcs/etc-atni/products/etc-atni-reports/etcacm_tp_2014_5_add_2011_aqmaps.

Horálek, J., et al., 2016a, *Application of FAIRMODE Delta tool to evaluate interpolated European air quality maps for 2012*, ETC/ACM Technical Paper 2015/2, http://www.eionet.europa.eu/etcs/etc-atni/products/etc-atni-reports/etcacm_tp_2015_2_delta_evaluation_aqmaps2012.

Horálek, J., et al., 2016b, *European air quality maps of PM and ozone for 2013 and their uncertainty,* ETC/ACM Technical Paper 2015/5, http://www.eionet.europa.eu/etcs/etc-atni/products/etc-atni-reports/etcacm_tp_2015_5_aqmaps2013.

Horálek, J., et al., 2017a, *Potential improvements on benzo(a)pyrene (BaP) mapping*, ETC/ACM Technical Paper 2016/3, http://www.eionet.europa.eu/etcs/etc-atni/products/etc-atni-reports/etcacm_tp_2016_3_bap_improved_mapping.

Horálek, J., et al., 2017b, *European air quality maps for 2014,* ETC/ACM Technical Paper 2016/6, http://www.eionet.europa.eu/etcs/etc-atni/products/etc-atni-reports/etcacm_tp_2016_6_aqmaps2014.

Horálek, J., et al., 2017c, *Inclusion of land cover and traffic data in NO_2 mapping methodology,* ETC/ACM Technical Paper 2016/12. http://www.eionet.europa.eu/etcs/etc-atni/products/etc-atni-reports/etcacm_tp_2016_12_lc_and_traffic_data_in_no2_mapping.

Horálek, J., et al., 2018a, *European air quality maps for 2015,* ETC/ACM Technical Paper 2017/7, http://www.eionet.europa.eu/etcs/etc-atni/products/etc-atni-reports/etcacm_tp_2017_7_aqmaps2015.

Horálek, J., et al., 2018b, *Satellite data inclusion and kernel based potential improvements in NO_2 mapping,* ETC/ACM Technical Paper 2017/14, http://www.eionet.europa.eu/etcs/etc-atni/products/etc-atni-reports/etcacm_tp_2017_14_improved_aq_no2mapping.

Horálek, J., et al., 2019a, *European air quality maps for 2016*, Eionet Report ETC/ACM 2018/8, http://www.eionet.europa.eu/etcs/etc-atni/products/etc-atni-reports/etc-acm-report-2018-8-european-air-quality-maps-for-2016.

Horálek, J., et al., 2019b, *Land cover and traffic data inclusion in PM mapping*, Eionet Report ETC/ACM 2018/18, http://www.eionet.europa.eu/etcs/etc-atni/products/etc-atni-reports/etc-acm-report-18-2018-land-cover-and-traffic-data-inclusion-in-pm-mapping.

JRC, 2009, *Population density disaggregated with Corine land cover 2000. 100x100 m^2 grid resolution,* EEA version popu01clcv5.tif of 24 Sep 2009. http://www.eea.europa.eu/data-and-maps/data/population-density-disaggregated-with-corine-land-cover-2000-2.

Mareckova, K., et al., 2018, *Inventory Review 2018. Review of emission data reported under the LRTAP Convention and NEC Directive. Stage 1 and 2 review & Status of gridded and LPS data.* EEA/CEIP Technical Report 2/2017. https://webdab01.umweltbundesamt.at/download/InventoryReport_2018_v2.pdf.

NILU, 2018, *EBAS, database of atmospheric chemical composition and physical properties* (NILU, Norway). http://ebas.nilu.no/.

NMI, 2018, *EMEP/MSC-W modelled air concentrations and depositions. Gridded data for 2017, using 2016 emission* (2018 Reporting), EMEP01deg, http://www.emep.int/mscw/mscw_ydata.html.

ORNL, 2008, *ORNL LandScan high resolution global population data set.* http://www.ornl.gov/sci/landscan/landscan_documentation.shtml.

Simpson, D., et al., 2012, The EMEP MSC-W chemical transport model – technical description. *Atmos. Chem. Phys.*, 12, 7825–7865, doi:10.5194/acp-12-7825-2012, http://www.atmos-chem-phys.net/12/7825/2012/acp-12-7825-2012.html.

UNECE, 2004, *Manual on methodologies and criteria for modelling and mapping critical loads and levels and air pollution effects, risks and trends*. UNECE Convention on Long-range Transboundary Air Pollution. http://www.icpmapping.org/Mapping_Manual.

UNECE, 2016, *Forest condition in Europe. 2016 report of ICP Forests.* UNECE Convention on Long-range Transboundary Air Pollution.
http://www.wsl.ch/info/mitarbeitende/schaub/ICPF_TR_2016.pdf.

WHO, 2005, *WHO Air quality guidelines for particulate matters, ozone, nitrogen dioxide and sulphur dioxide,* Global update 2005,
http://www.who.int/phe/health_topics/outdoorair/outdoorair_aqg/en/index.html.

WHO, 2013, *Health risks of air pollution in Europe – HRAPIE project. Recommendations for concentration–response functions for cost–benefit analysis of particulate matter, ozone and nitrogen dioxide.*
http://www.euro.who.int/__data/assets/pdf_file/0006/238956/Health_risks_air_pollution_HRAPIE_project.pdf.

Annexes

Annex 1 – Methodology

A1.1 Mapping method

Previous technical papers prepared by Horálek et al. (2005, 2007, 2008, 2010, 2014, 2017c, 2019b), De Smet et al. (2011), Denby et al. (2011a, 2011b) discuss methodological developments and details on spatial interpolations and their uncertainties. Compared to the preceding report (Horálek et al., 2019a), the improved mapping methodology for PM_{10} and $PM_{2.5}$ as developed in Horálek et al. (2019b) is used in this report. This annex summarizes the currently applied method for all the considered indicators. The mapping method has been evaluated with the FAIRMODE Delta tool in Horálek et al. (2016a). The method is called as the *Regression – Interpolation – Merging Mapping*.

Pseudo $PM_{2.5}$ and NO_x station data estimation

To supplement $PM_{2.5}$ measurement data, in the mapping procedure we also use data from so-called *pseudo $PM_{2.5}$ stations.* These data are the estimates of $PM_{2.5}$ concentrations at the locations of PM_{10} stations with no $PM_{2.5}$ measurement. These estimates are based on PM_{10} measurement data and different supplementary data, using linear regression:

$$\hat{Z}_{PM2.5}(s) = c + b.Z_{PM10}(s) + a_1.X_1(s) + ... + a_n.X_n(s) \quad \text{(A1.1)}$$

where $\hat{Z}_{PM2.5}(s)$ is the estimated value of $PM_{2.5}$ at the station *s*,

$Z_{PM10}(s)$ is the measurement value of PM_{10} at the station *s*,

$X_1(s),..., X_n(s)$ are the values of other supplementary variables at the station *s*,

$c, b, a_1,..., a_n$ are the parameters of the linear regression model calculated based on the data at the points of measuring stations with both $PM_{2.5}$ and PM_{10} measurements,

n is the number of other supplementary variables used in the linear regression model (apart from PM_{10}).

When applying this estimation method, all background stations (either classified as rural, urban or suburban) are handled together for estimating $PM_{2.5}$ values at background pseudo stations. For details, see Denby et al. (2011b). For estimating $PM_{2.5}$ values at urban traffic pseudo stations, Equation A1.1 is applied for the urban traffic stations. For details, see by Horálek et al. (2019b).

To supplement NO_x measurement data, we estimate NO_x values at the locations of NO_2 stations with no NO_x data. The estimates are calculated similarly as in Horálek et al. (2007), using quadratic regression:

$$\hat{Z}_{NOx}(s) = a.Z_{NO2}(s)^2 + b.Z_{NO2}(s) + c \quad \text{(A1.2)}$$

where $\hat{Z}_{NOx}(s)$ is the estimated value of NO_x at the station *s*,

$Z_{NO2}(s)$ is the measurement value of NO_2 at the station *s*,

a, b, c are the parameters of the quadratic regression calculated based on the data at the points of measuring stations with both NO_x and NO_2 measurements.

Interpolation

The mapping method used is a linear regression model followed by kriging of the residuals produced from that model (residual kriging). Interpolation is therefore carried out according to the relation:

$$\hat{Z}(s_0) = c + a_1.X_1(s_0) + a_2.X_2(s_0) + ... + a_n.X_n(s_0) + \eta(s_0) \quad \text{(A1.3)}$$

where $\hat{Z}(s_0)$ is the estimated value of the air pollution indicator at the point s_o,

$X_1(s_0), X_2(s_0),..., X_n(s_0)$ are the n number of individual supplementary variables at the point s_o

$c, a_1, a_2,..., a_n$ are the $n+1$ parameters of the linear regression model calculated based on the data at the points of measurement,

$\eta(s_0)$ is the spatial interpolation of the residuals of the linear regression model at the point s_o calculated based on the residuals at the points of measurement.

For different pollutants and area types (rural, urban background, and in the case of PM and NO_2 , also urban traffic), different supplementary data are used, depending on their improvement to the fit of the regression. Ordinary kriging is used to interpolate the residuals:

$$\hat{R}(s_0) = \sum_{i=1}^{N} \lambda_i R(s_i), \sum_{i=1}^{N} \lambda_i = 1, \quad \text{(A1.4)}$$

where $R(s_i)$ are the residuals in the points of the measuring stations s_i ,

$\lambda_1, ..., \lambda_N$ are the weights estimated based on variogram,

N is the number of the stations used in the interpolation.

The variogram (as a measure of a spatial correlation) is estimated using a spherical function (with parameters *nugget, sill, range*). For details, see Horálek et al. (2007), Section 2.3.5 and Cressie (1993).

For $PM_{2.5}$ and NO_x, both measurement data and the estimated data from the pseudo stations are used.

For the PM_{10} and $PM_{2.5}$ indicators we apply, prior to linear regression and interpolation, a logarithmic transformation to measurement and EMEP model concentrations. In the case of $PM_{2.5}$ rural map layer creation, population density is also log-transformed. After interpolation, we apply a back-transformation. For details, see De Smet et al. (2011) and Denby et al. (2008). In the case of urban background $PM_{2.5}$ map, we do not use any supplementary data – we apply just lognormal kriging.

For the vegetation related indicators (AOT40 for vegetation and forests and NO_x) we only construct rural maps based on rural background stations, based on the assumption that no vegetation is located in urban areas. For the health related indicators, we construct the rural and urban background map layers (and for PM and NO_2 also urban traffic map layer) separately and then we merge them.

Merging of rural and urban background (and urban traffic) map layers

Health related indicator map layers for ozone are constructed (using linear regression with kriging of its residuals) for the rural and urban background areas separately on a grid at 10x10 km^2 resolution. The rural map is based on rural background stations and the urban background map on urban and suburban background stations. Subsequent to this, the rural and urban background maps are merged into one combined air quality indicator map using a European-wide population density grid at 1x1 km^2 resolution. For the 1x1 km^2 grid cells with a population density less than a defined value of α_1, we select the rural map value and for grid cells with a population density greater than a defined value α_2, we select the urban background map value. For areas with population density within the interval (α_1, α_2) a weighting function of α_1 and α_2 is applied (for details and the setting of the parameters α_1 and α_2,

see Horálek et al., 2005, 2007, 2010). This applies to the grid cells where the estimated rural value is lower (PM_{10}, $PM_{2.5}$ and NO_2) or higher (ozone), than the estimated urban background map value. In limited areas when this criterion does not hold, we apply a joint urban/rural map layer (created using all background stations regardless their type), as far as its value lies in between the rural and urban background map value. For details, see De Smet et al. (2011).

Summarising, the separate ozone rural, urban and joint urban/rural map layers are constructed at a resolution of 10x10 km^2; their merging however takes place on the basis of the 1x1 km^2 resolution population density grid, resulting in a final combined pollutant indicator map on this 1x1 km^2 resolution grid. This map is used both for the population exposure estimates and for presentational purposes.

In the case of PM_{10}, $PM_{2.5}$ and NO_2, separate map layers are created for rural, urban background and urban traffic areas on a grid at 1x1 km^2 resolution. The rural background map layer is based on the rural background stations, the urban background map layer on the urban and the suburban background stations, and the urban traffic map layer on the urban and the suburban traffic stations. For different map layers (rural, urban background, urban traffic) different supplementary data are used, depending on their improvement to the fit of the regression. The three map layers are merged into one final map using a weighting procedure

$$\hat{Z}_F(s_0) = \left(1 - w_U(s_0)\right) \cdot \hat{Z}_R(s_0) + w_U(s_0)\left(1 - w_T(s_0)\right) \cdot \hat{Z}_{UB}(s_0) + w_U(s_0) w_T(s_0) \cdot \hat{Z}_T(s_0) \qquad \text{(A1.5)}$$

where $\hat{Z}_F(s_0)$ is the resulting estimated concentration in a grid cell s_o for the final map,

$\hat{Z}_{UB}(s_0)$ is the estimated concentration in a grid cell s_o for the urban background map layer,

$\hat{Z}_R(s_0)$ is the estimated concentration in a grid cell s_o for the rural background map layer,

$\hat{Z}_T(s_0)$ is the estimated concentration in a grid cell s_o for the urban traffic map layer,

$w_U(s_0)$ is the weight representing the ratio of the urban character of the a grid cell s_o,

$w_T(s_0)$ is the weight representing the ratio of areas exposed to traffic air quality in a grid cell s_o.

The weight $w_U(s_0)$ is based on the population density grid, while $w_T(s_0)$ is based on the buffers around the roads. For further details, see Horálek et al. (2017b and references therein).

In all calculations and map presentations the EEA standard projection ETRS89-LAEA5210 (also known as ETRS89 / LAEA Europe, see www.epsg-registry.org) is used. The interpolation and mapping domain consists of the areas of all EEA member and cooperating countries, and other microstates, as far as they fall into the EEA map extent *Map_2c* (EEA, 2018). The mapping area covers the whole Europe apart from Belarus, Moldova, Ukraine and the European parts of Russia and Kazakhstan.

A1.2 Calculation of population and vegetation exposure

Population and vegetation exposure estimates are based on the interpolated concentration maps, population density data and land cover data.

Population exposure

Population exposure for individual countries and for Europe as a whole is calculated for ozone from the air quality maps and population density data, both at 1x1 km^2 resolution. For each concentration class, the total population per country as well as the European-wide total is determined.

For PM and NO_2, the population exposure is calculated separately for the areas where the air quality is considered to be directly influenced by traffic and for the background (both rural and urban) areas. For each concentration class '*j*', the percentage population per country as well as the European-wide total is determined according to:

$$P_j = \frac{\sum_{i=1}^{N} I_{Bij}\left(1 - w_U(i)w_T(i)\right)p_i + \sum_{i=1}^{N} I_{Tij} w_U(i) w_T(i) p_i}{\sum_{i=1}^{N} p_i} \cdot 100 \qquad \text{(A1.6)}$$

where P_j is the percentage population living in areas of the *j*-th concentration class in either the country or in Europe as a whole,

p_i is the population in the *i*-th grid cell,

I_{Bij} is the Boolean 0-1 indicator showing whether the background air quality concentration (estimated by the combined rural/urban background map layer) in the *i*-th grid cell is within the *j*-th concentration class (I_{Bij} = 1), or not (I_{Bij} = 0),

I_{Tij} is the Boolean 0-1 indicator showing whether the traffic air quality concentration in the *i*-th grid cell is within the *j*-th concentration class (I_{Tij} = 1), or not (I_{Tij} = 0),

N is the number of grid cells in the country or in Europe as a whole.

In addition, we express per-country and European-wide exposure as the population-weighted concentration, i.e. the average concentration weighted according to the population in a 1x1 km^2 grid cell:

$$\hat{c} = \frac{\sum_{i=1}^{N} c_i p_i}{\sum_{i=1}^{N} p_i} \qquad \text{(A1.7)}$$

where $\hat{c}$ is the population-weighted average concentration in the country or in the whole of Europe,

p_i is the population in the i^{th} grid cell,

c_i is the concentration in the i^{th} grid cell (based on the final merged map),

N is the number of grid cells in the country or in Europe as a whole.

Estimation of trends

For detecting and estimating the trends in time series of annual values of population exposure, the non-parametric Mann-Kendall's test for testing the presence of the monotonic increasing or decreasing trend is used. Next to that, the non-parametric Sen's method for estimating the slope of a

linear trend is executed. For details, see Gilbert (1987). The significance of the Mann-Kendal test is shown by the usual way, i.e. + for 0.1, * for 0.05, ** for 0.01, and *** for 0.001.

Vegetation (and forest) exposure

Vegetation (and forest) exposure for individual countries and for Europe as a whole is calculated based on the air quality maps and land cover data, both in 2x2 km^2 grid resolution. For each concentration class, the total vegetation (and forest) area per country as well as European-wide is determined.

Next to this, we express per-country and European-wide exposure as the vegetation (forest)-weighted concentration, i.e. the average concentration weighted according to the vegetation (and forest) in a 1x1 km^2 grid cell, similarly like in Eq. A1.7.

A1.3 Methods for uncertainty analysis

The uncertainty estimation of the European map is based on cross-validation. The cross-validation method computes the quality of the spatial interpolation for each measurement point from all available information except from the point in question, i.e. it withholds one data point and then makes a prediction at the spatial location of that point. This procedure is repeated for all measurement points in the available set. The predicted and measurement values at these points are plotted in the form of a scatter plot. With help of statistical indicators the quality of the predictions is demonstrated objectively. The advantage of the nature of this cross-validation technique is that it enables evaluation of the quality of the predicted values at locations without measurements, as long as they are within the area covered by the measurements.

In addition, we make a simple comparison between the point measurements and interpolated values of the 10x10 km^2 grid for the separate rural and urban maps and the 1x1 km^2 grid for the final combined maps, for the health-related indicators, resp. the 2x2 km^2 grid in the case of AOT40 and NO_x. Note that the grid cell value is the averaged result of the interpolation in this grid cell area. The interpolated value within a grid cell will only approximate the predicted value(s) at the station(s) lying within that cell.

Another method to estimate uncertainties is based on geostatistical theory: together with the prediction, the prediction standard error is computed at all the grid cells, which represents in fact the interpolation uncertainty map (see Cressie, 1993 for a detailed discussion). Based on the concentration and the uncertainty map, the exceedance probability map is created.

Cross-validation

The results of cross-validation are described by the statistical indicators and scatter plots. The main indicator used is root mean squared error (RMSE) and additional is bias (mean prediction error, MPE):

$$RMSE = \sqrt{\frac{1}{N}\sum_{i=1}^{N}(\hat{Z}(s_i) - Z(s_i))^2} \quad \text{(A1.8)}$$

$$bias(MPE) = \frac{1}{N}\sum_{i=1}^{N}(\hat{Z}(s_i) - Z(s_i)) \quad \text{(A1.9)}$$

where $Z(s_i)$ is the air quality indicator value derived from the measured concentration at the i^{th} point, $i = 1, \ldots, N$,

$\hat{Z}(s_i)$ is the air quality estimated indicator value at the i^{th} point using other information, without the indicator value derived from the measured concentration at the i^{th} point,

N is the number of the measuring points.

Next to the RMSE expressed in the absolute units, one could express this uncertainty in relative terms by relating the RMSE to the mean of the air pollution indicator value for all stations:

$$RRMSE = \frac{RMSE}{\overline{Z}}.100 \quad \text{(A1.10)}$$

where $RRMSE$ is the relative RMSE, expressed in percent,

$\overline{Z}$ is the arithmetic average of the indicator values $Z(s_1), \ldots, Z(s_N)$, as derived from measurement concentrations at the station points $i = 1, \ldots, N$.

Other indicators are R^2 and the regression equation parameters *slope* and *intercept*, following from the scatter plot between the predicted (using cross-validation) and the observed concentrations.

RMSE should be as small as possible, bias (MPE) should be as close to zero as possible, R^2 should be as close to *1* as possible, slope *a* should be as close to *1* as possible, and intercept *c* should be as close to zero as possible (in the regression equation $y = a.x + c$).

In the cross-validation of $PM_{2.5}$ and NO_x, only stations with $PM_{2.5}$, resp. NO_x, measurement data are used (not the pseudo $PM_{2.5}$, resp. NO_x, stations).

Comparison of the point measurement and interpolated grid values

The comparison of point measurement and predicted grid values is described by the linear regression equation and its parameters and statistical values. The comparison is executed separately for rural and urban background maps and for the final combined map. In the case of $PM_{2.5}$ and NO_x, only the stations with actual $PM_{2.5}$ resp. NO_x measurement data are used (not the pseudo $PM_{2.5}$ resp. NO_x stations).

The point observation – point cross-validation prediction analysis (Annex 3) describes interpolation performance at point locations when there is no observation (as it follows the leave-one-out approach). In this case, the smoothing effect of the interpolation is most prevalent.

The point observation – grid prediction approach indicates performance of the value for the 10x10 km^2 (resp. 2x2 km^2 or 1x1 km^2) grid cell with respect to the observations that are located within that cell. As such, some variability is due to smoothing but it also includes smoothing due to spatial averaging into the 10x10 km^2 (2x2 km^2, 1x1 km^2) grid cells. As such, the point-grid validation approach tells us how well our interpolated and aggregated grid values approximate the measurements at the actual station (point) locations. Whereas the point-point approach tells us how well our interpolated values estimate the indicator at a point where there is no actual measurement at that location, under the constrained that the point lies within the area covered by measurements.

Annex 2 – Input data

The types of input data in this paper are not different from that of Horálek et al. (2019a). The air quality and meteorological data has been updated. No further changes in selecting and processing of the input data have been implemented. For readability of this paper, we reproduce here the list of the input data. The key data is the air quality measurements at the monitoring stations extracted from Air Quality e-Reporting database, including geographical coordinates (*latitude*, *longitude*). The supplementary data cover the whole mapping domain and are converted into the EEA reference projection ETRS89-LAEA5210 on a 1 x 1 km grid resolution (for health related indicators apart from ozone) resp. a 10x10 km^2 grid resolution (ozone). The data for the maps of vegetation related indicators (particularly AOT40) were converted – like in the previous reports (Horálek et al., 2019a and references cited therein) – into a 2 x 2 km^2 resolution to allow accurate land cover exposure estimates to be prepared for use in Core Set Indicator 005 of the EEA.

A2.1 Air quality monitoring data

Air quality station monitoring data for the relevant year as extracted from the official EEA Air Quality e-Reporting database, EEA (2019a), in January–March 2019 has been used. This data set is supplemented with several EMEP rural stations from the database EBAS (NILU, 2019) not reported to the Air Quality e-Reporting database. Specifically, 7 additional stations for PM_{10}, 4 for $PM_{2.5}$, 6 for NO_2 and 5 for NO_x from the EBAS database (NILU, 2019) are added. Only data from stations classified as *background* (for the three types of area, *rural*, *suburban* and *urban*) are used for ozone. *Industrial* and *traffic* station types are not considered; they represent local scale concentration levels not applicable at the mapping resolution employed. For PM and NO_2, next to the background stations, also the stations classified as *traffic* for the types of area *suburban* and *urban* are used.

The following pollutants and aggregations are considered:

PM_{10} – annual average [µg·m^{-3}], year 2017
– 90.4 percentile of the daily average values [µg·m^{-3}], year 2017

$PM_{2.5}$ – annual average [µg·m^{-3}], year 2017

Ozone – 93.2 percentile of the maximum daily 8-hour average values [µg·m^{-3}], year 2017
– SOMO35 [µg·m^{-3}·day], year 2017
– SOMO10 [µg·m^{-3}·day], year 2017
– AOT40 for vegetation [µg·m^{-3}·hour], year 2017
– AOT40 for forests [µg·m^{-3}·hour], year 2017

NO_2 – annual average [µg·m^{-3}], year 2017

NO_x – annual average [µg·m^{-3}], year 2017

NO – annual average [µg·m^{-3}], year 2017 (for the purposes of NO_x mapping only)

The exact values of percentiles are actually 90.41 in the case of PM_{10} daily means and 93.15 in the case of ozone maximum daily 8-hour means.

For a considerable number of stations NO_x is measured, but it is not reported as such but separately as NO and NO_2. For these stations reporting NO and NO_2 separately, the NO_x concentrations were derived according to the equation

$$NO_x = NO_2 + \frac{46}{30} \cdot NO \qquad \text{(A2.1)}$$

In this equation, all components are expressed in $\mu g \cdot m^{-3}$, with a molecular mass for NO of 30 $g \cdot mol^{-1}$ and for NO_2 of 46 $g \cdot mol^{-1}$.

SOMO35 is the annual sum of the differences between maximum daily 8-hour concentrations above 70 $\mu g \cdot m^{-3}$ (i.e. 35 ppb) and 70 $\mu g \cdot m^{-3}$. SOMO10 is the annual sum of the differences between maximum daily 8-hour concentrations above 20 $\mu g \cdot m^{-3}$ (i.e. 10 ppb) and 20 $\mu g \cdot m^{-3}$. AOT40 is the sum of the differences between hourly concentrations greater than 80 $\mu g \cdot m^{-3}$ (i.e. 40 ppb) and 80 $\mu g \cdot m^{-3}$, using only observations between 08:00 and 20:00 CET, calculated over the three months from May to July for AOT40 for vegetation and over the six months from April to September for AOT40 for forests.

Only the stations with annual data coverage of at least 75 percent are used. In the case of SOMO35, SOMO10 and AOT40 indicators, a correction for the missing data is applied according to the equation

$$I_{corr} = I \cdot \frac{N_{\max}}{N} \qquad \text{(A2.2)}$$

where I_{corr} is the corrected indicator (SOMO35, SOMO10, AOT40 for vegetation or AOT40 for forests),
I is the value of the given indicator without any correction,
N is the number of the available daily resp. hourly data in a year for the given station,
N_{max} is the maximum possible number of the days or hours applicable for the given indicator.

For the x^{th} highest values (i.e. for the PM_{10} indicator 36th highest daily mean and for the ozone indicator 26th highest maximum daily 8-hour running mean) used in earlier reports (Horálek et al., 2016b and references cited therein), no correction for missing data was applied. The most straightforward way to solve the missing data issue in these cases is to use percentiles instead of the x^{th} highest values. Since ETC/ACM Technical Paper 2016/6 with its 2014 maps, the 90.4 percentile of PM_{10} daily means and the 93.2 percentile of ozone maximum daily 8-hour means is used.

For the indicators relevant to human health (i.e. for all PM_{10} and $PM_{2.5}$ indicators, ozone indicators 93.2 percentile of maximum daily 8-hour means, SOMO35 and SOMO10, and NO_2 annual average), data from *rural*, *urban* and *suburban background* stations are considered. (Throughout the paper, the urban and suburban stations are handled together). For PM_{10} and $PM_{2.5}$ and NO_2, also *urban* and *suburban traffic* stations are considered. For the indicators relevant to vegetation damage (i.e. for both ozone AOT40 parameters and NO_x annual average), only *rural background* stations are considered. In case of existing data (with sufficient annual time coverage) from two or more different measurement devices in the same station location, the average of these data is used.

We excluded the stations from French overseas areas (departments), Svalbard, Azores, Madeira and Canary Islands. These areas outside the EEA map extent *Map_2c* (EEA, 2018) were excluded from the interpolation and mapping domain.

Table A2.1 shows the number of the measurement stations selected for the individual pollutants and their respective indicators.

Table A2.1 Number of stations selected for each pollutant indicator and area type, 2017

Station type	PM_{10}		$PM_{2.5}$	ozone					NO_2	NO_x
	Ann. avg.	90.4 perc. of d. means	Annual average	93.2 perc. of dmax- 8h	SOMO35	SOMO10	AOT40 for veg.	AOT40 for forests	Ann. avg.	Ann. avg.
Rural background	362	352	202	536	536	514	529	534	452	350
Urban/suburban backgr.	1385	1385	686	1148	1148	1078			1333	
Urban/suburban traffic	747	747	330						977	

Compared to 2016, the number of rural background stations selected for 2017 increased by approximately 5 % for NO_2, while it is about the same (i.e. with a change minor than 5 %) for other pollutants. The number of the urban/suburban background stations increased by approximately 5 % for PM_{10} and by approximately 9 % for $PM_{2.5}$, while it remained almost the same for ozone and NO_2. The number of the NO_2 urban/suburban traffic stations increased by approximately 19 %. For PM_{10} and $PM_{2.5}$, the urban/suburban traffic stations have been used for the first time in the regular mapping.

For the $PM_{2.5}$ mapping, 183 additional rural background, 683 additional urban/suburban background and additional 431 urban/suburban traffic PM_{10} stations (at locations without $PM_{2.5}$ measurement) have been also used for the purpose of calculating the pseudo $PM_{2.5}$ station data.

In the case of NO_x, 303 stations with NO_x reported data have been used, while for 47 stations NO_x values are calculated from reported NO_2 and NO data using Eq. A2.1. Next to this, for the NO_x mapping 110 additional rural background NO_2 stations (at locations without NO_x measurement) were also used for the purpose of calculating the pseudo NO_x station data.

A2.2 EMEP MSC-W model output

The chemical dispersion model used in this paper is the EMEP MSC-W (formerly called Unified EMEP) model (version rv4.17a), which is an Eulerian model. Simpson et al. (2012) and https://wiki.met.no/emep/page1/emepmscw_opensource (web site of Norwegian Meteorological Institute) describe the model in more detail. Emissions for the previous year 2016 (Mareckova et al., 2018) are used and the model is driven by ECMWF meteorology for the relevant year 2017. EMEP (2018) provides details on the EMEP modelling for 2017 using 2016 emission. The resolution of the model is 0.1°x0.1°, i.e. circa 10x10 km^2. For the first time, the model output based on the emission for the previous (not actual) year has been used, in agreement with conclusion of Horálek et al. (2016b), in order to enable the map creation a half year earlier that if used the model results based on the actual emission.

We downloaded the EMEP data from NMI (2019) in the form of annual means. Next to this, we received the EMEP data in the form of daily means for PM_{10} and $PM_{2.5}$ and hourly means for ozone, and we aggregated these primary data to the same set of parameters as we have for the air quality observations:

PM_{10} – annual average [$\mu g \cdot m^{-3}$], year 2017
– 90.4 percentile of the daily average value [$\mu g \cdot m^{-3}$], year 2017 (aggregated from daily means)

$PM_{2.5}$ – annual average [$\mu g \cdot m^{-3}$], year 2017

Ozone – 93.2 percentile of the highest maximum daily 8-hour average value [$\mu g \cdot m^{-3}$], year 2016 (aggregated from hourly means)
– SOMO35 [$\mu g \cdot m^{-3} \cdot day$], year 2017 (aggregated from hourly means)
– SOMO10 [$\mu g \cdot m^{-3} \cdot day$], year 2017 (aggregated from hourly means)
– AOT40 for vegetation [$\mu g \cdot m^{-3} \cdot hour$], year 2017 (aggregated from hourly means)
– AOT40 for forests [$\mu g \cdot m^{-3} \cdot hour$], year 2017 (aggregated from hourly means)

NO_2 – annual average [$\mu g \cdot m^3$], year 2017

NO_x – annual average [$\mu g \cdot m^3$], year 2017

Due to the complete temporal data coverage available at the modelled data, the PM_{10} indicator 90.4 percentile of daily means is identical with the 36th highest daily mean and the ozone indicator 93.2 percentile of maximum daily 8-hour means is identical with the 26th highest maximum daily 8-hour mean.

In the original format of the model results, a point represents the centre of a grid cell (in 0.1°x0.1° resolution). The data was imported into *ArcGIS* as a point shapefile and converted into ETRS89-LAEA5210 projection, subsequently converted into a 100x100 m^2 resolution raster grid and spatially aggregated into the reference EEA 10x10 km^2 grid (for ozone health related indicators), 1x1 km^2 grid (for PM and NO_2), resp. into the 2x2 km^2 grid (for vegetation related indicators).

A3.3 Other supplementary data

Altitude

We use the altitude data field (in meters) of *Global Multi-resolution Terrain Elevation Data 2010 (GMTED2010)*, with an original grid resolution of 15x15 arcseconds (some 463x463 m at 60N). Source: U.S. Geological Survey Earth Resources Observation and Science, see Danielson et al. (2011). We converted the field into the ETRS 1989 LAEA projection. (The resolution after projection was in 449.2x449.2 m). In the following step, we resampled the raster dataset to 100x100 m^2 resolution and shifted it to the extent of EEA reference grid. As a final step, the dataset was spatially aggregated into 1x1 km^2, 2x2 km^2 and 10x10 km^2 resolutions.

Meteorological parameters

Actual meteorological surface layer parameters were extracted from the *Meteorological Archival and Retrieval System (MARS)* of the *ECMWF (European Centre for Medium-range Weather Forecasts)*. Currently we use the following ECMWF variables (details specified in Horálek et al. 2007, Section 4.5) on a 0.25x0.25 degrees (about 28x28 km at 60N) resolution as supplementary data in the regressions:

Wind speed	– annual average [$m.s^{-1}$], year 2017 (aggregated from 6-hour means)
Surface solar radiation	– annual average of daily sum [$MWs.m^{-2}$], year 2017 (aggregated from daily sums)

The 6-hour mean wind speed used in the aggregation is derived from the 10 meter height wind speed in U (*10U*) and V (*10V*) directions (where U and V are perpendicular vectors in horizontal directions) with magnitude $\sqrt{(10U)^2 + (10V)^2}$.

The data are imported into *ArcGIS* as a point shapefile. Each point represents the centre of a grid cell. The shapefile is converted into ETRS89-LAEA5210 projection, converted into a 100x100 m^2 resolution raster grid and spatially aggregated into the reference EEA 1x1 km^2 grid, 10x10 km^2 grid, and 2x2 km^2 grid.

Population density and population totals

Population density (in $inhbs.km^{-2}$, census 2011) is based on *Geostat 2011* grid dataset, Eurostat (2014). The dataset is in 1x1 km^2 resolution, in the EEA reference grid.

For regions not included in the Geostat 2011, alternative sources were used. Primarily, *JRC (Joint Research Centre)* population data in resolution 100x100 m^2 were used (JRC, 2009). The JRC 100x100 m^2 population density data is spatially aggregated into the reference 1x1 km^2 EEA grid. For regions that are neither included in the Geostat 2011 nor in the JRC database, we used population density data from *ORNL LandScan Global Population Dataset* (ORNL, 2008). This dataset is in 30x30 arcsec resolution; its values are based on the annual mid-year national population estimates for 2008 from the Geographic Studies Branch, US Bureau of Census, http://www.census.gov. The ORNL data is re-projected and converted from its original WGS1984 30x30 arcsecs grids into EEA's reference projection

ETRS89-LAEA5210 at 1x1 km^2 resolution by EEA (eea_r_3035_1_m_landscan-eurmed_2008, EEA, 2008).

The areas lacking Geostat 2011 data, and supplemented with JRC or ORNL data were: Gibraltar (JRC); Faroe Islands, British crown dependencies (Jersey, Guernsey and Man) and northern Cyprus (ORNL). As such, the Geostat 2011 1x1 km^2 data and these supplements cover the entire mapping area.

To verify the consistency of merging Geostat 2011 with JRC and ORNL data, we compared the Geostat 2011 data and the JRC supplemented with ORNL data on the basis of the national population totals of the individual countries. Additionally, we verified the national population totals for the Geostat 2011 gridded data with the Eurostat national population data for 2017 (Eurostat, 2019). Figure A2.1 presents both comparisons. From these verifications, one can conclude a high correlation of the national population totals of each data source. Slight underestimation of the supplemented JRC and ORNL data in comparison with the Geostat 2011 data can be seen, which is caused by the fact that the Geostat 2011 data is more up-to-date than both the JRC and the ORNL data source. Geostat 2011 and Eurostat 2017 data correlate even better and leads to a similar conclusion. Based on this, we used in the further calculations on national population totals the actual Eurostat data for 2017 (Eurostat, 2019), as described further.

Population density data can be used to classify the spatial distribution of each type of area (rural, urban or mixed population density) in Europe. We use this information to select and weight the air quality values, grid cell by grid cell and merge them into a final combined map (Annex 1). Furthermore, we use it to estimate population health exposure and exceedance numbers per country and for Europe as a whole, including involved uncertainties. These activities take place on the 1x1 km^2 resolution grid in accordance with the recommendations of Horálek et al. (2010). The supplemented Geostat data (as described above) are used in all the calculations.

Figure A2.1 Correlation of national population totals for JRC supplemented with ORNL (left) and Eurostat 2017 (right) with Geostat 2011

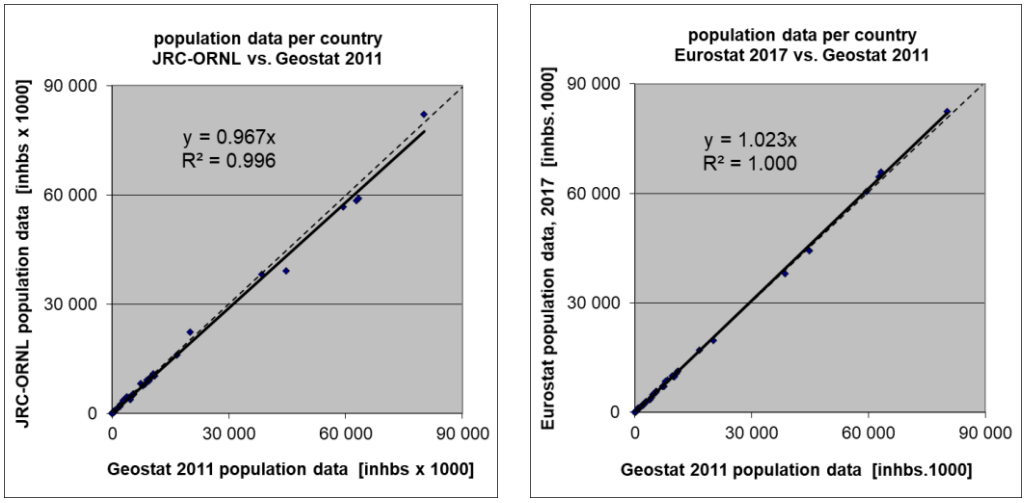

National population totals presented in the exposure tables of this paper are based on Eurostat national population data for 2017 (Eurostat, 2019). For France, Portugal and Spain, the population totals of areas outside the mapping area (i.e. French oversea departments Azores, Madeira and Canarias) are subtracted. For Andorra and Monaco with 2017 data not available, the average of 2016 and 2018 numbers is used. For northern part of Cyprus which do not have 2017 data in the Eurostat database, the population total is based on alternative data (namely http://www.devplan.org/frame-eng.html).

Land cover

CORINE Land Cover 2012 – grid 100 x 100 m^2, Version 18.5 (09/2016) is used (EEA, 2016). The country missing in this database is Andorra, the area missing in this database is the Faroe Islands. Due to the lack of land cover data for Andorra, we excluded this country from the process of exposure estimates related to the vegetation based AOT40 ozone indicators.

In agreement with Horálek et al. (2017b), the 44 CLC classes have been re-grouped into the 8 more general classes. In this paper we use four of these general classes, see Table A2.2.

Table A2.2 General land cover classes, based on CLC2012 classes, used in mapping

Label	General class description	CLC classes grid codes	CLC classes codes	CLC classes description
HDR	High density residential areas	1	111	Continuous urban fabric
LDR	Low density residential areas	2	112	Discontinuous urban fabric
AGR	Agricultural areas	12 – 22	211 – 244	Agricultural areas
NAT	Natural areas	23 – 34	311 – 335	Forest and semi natural areas

Two aggregations are used, i.e. into 1x1 km^2 grid and into the circle with radius of 5 km. For each general CLC class we spatially aggregated the high land use resolution into the 1x1 km^2 EEA standard grid resolution. The aggregated grid square value represents for each general class the total area of this class as percentage of the total 1x1 km^2 square area. For details, see Horálek (2017b).

Road type vector data

GRIP (Meijer et al., 2016) vector road type data base provided by PBL is used. The road types are distributed into 5 classes, from highways to local roads and streets. In agreement with Horálek et al. (2017b), road classes No. 1 “Highways”, No. 2 “Primary roads” and No. 3 “Secondary roads” are used.

Percentage of the area influenced by traffic is represented by buffers around the roads: for the individual classes 1 – 3 and for classes 1 – 3 together, at all 1x1 km^2 grid cells; a buffer of 75 metres distance at each side from each road vector is taken for the roads of classes 1 and 2, while a buffer of 50 metres is taken for the roads of class 3. For motivation and calculation details, see Horálek et al. (2017b).

Satellite data

Annual average NO_2 dataset was constructed from data acquired by the *OMI* instrument onboard the Aura platform. The parameter used is

NO_2 – annual average tropospheric vertical column density (VCD) [number of NO_2 molecules per cm^2 of earth surface], year 2017 (aggregated from daily data).

The OMNO2d product generated by NASA was used as a basis, NASA (2019). The tropospheric column was used. All the orbits within a given day (typically observed between 13:00 and 14:00 local time) are mapped into a 0.25x0.25 degrees grid. For details, see Horálek et al. (2018b). The data were converted to ArcGIS and spatially transformed to the reference EEA 1x1 km^2 grid, like in the case of modelled data.

Annex 3 – Technical details and mapping uncertainties

This annex contains technical details on the linear regression models and the residual kriging, including the performance. Furthermore, uncertainty estimates for the maps of the indicators are given.

A3.1 PM_{10}

Technical details on the interpolation model and uncertainty estimates for both PM_{10} indicators maps annual average (Map 2.1) and 90.4 percentile of daily means (Map 2.2) are presented in this section.

Technical details on the interpolation model

Table A3.1 presents the estimated parameters of the linear regression models (c, a_1, a_2, …) and of the residual kriging (nugget, sill, range) and includes the statistical indicators of both the regression and the kriging, for both PM_{10} indicators. The linear regression and ordinary kriging on its residuals is applied on the logarithmically transformed data of both measurement and modelled PM_{10} values. In Table A3.1 the standard error and variogram parameters (nugget, sill and range) refer to these transformed data, whereas RMSE and bias refer to the interpolation after a back-transformation.

In 2017, an updated methodology as developed and tested under Horálek et al. (2019b) has been used, i.e. including the land cover among the supplementary data and using the traffic urban map layer.

The adjusted R^2 and standard error are indicators for the fit of the regression relationship, where the adjusted R^2 should be as close to 1 as possible and the standard error should be as small as possible. The adjusted R^2 for the rural areas was 0.69 at the annual average and 0.63 at the P90.4; for the urban background areas 0.27 at the annual average and 0.28 at the P90.4; for the urban traffic areas 0.42 at the annual average and 0.34 at the P90.4.

RMSE (the smaller the better) and bias (the closer to zero the better), highlighted by orange, are the cross-validation indicators, showing the quality of the resulting map. The bias indicates to what extent the predictions are under- or overestimated on average. Further in this section, more detailed uncertainty analysis is presented.

Table A3.1 Parameters and statistics of linear regression model and ordinary kriging of PM_{10} indicators annual average and 90.4 percentile of daily means for 2017 in rural, urban background and urban traffic areas for the final combined map

		Annual average			90.4 percentile of daily means		
		Rural areas	Urb. b. ar.	Urb. tr. ar.	Rur. ar.	Urb. b. ar.	Urb. tr. ar.
Linear regresion model (LRM, Eq. A1.3)	c (constant)	4.39	1.72	2.21	4.09	1.76	2.68
	a1 (log. EMEP model)	0.586	0.562	0.45	0.524	0.622	0.40
	a2 (altitude GMTED)	-0.00034			-0.00034		
	a3 (wind speed)	-0.038		-0.051	-0.062		-0.065
	a4 (s. solar radiation)	-0.029			-0.021		
	a5 (land cover NAT)	-0.002			-0.002		
	Adjusted R^2	**0.69**	**0.27**	**0.42**	**0.63**	**0.28**	**0.34**
	Stand. Error [µg.m^{-3}]	**0.24**	**0.37**	**0.29**	**0.26**	**0.40**	**0.32**
Ordinary kriging (OK) of LRM residuals	nugget	0.027	0.032	0.019	0.027	0.023	0.028
	sill	0.053	0.080	0.050	0.055	0.105	0.065
	range [km]	900	720	210	470	670	210
LRM + OK of its residuals	**RMSE [µg.m^{-3}]**	**3.2**	**7.3**	**5.3**	**7.0**	**14.1**	**10.9**
	Relative RMSE [%]	**20.1**	**28.8**	**21.9**	**24.2**	**30.8**	**25.8**
	Bias (MPE) [µg.m^{-3}]	**0.1**	**-0.1**	**-0.2**	**0.2**	**-0.2**	**-0.3**

Uncertainty estimated by cross-validation

Using RMSE as the most common indicator, the *absolute mean uncertainty* of the final combined map at areas 'in between' the station measurements can be expressed in µg·m^{-3}. Table A3.1 shows that the absolute mean uncertainty of the final combined map of PM_{10} annual average resp. 90.4 percentile of daily means expressed by RMSE is 3.2 µg·m^{-3} resp. 7.0 µg·m^{-3} for the rural areas, 7.3 µg·m^{-3} resp. 14.1 µg·m^{-3} for the urban background areas, and 5.3 µg·m^{-3} resp. 10.9 µg·m^{-3} for the urban traffic areas. Alternatively, one can express this uncertainty in relative terms by relating the absolute RMSE uncertainty to the mean air pollution indicator value for all stations. This *relative mean uncertainty* (Relative RMSE) of the final combined map of PM_{10} annual average resp. 90.4 percentile of daily means is 20.1 % resp. 24.2 % for rural areas, 28.8 % resp. 30.8 % for urban background areas, and 21.9 % resp. 25.8 % for urban traffic areas. These quite high numbers in urban background areas compared to previous years up to 2015 are caused by inclusion of Turkey since 2016 mapping. For the mapping results without Turkey, the relative mean uncertainty is 18.3 % resp. 20.9 % for rural areas, 19.9 % resp. 22.5 % for urban background areas and 20.3 % resp. 23.8 % for urban traffic areas. Nevertheless, the relative uncertainty values including Turkey fulfil the data quality objectives for models as set in Annex I of the air quality Directive 2008/50/EC (EU, 2008).

Figure A3.1 shows the cross-validation scatter plots, obtained according to Annex 1, for rural, urban background and urban traffic areas, for both PM_{10} indicators. The R^2 indicates that the variability is attributable to the interpolation for about 79 % resp. 74 % at the rural areas, for about 68 % resp. 71 % at the urban background areas, and for about 65 % resp. 73 % at the urban traffic areas.

Figure A3.1 Correlation between cross-validated predicted (y-axis) and measurement values for PM_{10} indicators annual average (top) and 90.4 percentile of daily means (bottom) for 2016 for rural (left) and urban background (middle) and urban traffic (right) areas

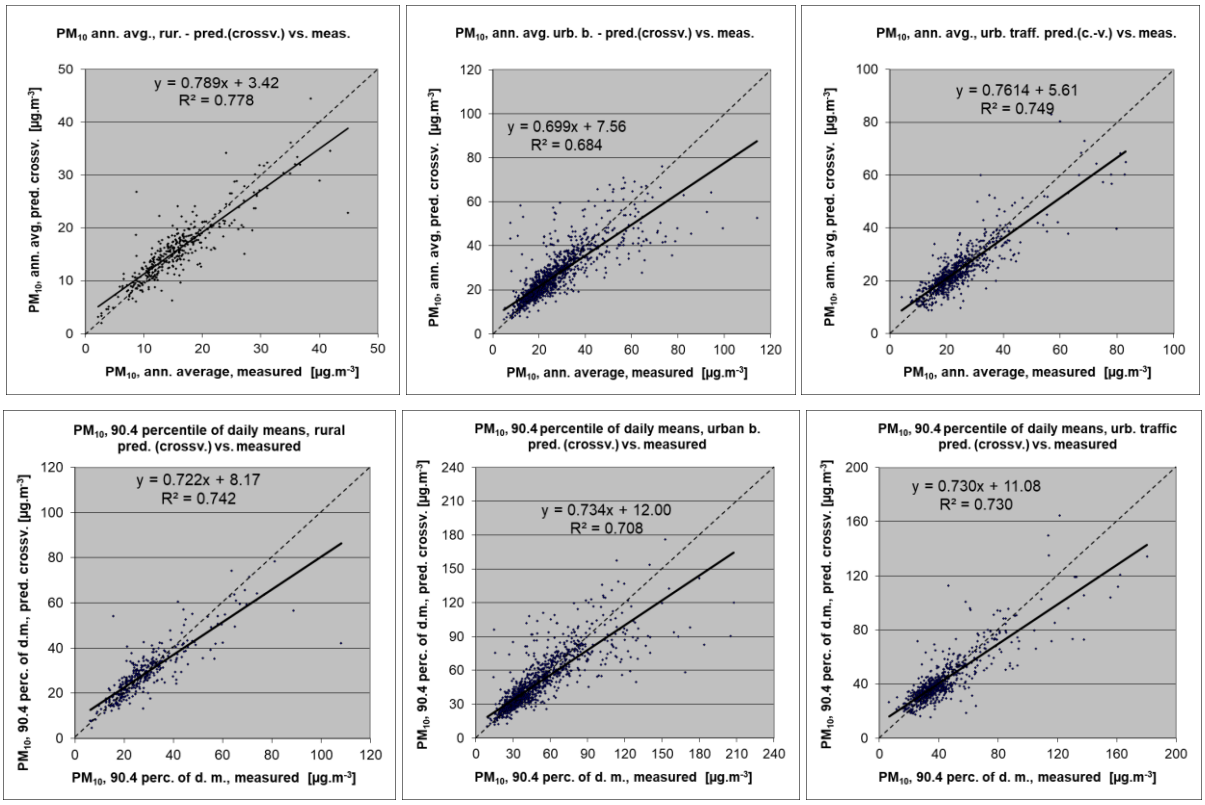

The trend line in the scatter-plots deviates at the lowest values somewhat above, and at the higher values under the symmetry axis, indicating that the interpolation methods tend to underestimate the high concentrations and overestimate the low concentrations. For example, in urban background areas for annual average an observed value of 55 µg·m^{-3} is estimated in the interpolations to be about 46 µg·m^{-3}, about 16 % lower. This underestimation at high values is common to all spatial interpolation methods. It could be reduced by either using a higher number of stations with an improved spatial distribution, or by introducing an improved regression that uses either other supplementary data or more advanced chemical transport model (resp. model in finer resolution).

Comparison of point measurement values with the predicted grid value

In addition to the above *point observation – point prediction* cross-validation, a simple comparison has been made between the point observation values and interpolated prediction values spatially averaged at grid cells. This *point observation – grid averaged prediction* comparison indicates to what extent the predicted value of a grid cell represents the corresponding measurement values at stations located in that cell. The comparison has been made primarily for the separate rural, urban background and urban traffic map layers at 1x1 km^2 resolution. (One can directly relate this comparison result to the cross-validation results of Figure A3.1). Next to this, the comparison has been done also for the final combined maps at the same 1x1 km^2 resolution. Figure A3.2 shows the scatterplots for these comparisons, for PM_{10} annual average only as an illustration. The results of the point observation – point prediction cross-validation of Figure A3.1 and those of the point observation – grid averaged prediction validation for separate rural and separate urban background maps, and for the final combined maps are summarised in Table A3.2 for both PM_{10} indicators.

Figure A3.2 Correlation between predicted grid values from rural (upper left), urban background (upper middle) and urban traffic (upper right) map layer and final combined map (all bottom) (y-axis) versus measurements from rural (left), urban/suburban background (middle) and urban/suburban traffic stations (right) (x-axis) for PM_{10} annual average 2017

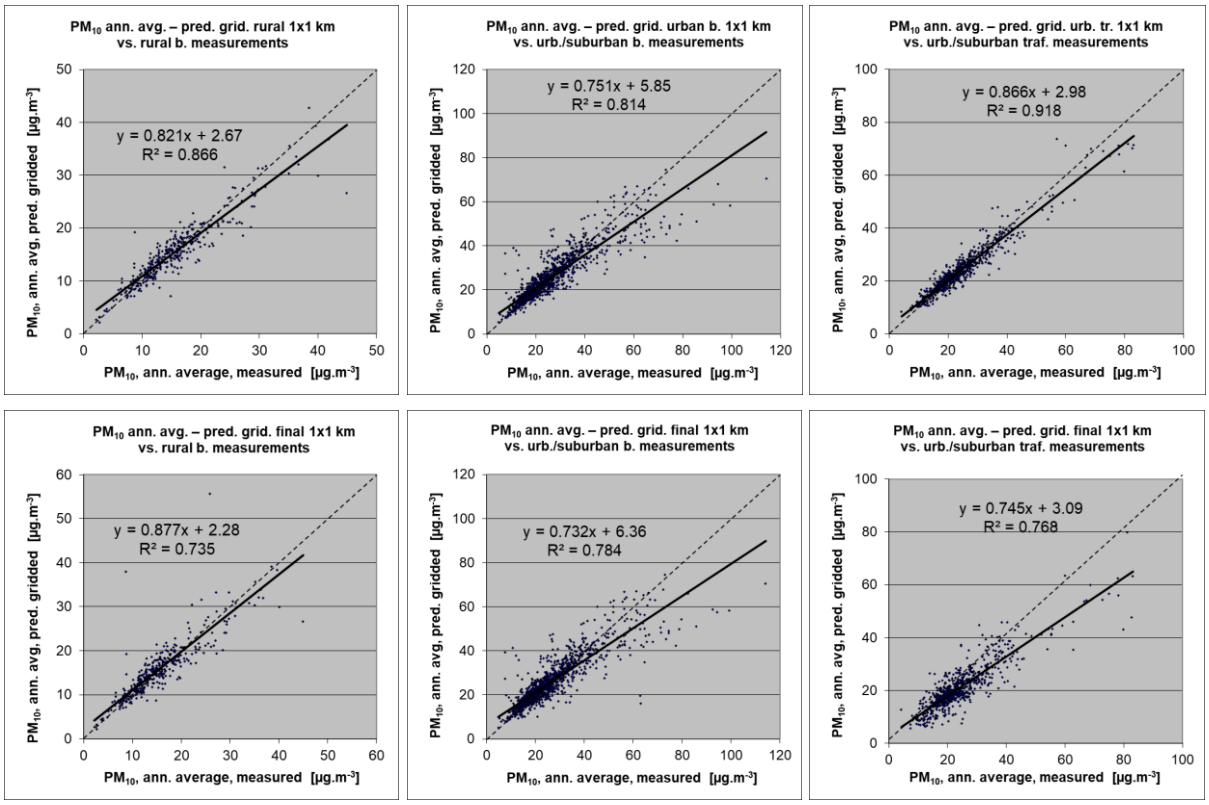

Table A3.2 Statistical indicators from the scatter plots for the predicted grid values from separate (rural, urban background or urban traffic) map layers and final combined map versus the measurement point values for rural (upper left), urban background (upper right) and urban traffic (bottom left) stations for PM_{10} indicators annual average (top) and 90.4 percentile of daily means (bottom) for 2017

PM_{10}	rural backgr. stations				urban/suburban backgr. stations			
	RMSE	bias	R^2	lin. r. equation	RMSE	bias	R^2	lin r. equation
Annual average								
cross-valid. prediction, separate (r or ub) map	3.2	0.1	0.778	y = 0.789x + 3.42	7.3	-0.1	0.684	y = 0.699x + 7.56
grid prediction, 1x1 km separate (r or ub) map	2.5	-0.2	0.866	y = 0.821x + 2.67	5.7	-0.5	0.814	y = 0.751x + 5.85
grid prediction, 1x1 km final combined map	3.7	0.3	0.735	y = 0.877x + 2.28	6.1	-0.4	0.784	y = 0.732x + 6.36
90.4 percentile of daily means								
cross-valid. prediction, separate (r or ub) map	7.0	0.2	0.742	y = 0.722x + 8.17	14.1	-0.2	0.708	y = 0.734x + 12.0
grid prediction, 1x1 km separate (r or ub) map	5.1	-0.4	0.872	y = 0.779x + 5.99	9.5	-0.8	0.872	y = 0.810x + 7.95
grid prediction, 1x1 km final combined map	6.8	0.5	0.761	y = 0.832x + 5.34	10.4	-0.8	0.847	y = 0.787x + 9.01

PM_{10}	urban/suburban traffic stations			
	RMSE	bias	R^2	lin. r. equation
Annual average				
cross-valid. prediction, urban traffic map	5.3	-0.2	0.749	y = 0.761x + 5.61
grid prediction, 1x1 km urban traffic map	3.1	-0.3	0.918	y = 0.866x + 2.98
grid prediction, 1x1 km final merged map	6.0	-3.1	0.768	y = 0.745x + 3.09
90.4 percentile of daily means				
cross-valid. prediction, urban traffic map	10.9	-0.3	0.730	y = 0.730x + 11.1
grid prediction, 1x1 km urban traffic map	6.6	-0.7	0.906	y = 0.834x + 6.34
grid prediction, 1x1 km final merged map	11.5	-5.0	0.756	y = 0.770x + 4.75

By comparing the scatterplots and the statistical indicators for the separate rural and separate urban background map with the final combined maps in both resolutions, one can evaluate the level of representation of the rural resp. urban background areas in the final combined maps. Both the rural and the urban air quality are fairly well represented in the 1x1 km^2 final combined map, while the traffic air quality is underestimated in this spatial resolution. One can conclude that the final combined map in 1x1 km^2 resolution is representative for rural and urban background areas, but not for urban traffic areas.

The Table A3.2 shows a better relation (i.e. lower RMSE, higher R^2, smaller intercept and slope closer to 1) between station measurements and the interpolated values of the corresponding grid cells at either rural, urban background or urban traffic areas than it does at the point cross-validation predictions. That is because the simple comparison between point measurements and the gridded interpolated values shows the uncertainty at the actual station locations (points), while the point cross-validation prediction simulates the behaviour of the interpolation at point positions assuming no actual measurement would exist at that point. The uncertainty at measurement locations is introduced partly by the smoothing effect of the interpolation and partly by the spatial averaging of the values in the 1x1 km^2 grid cells. The level of the smoothing effect leading to underestimation at areas with high values is there smaller than in situations where no measurement is represented in such areas. For example, in urban background areas the predicted interpolation gridded annual average value in the separate urban background map will be about 47 $\mu g \cdot m^{-3}$ at the corresponding station point with the measurement value of 50 $\mu g \cdot m^{-3}$. This means an underestimation of about 14 %. It is a slightly less than the prediction underestimation of 16 % at the same point location, when leaving out this one actual measurement point and the interpolation is done without this station (see the previous subsection).

A3.2 $PM_{2.5}$

Technical details and uncertainty estimates for Map 3.1 with the $PM_{2.5}$ annual average are presented in this section.

Technical details on the interpolation model

Like for PM_{10}, an updated methodology as developed and tested under Horálek et al. (2019b) has been used, i.e. including the land cover among supplementary data and using the traffic urban map layer.

Table A3.3 presents the regression coefficients determined for pseudo $PM_{2.5}$ stations data estimation, based on the 738 rural and urban/suburban background and 296 urban/suburban traffic stations that have both $PM_{2.5}$ and PM_{10} measurements available (see Section 2.1.1).

Table A3.3 Parameters and statistics of linear regression model for generation of pseudo $PM_{2.5}$ data, regardless of rural or urban/suburban area, for $PM_{2.5}$ annual average 2017

		Rural and urban background areas	Urban traffic areas
Linear regresion model (LRM, Eq. A1.1)	c (constant)	22.9	34.4
	b (PM_{10} measurement data)	0.717	0.594
	a1 (surface solar radiation)	-0.940	-1.022
	a2 (latitude)	-0.305	-0.492
	a3 (longitude)	0.098	0.087
	Adjusted R^2	**0.90**	**0.81**
	Standard Error [µg.m^{-3}]	**2.0**	**2.6**

The same supplementary data as in Horálek et al. (2019b) has been used, apart from the wind speed, which was found not significant.

Table A3.4 presents the estimated parameters of the linear regression models (c, a_1, a_2,…) and of the residual kriging (*nugget, sill, range*) and includes the statistical indicators of both the regression and the kriging of its residuals. Like in the case of PM_{10}, the linear regression is applied on the logarithmically transformed data of both measurement and modelled $PM_{2.5}$ values. Thus, the standard error and variogram parameters refer to these transformed data, whereas RMSE and bias refer to the interpolation after the back-transformation.

Table A3.4 Parameters and statistics of linear regression model and ordinary kriging of $PM_{2.5}$ annual average 2017 in rural, urban background and urban traffic areas for final combined map

$PM_{2.5}$		**Annual average**		
		Rural areas	**Urban b. areas**	**Urban tr.. areas**
Linear regresion model (LRM, Eq. A1.3)	c (constant)	0.84	1.47	1.12
	a1 (log. EMEP model)	0.762	0.53	0.591
	a2 (altitude GMTED)	-0.00011		
	a3 (wind speed)	*n. sign.*		
	a4 (land cover NAT1)	-0.0024		
	Adjusted R^2	**0.64**	**0.27**	**0.50**
	Standard Error [µg.m^{-3}]	**0.30**	**0.37**	**0.35**
Ordinary kriging (OK) of LRM residuals	nugget	0.048	0.017	0.029
	sill	0.077	0.107	0.083
	range [km]	410	920	360
LRM + OK of its residuals	**RMSE [µg.m^{-3}]**	**2.4**	**2.6**	**3.7**
	Relative RMSE [%]	**22.6**	**17.6**	**27.3**
	Bias (MPE) [µg.m^{-3}]	**-0.1**	**0.1**	**-1.8**

The adjusted R^2 (the closer to 1 the better) and standard error (the smaller the better) are indicators for the *quality of the fit of the regression relation*. The adjusted R^2 is 0.64 for the rural areas, 0.27 for urban background areas and 0.50 for urban traffic areas. Somewhat weaker regression relation in the urban background areas causes a higher impact of the interpolation part of the interpolation-regression-merging mapping methodology in these areas.

RMSE and bias – highlighted in orange – are the cross-validation indicators, showing the *quality of the resulting map*; the bias indicates to what extent the predictions are under- or overestimated on average. Only stations with $PM_{2.5}$ measurement data are used for calculating the RMSE and the bias (i.e. only non-pseudo $PM_{2.5}$ stations are used). These statistical indicators are calculated excluding the pseudo stations because they are estimated values only, not actual measurement values. According to Denby et al (2011b), the pseudo $PM_{2.5}$ data does not satisfy the quality objectives for fixed monitoring alone. The pseudo stations are used as they improve the mapping estimate. Whereas the actual measurements can be used for evaluating the *quality of the map*. For the future, we consider to quit the application of the $PM_{2.5}$ pseudo stations as the current number of the actual $PM_{2.5}$ measurement stations has increased over time such that the use of pseudo $PM_{2.5}$ stations may not contribute enough any longer to improve the mapping estimates.

Due to the lack of rural stations in Turkey for $PM_{2.5}$, no proper interpolation results could be presented for this country in a rural map, so we do not present the estimated $PM_{2.5}$ values for Turkey in the final map. Thus, the stations located in Turkey have not been used in the uncertainty estimates (although used in the mapping process), as they lie outside the mapping area.

Uncertainty estimated by cross-validation

Table A3.4 shows that the absolute mean uncertainty of the final combined map of $PM_{2.5}$ annual average expressed as RMSE is 2.4 $\mu g \cdot m^{-3}$ for the rural areas and 2.6 $\mu g \cdot m^{-3}$ for the urban background areas and 3.7 $\mu g \cdot m^{-3}$ for the urban traffic areas. On the other hand, the *relative mean uncertainty* (Relative RMSE) of the final combined map of $PM_{2.5}$ annual average is 22.6 % for rural areas, 17.6 % for urban background areas and 27.3 % for urban traffic areas. These relative uncertainty values fulfil the data quality objectives for models as set in Annex I of the air quality Directive 2008/50/EC (EU, 2008).

Figure A3.3 shows the cross-validation scatter plots, obtained according to Section A1.3, for both the rural and urban areas. The R^2 indicates that about 80 % of the variability is attributable to the interpolation for the rural areas and 84 % for the urban background areas and 84 % for the urban traffic areas.

Figure A3.3 Correlation between cross-validated predicted and measurement values for $PM_{2.5}$ annual average 2017 for rural (left), urban background (middle) and urban traffic (right) areas

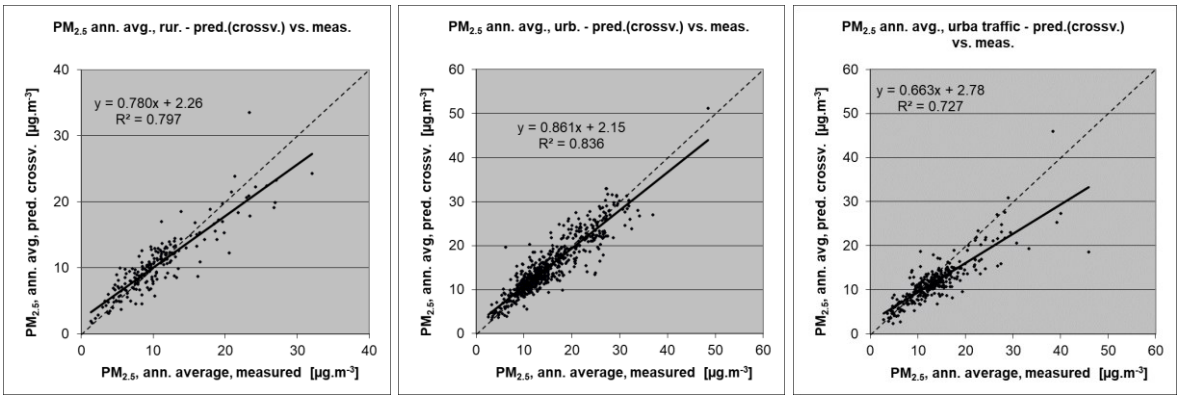

The scatter plots indicate that in areas with high concentrations the interpolation methods tend to underestimate the levels. For example, in rural areas an observed value of 25 µg·m^{-3} is estimated in the interpolations to be about 22 µg·m^{-3}, which is an underestimated prediction of about 13 %. This underestimation at high values is an inherent feature of all spatial interpolations. It could be reduced by either using a higher number of the stations at improved spatial distribution, or by introducing a closer regression that uses either other supplementary data or more improved CTM output.

Comparison of point measurement values with the predicted grid value

Next to the cross-validation comparison, a simple comparison has been made between the point observation values and interpolated prediction values spatially averaged in grid cells. This point-grid comparison indicates to what extent the predicted value of a grid cell represents the corresponding measurement values at stations located in that cell. The comparison has been made primarily for the separate rural, urban background and urban traffic map layers at 1x1 km^2 resolution. Next to this, the comparison has been done also for the final combined maps at the same 1x1 km^2 resolution. Figure A3.4 shows the scatterplots for these comparisons.

The results of the point observation – point prediction cross-validation of Figure A3.3 and those of the point observation – grid averaged prediction validation of Figure A3.4 for separate map layers and for the final combined map are summarised in Table A3.5.

Figure A3.4 Correlation between predicted grid values from rural (upper left), urban background (upper middle) and urban traffic (upper right) map layer and final combined map (all bottom) (y-axis) versus measurements from rural (left), urban/suburban background (middle) and urban/suburban traffic stations (right) (x-axis) for $PM_{2.5}$ annual average 2017

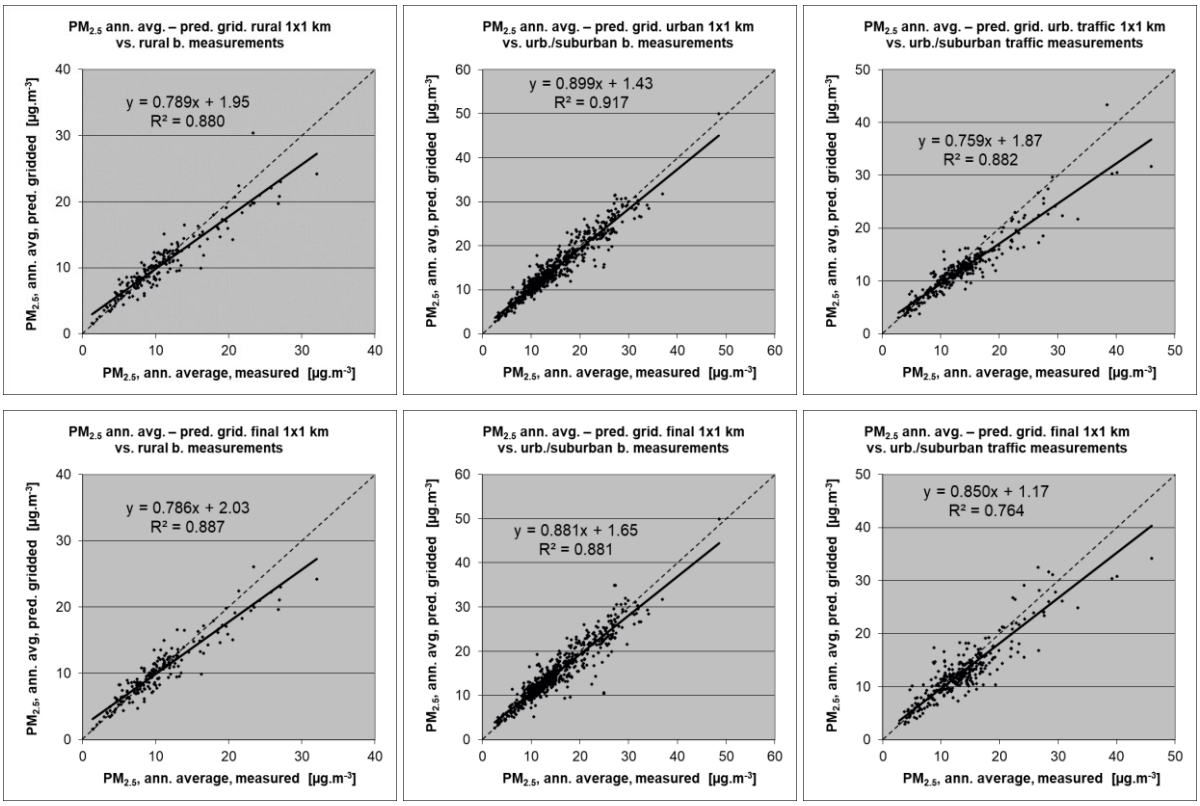

By comparing the scatterplots and the statistical indicators for separate rural, urban background and urban traffic map layers with the final combined maps, one can evaluate the level of representation of the rural, urban background and urban traffic areas in the final combined map. Similar results as for

PM_{10} can be observed: the final combined map in 1x1 km^2 resolution is fairly well representative for rural and urban background areas, but not for urban traffic areas.

Like in the case of PM_{10}, Table A3.5 shows a better correlated relation with the station measurements (i.e. lower RMSE, higher R^2, smaller intercept and slope closer to 1) for the simply interpolated gridded values than for the point cross-validation predictions, at both rural and urban background map areas. That is because the simple comparison shows the uncertainty at the actual station locations, while the cross-validation prediction simulates the behaviour of the interpolation (within the area covered by measurements) at point positions assuming no actual measurements would exist at these points.

Table A3.5 Statistical indicators from the scatter plots for the predicted grid values from separate (rural, urban background or urban traffic) map layers and final combined map versus the measurement point values for rural (upper left), urban background (upper right) and urban traffic (bottom left) stations for $PM_{2.5}$ annual average 2017

$PM_{2.5}$	rural backgr. stations				urban/suburban backgr. stations			
	RMSE	bias	R^2	lin. r. equation	RMSE	bias	R^2	lin r. equation
cross-valid. prediction, separate (r or ub) map	2.4	-0.1	0.797	y = 0.780x + 2.26	2.6	0.1	0.836	y = 0.861x + 2.15
grid prediction, 1x1 km separate (r or ub) map	1.9	-0.3	0.880	y = 0.789x + 1.95	1.9	-0.1	0.917	y = 0.899x + 1.43
grid prediction, 1x1 km final merged map	1.9	-0.2	0.887	y = 0.786x + 2.03	2.2	-0.1	0.881	y = 0.881x + 1.65

$PM_{2.5}$	urban/suburban traffic stations			
	RMSE	bias	R^2	lin. r. equation
cross-valid. prediction, urban traffic map	3.7	-1.8	0.727	y = 0.663x + 2.78
grid prediction, 1x1 km urban traffic map	2.7	-1.4	0.882	y = 0.759x + 1.87
grid prediction, 1x1 km final merged map	3.2	-0.9	0.764	y = 0.850x + 1.17

The uncertainty at measurement locations is introduced partly by the smoothing effect of the interpolation and partly by the spatial averaging of the values in the 1x1 km^2 grid cells. For example, in urban background areas the predicted interpolation gridded value in the final map will be about 28 $\mu g \cdot m^{-3}$ at the corresponding station point with the measurement value of 30 $\mu g \cdot m^{-3}$ (calculated based on the linear regression equation), which coincides with an underestimation of about 6 %.

A3.3 Ozone

In this section, we present the technical details and the uncertainty estimates for the maps of ozone health-related indicators 93.2 percentile of maximum daily 8-hour means, SOMO35 and SOMO10 (Maps 4.1 – 4.3), as well as for the maps of ozone vegetation-related indicators AOT40 for vegetation and AOT40 for forests (Maps 4.4 and 4.5).

Technical details on the interpolation model

Table A3.6 presents the estimated parameters of the linear regression models and of the residual kriging, including the statistical indicators of both the regression and the kriging.

The adjusted R^2 and standard error show the quality of the fit of the regression relation. For the rural areas, all indicators show the value of the adjusted R^2 between 0.62 and 0.70. For the urban areas, the adjusted R^2 is 0.55 for 93.2 percentile of daily 8-hour maximums and 0.57 for SOMO35, while for SOMO10 is it 0.37 only. For the vegetation-related indicators the urban maps are not constructed.

Table A3.6 Parameters and statistics of linear regression model and ordinary kriging for ozone indicators 93.2 percentile of maximum daily 8-hourly means, SOMO35 and SOMO10 in rural and urban areas for the final combined map and for O_3 indicators AOT40 for vegetation and for forests in rural areas for 2017

		93.2 perc. of dmax 8h		SOMO35		SOMO10		AOT40v	AOT40f
		Rur. areas	Urb. ar.	Rur. ar.	Urb.ar.	Rur. ar.	Urb.ar.	Rur. ar.	Rur. ar.
Linear regresion model (LRM, Eq. A1.3)	c (constant)	-41.0	2.9	-3029	-1188	-144	2984	-12672	-21283
	a1 (EMEP model)	1.24	0.97	0.72	0.56	0.68	0.47	0.87	0.72
	a2 (altitude GMTED)			0.75		1.57		*n. sign.*	*n. sign.*
	a3 (wind speed)		-2.47		-153.27		*n. sign.*		
	a4 (s. solar radiation)	1.42	0.64	322.0	231.3	457.8	466.0	1279.4	2213.6
	Adjusted R^2	**0.65**	**0.55**	**0.68**	**0.57**	**0.62**	**0.37**	**0.67**	**0.70**
	Stand. Err. [µg.m^{-3}.x]*	**10.1**	**12.2**	**1645**	**1643**	**2470**	**3049**	**5979**	**9641**
Ord. krig. (OK) of LRM	nugget	23	42	2.0E+06	1.6E+06	0.0E+00	3.3E+06	2.1E+07	5.5E+07
	sill	67	89	2.2E+06	3.5E+06	4.9E+06	4.8E+06	3.0E+07	7.3E+07
	range [km]	45	270	170	180	20	240	180	150
LRM + OK of its residuals	**RMSE [µg.m^{-3}.x]***	**9.7**	**9.4**	**1618**	**1314**	**2416**	**2443**	**5257**	**8803**
	Relative RMSE [%]	**8.6**	**8.7**	**29.7**	**30.4**	**11.3**	**12.9**	**34.2**	**34.7**
	Bias (MPE) [µg.m^{-3}.x]*	**0.0**	**0.0**	**-41**	**24**	**-102**	**38**	**-76**	**-144**

*) Units – 93.2 percentile of daily 8-h maximums: [µg·m^{-3}], SOMO35: [µg·m^{-3}·d], AOT40v and AOT40f: [µg·m^{-3}·h].

RMSE and bias – highlighted by orange – are the cross-validation indicators, showing the quality of the resulting map.

Uncertainty estimated by cross-validation

The basic uncertainty analysis is provided by cross-validation. Table A3.6 shows both absolute and relative mean uncertainty, expressed by RMSE and Relative RMSE. The relative mean uncertainty of the 2017 ozone map is at the 93.2 percentile of daily 8-h maximums about 9 % for both rural and urban areas, around 30 % for both rural and urban areas at the SOMO35, around 11–13 % for SOMO10 and about 35 % at AOT40 for both vegetation and forests. The small levels of the relative uncertainty for the 93.2 percentile of maximum daily 8-h means and SOMO10 are highly influenced by the low ratio between the relevant standard error and mean calculated based on all annual station concentration data: for these two indicators the ratio is at the level of about 0.15 – 0.20, while for SOMO35 and for both AOT40 indicators it is at the level of about 0.5 – 0.7.

Figure A3.5 shows the cross-validation scatter plots for both the rural and urban areas of the 2017 map for the health-related ozone indicators.

The R^2, an indicator for the interpolation correlation with the observations, shows that for the health related ozone indicators, about 64 – 69 % is attributable to the interpolation in the rural areas, while in the urban areas it is about 72 % for the 93.2 percentile of maximum daily 8-h means, about 74 % for SOMO35 and about 59 % for SOMO10.

Figure A3.5 Correlation between cross-validated predicted (y-axis) and measurement values for ozone indicators 93.2 percentile of max. daily 8-hourly means (top), SOMO35 (middle) and SOMO10 (bottom) for 2017 for rural (left) and urban (right) areas

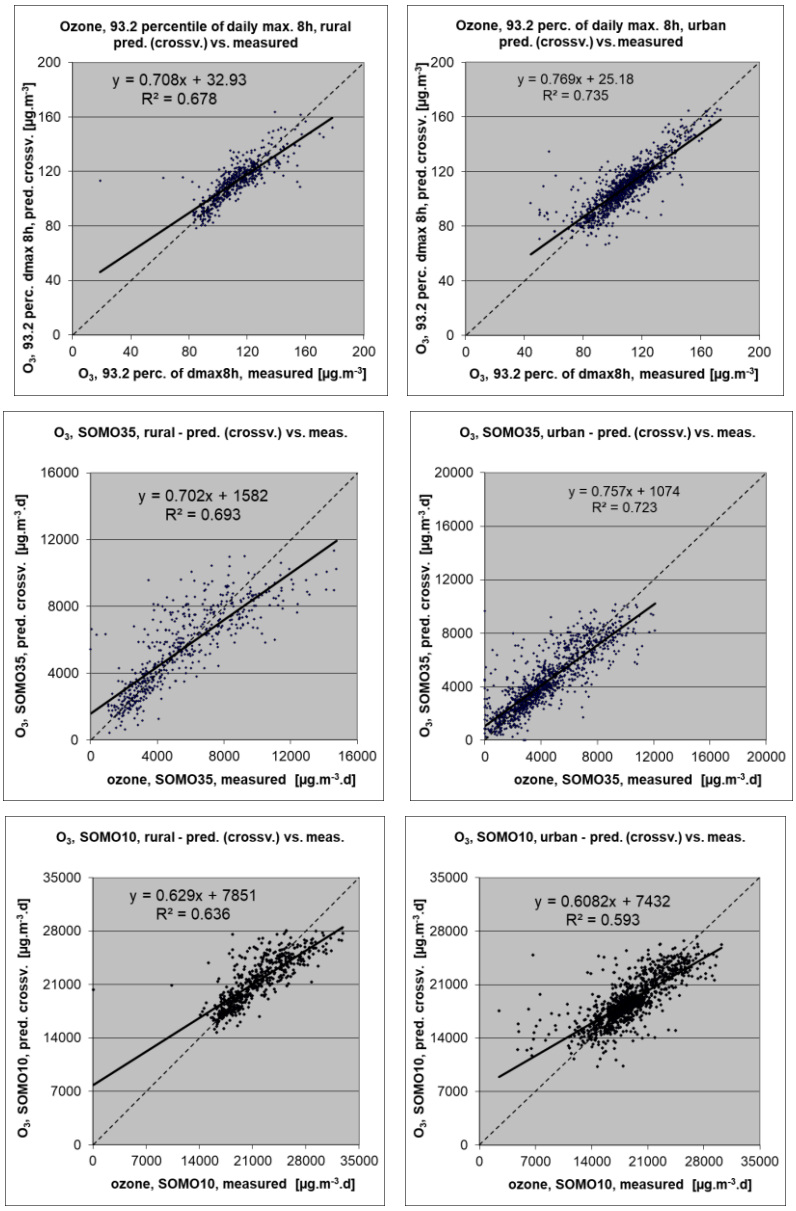

The scatter plots indicate that the higher values are underestimated and the lower values somewhat overestimated by the interpolation method; a typical smoothing effect inherent to the interpolation method with the linear regression and its residuals kriging. For example, in the case of the 93.2 percentile of daily 8-h maximums, in urban areas (Figure A.3.5, upper right panel) an observed value of 160 µg·m^{-3} is estimated in the interpolation as 148 µg·m^{-3}, which is 7 % lower. Or, in the case of SOMO35, in rural areas (Figure A3.5, bottom left panel) an observed value of 9 000 µg·m^{-3}·d is estimated in the interpolation as about 7 900 µg·m^{-3}·d, which is 12 % lower.

Figure A3.6 shows the cross-validation scatter plots of the AOT40 for both vegetation and forests. R^2 indicates that about 74 % of the variability is attributable to the interpolation, for both AOT40 indicators.

The cross-validation scatter plots show again that in areas with higher accumulated ozone concentrations the interpolation methods tend to deliver underestimated predicted values. For example, in agricultural areas (Figure A3.6, left panel) an observed value of 30 000 µg·m^{-3}·h is estimated in the interpolation as about 26 500 µg·m^{-3}·h, i.e. an underestimation of about 12 %. In addition, an overestimation at the lower end of predicted values occurred. One could reduce this under- and overestimation by extending the number of measurement stations and by optimising the spatial distribution of those stations, specifically in areas with elevated values over years.

Figure A3.6 Correlation between cross-validated predicted (y-axis) and measurement values for ozone indicators AOT40 for vegetation (left) and AOT40 for forests (right) for 2017 for rural areas

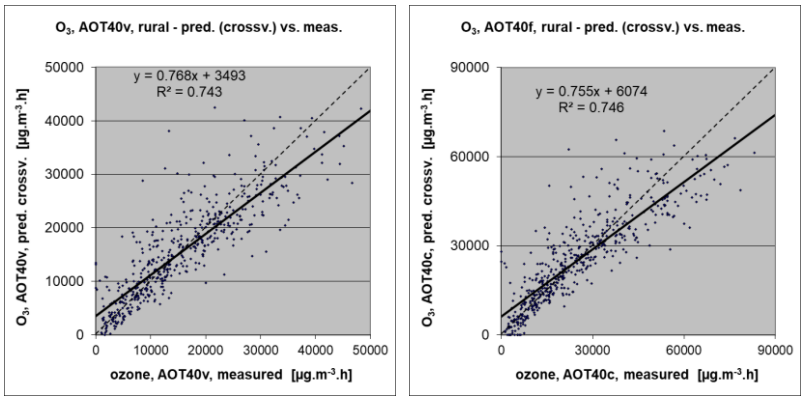

Comparison of point measurement values with the predicted grid value

In addition to the above point observation – point prediction cross-validation, a simple comparison has been made between the point observation values and interpolated predicted grid values.

For health related indicators, the comparison has been made primarily for the separate rural and separate urban background maps at 10x10 km^2 resolution. (One can directly relate this comparison result to the cross-validation of the previous section.) Next to this, the comparison has been done also for the final combined maps at 1x1 km^2 resolution.

Figure A3.7 shows the scatterplots for these comparisons, for ozone indicator 93.2 percentile of maximum daily 8-hour means only, as an illustration.

The results of the point observation – point prediction cross-validation of Figure A3.6 and those of the point observation – grid averaged prediction validation for the separate rural and the separate urban background map, and for the final combined maps are summarised in Table A3.7.

By comparing the scatterplots and the statistical indicators for the separate rural and separate urban background map with the final combined maps, one can evaluate the level of representation of the rural resp. urban background areas in the final combined maps. Both the rural and the urban air quality are fairly well represented in the 1x1 km^2 final combined map.

The uncertainty of the rural and urban background maps at measurement locations is caused partly by the smoothing effect of interpolation and partly by the spatial averaging of the values in the 10x10 km^2 grid cells. The level of smoothing, which leads to underestimation in areas with high values, is weaker in areas where measurements exist than in areas where a measurement point is not available. For example, in the case of the SOMO35, in rural areas an observed value of 9 000 µg·m^{-3}·d is estimated in the interpolation as about 8 200 µg·m^{-3}·d, which is about 8 % lower. It is less than the cross-validation

underestimation of 12 % at the same point location, when leaving out this one actual measurement point and the interpolation without this station is done (see the previous subsection).

Figure A3.7 Correlation between predicted grid values from rural 10x10 km² (upper left), urban 10x10 km² (bottom left) and final combined 1x1 km² (both right) map (y-axis) versus measurements from rural (top), resp. urban/suburban (bottom) background stations (x-axis) for ozone indicator 93.2 percentile of daily max. 8-hourly means for 2017

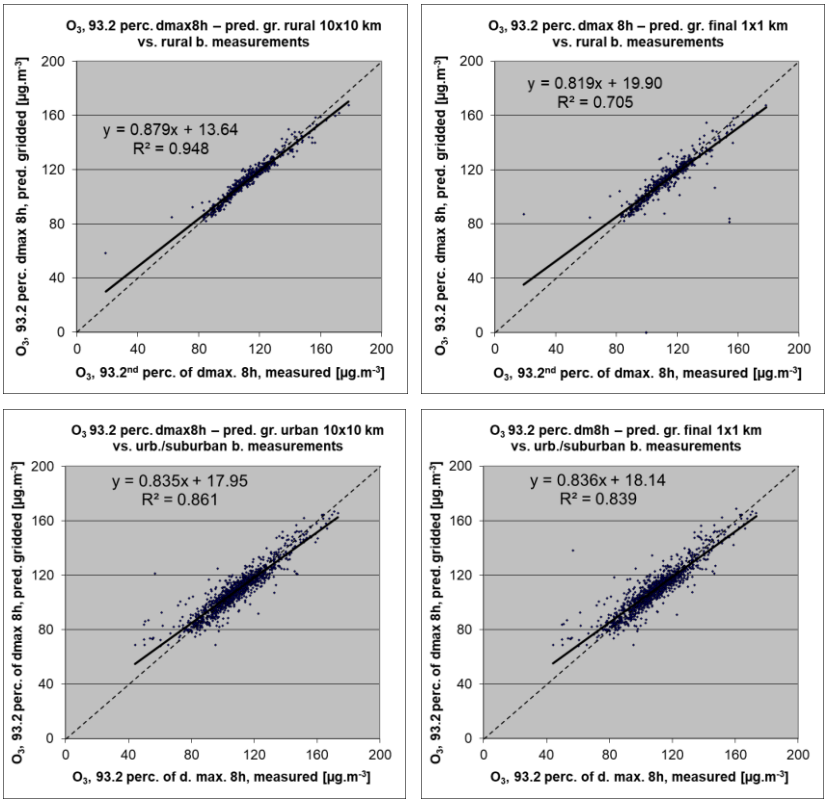

Table A3.7 Statistical indicators from the scatter plots for the predicted point values based on cross-validation and the predicted grid values from separate (rural resp. urban) 10x10 km² and final combined 1x1 km² map versus the measurement point values for rural (left) and urban (right) background stations for ozone indicators 93.2 percentile of daily max 8h means (top), SOMO35 (middle) and SOMO10 (bottom) for 2017

Ozone	rural backgr. stations				urban/suburban backgr. stations			
	RMSE	bias	R^2	lin. r. equation	RMSE	bias	R^2	lin r. equation
93.2 percentile of daily max. 8-hour means								
cross-valid. prediction, separate (r or ub) map	9.7	0.0	0.678	y = 0.708x + 32.9	9.4	0.0	0.735	y = 0.769x + 25.2
grid prediction, 10x10 km separate (r or ub) map	4.1	0.0	0.948	y = 0.879x + 13.6	6.8	0.0	0.861	y = 0.835x + 18.0
grid prediction, 1x1 km final merged map	9.6	-0.5	0.705	y = 0.819x + 19.9	7.3	0.4	0.839	y = 0.836x + 18.1
SOMO35								
cross-valid. prediction, separate (r or ub) map	1618	-41	0.693	y = 0.702x + 1582	1314	24	0.723	y = 0.757x + 1074
grid prediction, 10x10 km separate (r or ub) map	1441	-39	0.757	y = 0.734x + 1411	898	8	0.871	y = 0.837x + 712
grid prediction, 1x1 km final merged map	1495	-188	0.743	y = 0.721x + 1331	1036	72	0.828	y = 0.839x + 769
SOMO10								
cross-valid. prediction, separate (r or ub) map	2416	-102	0.636	y = 0.629x + 7851	2443	38	0.593	y = 0.608x + 7432
grid prediction, 10x10 km separate (r or ub) map	716	-14	0.974	y = 0.899x + 2153	1952	23	0.744	y = 0.688x + 5908
grid prediction, 1x1 km final merged map	1445	-154	0.872	y = 0.845x + 3180	2049	203	0.716	y = 0.706x + 5756

Table A3.8 presents the results of the point observation – point prediction cross-validation of Figure A3.6 and those of the point-grid validation for the rural map, for vegetation related indicators AOT40 for vegetation and AOT40 for forests. Again, one can see for both indicators a better correlation between the station measurements and the averaged interpolated predicted values of the corresponding grid cells, than at the point cross-validation predictions, of Figure A3.6.

Table A3.8 Statistical indicators from the scatter plots for predicted point values based on cross-validation and predicted grid values from rural 2x2 km² map versus measurement point values for rural background stations for O_3 indicators AOT40 for vegetation (top) and for forests (bottom) for 2017

Ozone	rural backgr. stations			
	RMSE	bias	R^2	linear regression equation
AOT40 for vegetation				
cross-valid. prediction, rural map	5257	-76	0.743	y = 0.768x + 3493
grid prediction, 2x2 km rural map	3921	-28	0.858	y = 0.825x + 2665
AOT40 for forests				
cross-valid. prediction, rural map	8803	-144	0.746	y = 0.755x + 6074
grid prediction, 2x2 km rural map	6783	-111	0.851	y = 0.813x + 4638

A3.4 NO_2 and NO_x

In this section, the technical details and the uncertainty estimates for the maps of NO_2 annual average and NO_x annual average, for Maps 5.1 and 5.2, are presented.

Technical details on the interpolation model

In agreement with Horálek et al. (2007) and Annex 1, the NO_x measurements are supplemented by the so-called *pseudo* NO_x stations. The pseudo NO_x data are calculated based on the NO_2 data, using quadratic regression Eq. A1.2. The regression coefficients were estimated based on the rural background stations with both NO_x and NO_2 measurements (see Section 2.1.1). The number of such stations is 342. The estimated coefficients of Eq. A1.2 are: a = 0.019, b = 1.054, c = 0.61. Adjusted R^2 is 0.94, the standard error is 2.0 $\mu g \cdot m^{-3}$.

Table A3.9 presents the estimated parameters of the linear regression models and of the residual kriging and includes the statistical indicators of both the regression and the kriging.

Only stations with actual measurement data of the relevant pollutant (i.e. not the pseudo stations) are used for calculating of the cross-validation parameters RMSE and bias.

Table A3.9 Parameters and statistics of linear regression model and ordinary kriging of NO_2 annual average for 2017 in rural, urban background and urban traffic areas for the final combined map (left) and NO_x annual average for 2017 in rural areas (right)

		NO_2 Annual average			NO_x Annual average
		Rural areas	Urb. b. areas	Urb. tr. areas	Rural areas
Linear regresion model (LRM, Eq. A1.3)	c (constant)	8.2	23.2	27.98	16.8
	a1 (EMEP model)	0.436	0.184	0.224	0.975
	a2 (altitude)	-0.0095	*non signif.*	*non signif.*	-0.0055
	a3 (altitude_5km_radius)	0.0093	*non signif.*	*non signif.*	
	a4 (wind speed)	-1.15	-3.16	-2.31	-2.75
	a5 (satellite OMI)	1.16	1.30	1.52	
	a6 (population*1000)	0.00231	0.00028		
	a7 (NAT_1km)		-0.0731		
	a8 (AGR_1km)		-0.0320		
	a9 (TRAF_1km)		0.0928		
	a10 (LDR_5km_radius)	0.0471	0.0519	0.1872	
	a11 (HDR_5km_radius)		0.1616	0.3570	
	a12 (NAT_5km_radius)	-0.0451			
	Adjusted R^2	**0.80**	**0.44**	**0.38**	**0.61**
	Standard Error [µg.m^{-3}]	**2.6**	**6.8**	**10.1**	**5.6**
Ordinary kriging (OK) of LRM residuals	nugget	6	11	12	21
	sill	7	27	24	29
	range [km]	160	270	270	140
LRM + OK of its residuals	**RMSE [µg.m^{-3}]**	**2.5**	**5.6**	**8.3**	**4.6**
	Relative RMSE [%]	**29.7**	**27.3**	**23.9**	**41.2**
	Bias (MPE) [µg.m^{-3}]	**0.1**	**0.0**	**0.1**	**0.2**

Uncertainty estimated by cross-validation

Table A3.9 shows both absolute and relative mean uncertainty, expressed by RMSE and Relative RMSE. The absolute mean uncertainty of the final combined map of NO_2 annual average expressed as RMSE is 2.6 µg·m^{-3} for the rural areas, 5.6 µg·m^{-3} for the urban background areas and 8.3 µg·m^{-3} for the urban traffic areas. For the NO_x rural map it is 4.6 µg·m^{-3}.

The relative mean uncertainty of the NO_2 annual average map is 30 % for rural, 27 % for urban background areas and 24 % for the urban traffic areas. The NO_x annual average rural map has a relative mean uncertainty of 42 %.

Figure A3.8 shows the point observation – point prediction cross-validation scatter plots for NO_2 annual average. The R^2 indicates that about 81 % of the variability is attributable to the interpolation for the rural areas, while for the urban background areas it is 62 % and for the urban traffic 59 %.

Figure A3.8 Correlation between cross-validated predicted and measurement values for NO_2 annual average 2017 for rural (left), urban background (middle) and urban traffic (right) areas

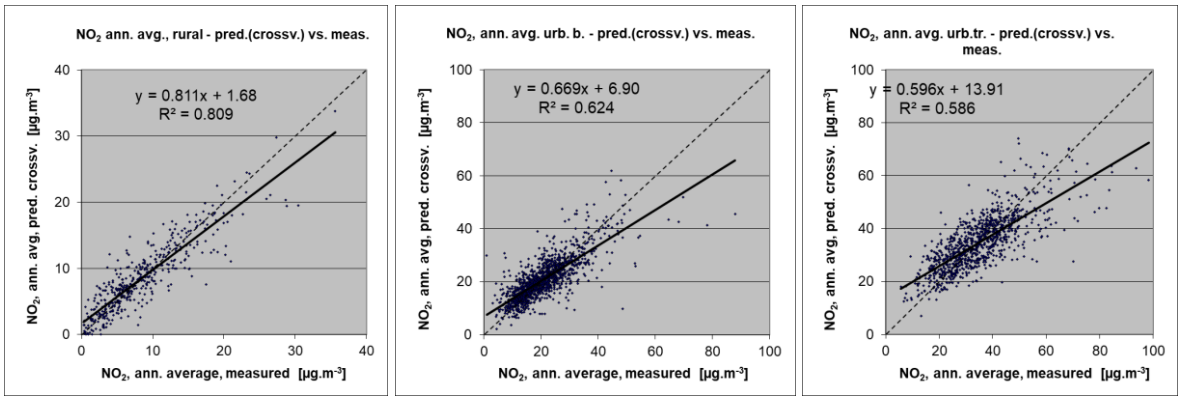

Like in the case of other pollutants, the cross-validation scatter plots show the underestimation of predictions at high concentrations at locations with no measurements. For example, in urban areas an observed value of 40 $\mu g \cdot m^{-3}$ is estimated in the interpolations to be about 34 $\mu g \cdot m^{-3}$, which is an underestimated prediction of about 14 %.

Figure A3.9 shows the cross-validation scatter plot for NO_x annual average rural map. The R^2 indicates that about 63 % of the variability is attributable to the interpolation.

Figure A3.9 Correlation between cross-validated predicted and measurement values for NO_x annual average 2017 for rural areas

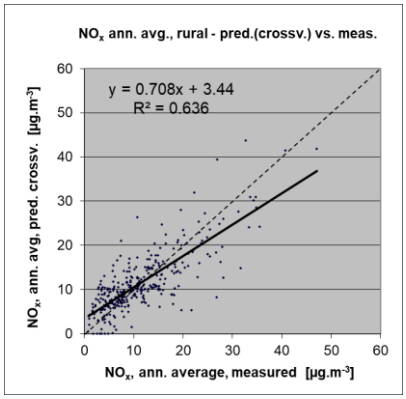

Comparison of point measurement values with the predicted grid value

Next to the above presented cross-validation, a simple comparison was made between the point observation values and interpolated predicted 1x1 km^2 resp. 2x2 km^2 grid values.

For NO_2 annual average, the comparison has been made primarily for the separate rural, separate urban background and separate urban traffic map layers at 1x1 km^2 resolution. Besides, the comparison has been done also for the final combined map. Table A3.10 presents the results of this comparison, together with the results of cross-validation prediction of Figure A3.8. One can conclude that the final combined map in 1x1 km^2 resolution is representative for rural and urban background areas, but not for urban traffic areas.

Table A3.10 Statistical indicators from the scatter plots for the predicted grid values from separate (rural, urban background or urban traffic) map layers and final combined map versus the

measurement point values for rural (upper left), urban background (upper right) and urban traffic (bottom left) stations for NO_2 annual average 2017

NO_2	rural backgr. stations				urban/suburban backgr. stations			
	RMSE	bias	R^2	lin. r. equation	RMSE	bias	R^2	lin r. equation
cross-valid. prediction, separate (r or ub) map	2.5	0.1	0.809	y = 0.811x + 1.68	5.6	0.0	0.624	y = 0.669x + 6.90
grid prediction, 1x1 km separate (r or ub) map	2.5	-0.4	0.826	y = 0.763x + 1.66	4.0	0.0	0.813	y = 0.772x + 4.72
grid prediction, 1x1 km final merged map	2.8	0.3	0.785	y = 0.878x + 1.31	4.6	0.5	0.749	y = 0.781x + 5.02

NO_2	urban/suburban traffic stations			
	RMSE	bias	R^2	lin. r. equation
cross-valid. prediction, urban traffic map	8.3	-0.1	0.586	y = 0.596x + 13.91
grid prediction, 1x1 km urban traffic map	6.4	0.0	0.756	y = 0.694x + 10.53
grid prediction, 1x1 km final merged map	14.5	-11.3	0.507	y = 0.451x + 7.75

Table A3.11 presents the cross-validation results of Figure A3.9 and those of the point observation – grid averaged prediction validation for the rural map of NO_x annual average.

Table A3.11 Statistical indicators from the scatter plots for predicted point values based on cross-validation and predicted grid values from rural 2x2 km^2 map versus measurement point values for rural background stations for NO_x annual average 2017

NO_x	rural background stations			
	RMSE	bias	R^2	linear regression equation
cross-valid. prediction, rural map	4.6	0.2	0.636	y = 0.708x + 3.34
grid prediction, 2x2 km rural map	3.5	0.1	0.790	y = 0.787x + 2.50

Annex 4 – Inter-annual changes

In this annex, inter-annual differences between 2016 and 2017 are presented, both for the mapped concentrations and for the population-weighted and vegetation-weighted concentrations. In the case of PM_{10} and $PM_{2.5}$, both 2016 and 2017 maps created based on the updated methodology are used. In the case of ozone, NO_2 and NO_X, 2016 maps as presented in Horálek et al. (2019a) are used.

A4.1 PM_{10}

Air concentrations

Map A4.1 presents the inter-annual difference between 2016 and 2017 for annual average and the 90.4 percentile of daily means for PM_{10}. Red areas show an increase of PM_{10} concentration in 2017, while blue areas show a decrease.

Map A4.1 Difference concentrations between 2016 and 2017 for PM_{10} indicators annual average (left) and 90.4 percentile (right)

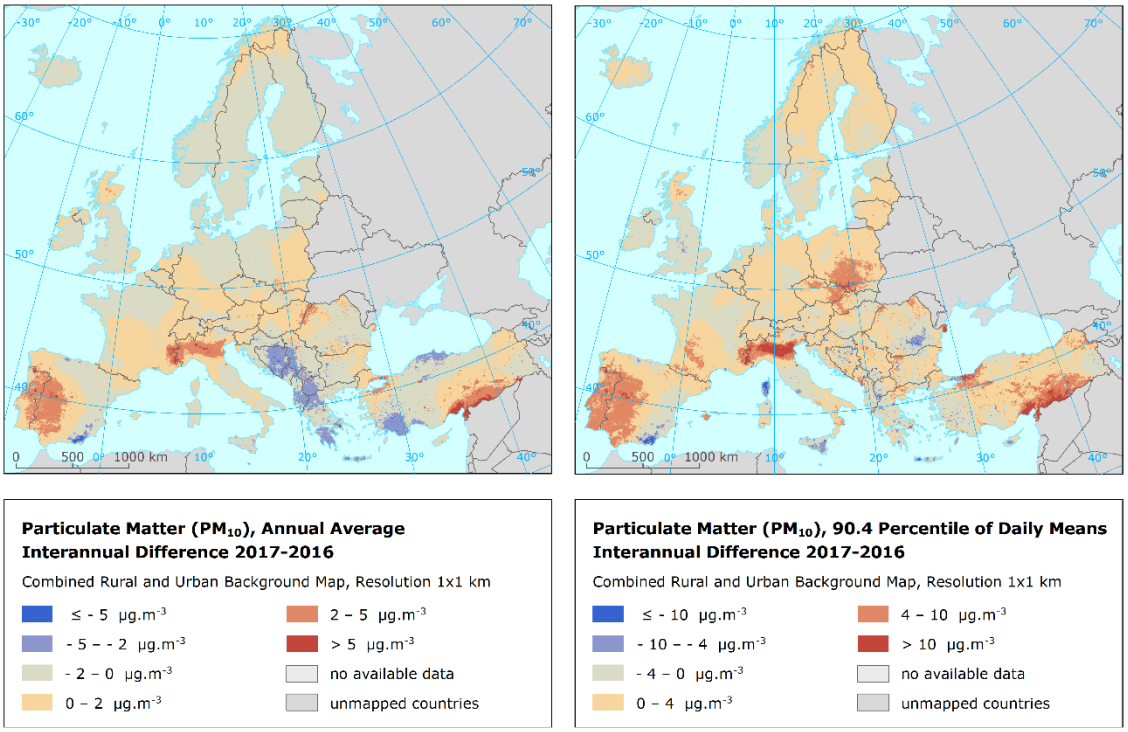

At the annual average PM_{10} difference map the highest increases are observed in Portugal and western Spain, Po valley in northern Italy and southern Turkey near the borders with Syria. Contrary to that, decreases occur in the area of the western Balkans.

At the 90.4 percentile of daily means for PM_{10} the highest increases are observed again in Portugal and western Spain, Po valley in northern Italy and southern Turkey, and also in southern Poland and north-eastern Czechia. The decreases are seen in southern Spain in Almeria region, i.e. opposite of the 2016-2015 difference in Horálek et al (2019a).

Be it noted that besides the actual changes in the concentrations, the variability of the linear regression model and variogram parameters, changes in the measurement network and changes in the dispersion model may cause minor differences in the concentration levels estimated.

Population exposure

Table A4.1 shows the inter-annual difference of the population-weighted concentrations between 2016 and 2017 for PM_{10} annual average and the 90.4 percentile of daily PM_{10} means, for individual countries and for Europe as a whole.

In 2017, the overall average population-weighted annual mean PM_{10} concentration for the whole of Europe was 23.1 $\mu g \cdot m^{-3}$, i.e. its value increased by about 0.2 $\mu g \cdot m^{-3}$ compared to the previous year. The steepest decreases per country were detected in Bosnia & Herzegovina and Malta, the highest increases were estimated in Greece, North Macedonia and Serbia (including Kosovo) .

In the case of the 90.4 percentile of daily means, the average European-wide population-weighted concentration for 2017 is estimated at 42 $\mu g \cdot m^{-3}$, which is of almost 1 $\mu g \cdot m^{-3}$ more than in 2016. The steepest decreases were estimated in Bosnia & Herzegovina, Croatia and Montenegro, while the highest increases in and Greece, Czechia, Portugal and Serbia. Note that the increases in Greece are estimated only by modelling and measurements in other countries, as the Greek measurement data was not available.

Table A4.1 Population-weighted concentration in 2016 and 2017 and its difference between 2016 and 2017 for PM_{10} indicators annual average (left) and 90.4 percentile of daily means (right).

Country		Population-weighted conc. [$\mu g.m^{-3}$]						Country		Population-weighted conc. [$\mu g.m^{-3}$]					
		Annual average			90.4 perc. of d. m.					Annual average			90.4 perc. of d. m.		
		2016	2017	'17 - '16	2016	2017	'17 - '16			2016	2017	'17 - '16	2016	2017	'17 - '16
Albania	AL	33.9	34.3	0.4	66.4	62.1	-4.2	Luxembourg	LU	17.0	16.4	-0.6	28.2	27.8	-0.4
Andorra	AD	23.3	25.7	2.3	45.3	49.8	4.5	Malta	MT	29.8	25.9	-3.9	45.5	39.4	-6.1
Austria	AT	16.9	17.3	0.5	30.5	31.4	1.0	Monaco	MC	21.4	22.3	0.9	35.7	33.8	-1.9
Belgium	BE	19.6	19.5	-0.2	34.1	34.0	-0.1	Montenegro	ME	27.7	26.0	-1.7	56.3	49.5	-6.8
Bosnia-Herzegovina	BA	34.2	29.6	-4.6	77.6	60.6	-17.0	Netherlands	NL	18.0	18.2	0.2	30.0	29.8	-0.2
Bulgaria	BG	34.3	32.3	-2.0	66.1	61.4	-4.7	North Macedonia	MK	45.0	47.3	2.4	100.3	100.3	0.1
Croatia	HR	26.4	24.2	-2.2	54.5	47.3	-7.2	Norway	NO	10.6	9.6	-1.0	19.8	18.0	-1.7
Cyprus	CY	37.9	37.6	-0.3	56.1	55.8	-0.3	Poland	PL	27.9	28.5	0.6	49.9	53.2	3.3
Czechia	CZ	22.1	22.8	0.8	39.2	44.1	4.9	Portugal	PT	18.3	19.7	1.4	29.5	34.3	4.7
Denmark	DK	15.2	15.1	-0.1	25.3	26.3	1.0	Romania	RO	25.3	24.9	-0.4	44.4	42.2	-2.2
Estonia	EE	11.5	10.5	-1.1	20.3	18.1	-2.2	San Marino	SM	21.0	22.0	1.1	40.1	40.4	0.3
Finland	FI	9.5	8.6	-0.9	16.5	15.2	-1.3	Serbia (incl. Kosovo*)	RS	34.3	36.7	2.4	67.5	72.3	4.7
France	FR	17.1	17.2	0.0	29.3	29.0	-0.3	Slovakia	SK	23.7	25.2	1.5	43.9	48.2	4.3
Germany	DE	16.9	16.9	0.0	28.6	29.2	0.6	Slovenia	SI	22.6	22.6	0.0	43.8	42.2	-1.6
Greece	GR	30.6	36.5	5.9	52.8	65.6	12.7	Spain	ES	20.6	21.8	1.2	33.0	37.2	4.3
Hungary	HU	25.3	26.4	1.1	47.1	48.5	1.4	Sweden	SE	11.4	10.7	-0.7	20.4	19.2	-1.2
Iceland	IS	9.3	11.6	2.3	17.5	19.7	2.2	Switzerland	CH	15.0	14.8	-0.2	27.5	26.3	-1.2
Ireland	IE	12.1	11.2	-0.9	22.0	19.9	-2.0	Turkey	TR	40.0	40.2	0.2	74.4	75.8	1.4
Italy	IT	25.1	26.1	1.1	44.1	47.6	3.5	United Kingdom	UK	15.7	14.6	-1.1	27.3	25.1	-2.2
Latvia	LV	16.5	15.2	-1.2	28.4	27.0	-1.4	**Total**		**22.9**	**23.1**	**0.2**	**40.7**	**41.6**	**1.0**
Liechtenstein	LI	13.5	12.8	-0.7	25.4	24.1	-1.4	**Total without Turkey**		**20.5**	**20.8**	**0.2**	**36.1**	**37.0**	**0.9**
Lithuania	LT	18.3	17.2	-1.1	31.4	30.8	-0.6	**EU-28**		**20.2**	**20.4**	**0.2**	**35.0**	**36.1**	**1.1**

*) under the UN Security Council Resolution 1244/99

A4.2 $PM_{2.5}$

Air concentrations

Map A4.2 presents the inter-annual difference between 2017 and 2016 for annual average $PM_{2.5}$.

The highest increases are seen in the Po valley in northern Italy, eastern Romania, and different Serbian cities. Decreases are estimated in the western Balkans, Corsica and some Greek rural areas.

Map A4.2 Difference $PM_{2.5}$ annual average concentrations between 2016 and 2017

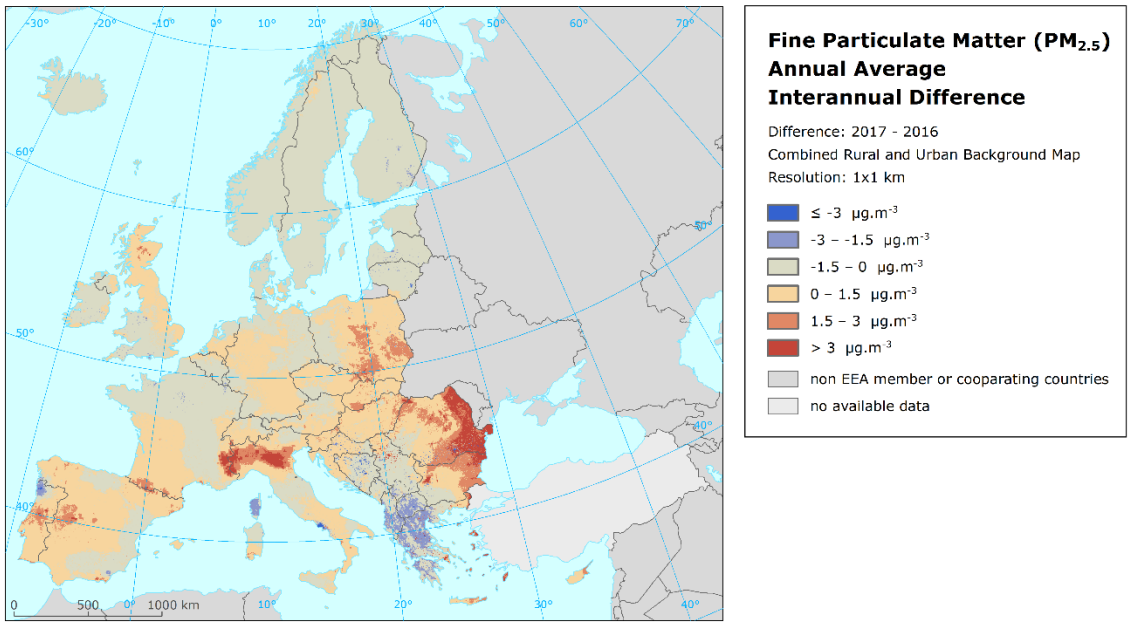

Population exposure

Table A4.2 presents the inter-annual difference of the population-weighted concentrations between 2016 and 2017 for $PM_{2.5}$ annual average, for individual countries and for Europe as a whole (without Turkey, which was not mapped neither for 2016 nor for 2017).

In 2017, the average European-wide population-weighted concentration is estimated at 13.8 µg·m^{-3}, which means a slight increase of about 0.3 µg·m^{-3} compared to 2016. The steepest decreases are shown in Bosnia & Herzegovina, Croatia, Lithuania and Montenegro, while the highest increases in Greece, Serbia and Slovakia. The estimate for Greece is again influenced by the lack of Greek measurement data.

Table A4.2 Population-weighted concentration in 2016 and 2017 and its difference between 2016 and 2017 for $PM_{2.5}$ annual average.

Country		Pop.-weighted conc. [µg.m^{-3}]			Country		Pop.-weighted conc. [µg.m^{-3}]			Country		Pop.-weighted conc. [µg.m^{-3}]		
		2016	2017	'17 - '16			2016	2017	'17 - '16			2016	2017	'17 - '16
Albania	AL	23.2	23.1	-0.1	Greece	GR	19.7	30.0	10.3	Norway	NO	6.0	5.2	-0.8
Andorra	AD	11.9	12.5	0.6	Hungary	HU	17.8	18.8	1.0	Poland	PL	20.8	21.4	0.6
Austria	AT	12.0	12.3	0.3	Iceland	IS	5.0	5.1	0.1	Portugal	PT	8.9	9.1	0.2
Belgium	BE	12.7	12.5	-0.2	Ireland	IE	7.0	6.2	-0.9	Romania	RO	17.0	17.9	0.9
Bosnia-Herzegovina	BA	27.3	22.6	-4.7	Italy	IT	16.5	17.0	0.5	San Marino	SM	14.0	14.2	0.2
Bulgaria	BG	23.1	22.4	-0.7	Latvia	LV	11.2	9.5	-1.8	Serbia (incl. Kosovo*)	RS	25.7	28.3	2.6
Croatia	HR	19.6	17.6	-2.0	Liechtenstein	LI	10.1	9.4	-0.7	Slovakia	SK	17.6	18.8	1.2
Cyprus	CY	15.3	15.7	0.4	Lithuania	LT	12.3	10.3	-2.0	Slovenia	SI	16.0	16.2	0.2
Czechia	CZ	16.6	17.1	0.5	Luxembourg	LU	11.4	10.0	-1.4	Spain	ES	11.3	12.0	0.7
Denmark	DK	9.3	8.5	-0.8	Malta	MT	11.3	11.8	0.4	Sweden	SE	5.9	5.0	-0.9
Estonia	EE	6.1	5.4	-0.7	Monaco	MC	13.8	13.2	-0.7	Switzerland	CH	10.2	9.9	-0.3
Finland	FI	5.3	4.4	-1.0	Montenegro	ME	20.6	18.6	-2.0	United Kingdom	UK	9.7	9.3	-0.4
France	FR	11.1	10.6	-0.5	Netherlands	NL	11.3	11.3	0.0	**Total**		**13.6**	**13.8**	**0.3**
Germany	DE	11.8	11.8	0.0	North Macedonia	MK	36.7	36.3	-0.4	**EU-28**		**13.3**	**13.5**	**0.3**

*) under the UN Security Council Resolution 1244/99

A4.3 Ozone

Air concentrations

Map A4.3 presents the inter-annual difference between 2016 and 2017 for four ozone indicators.

Map A4.3 Difference concentrations between 2016 and 2017 for ozone indicators 93.2 percentile of daily 8-hour maximums (top left), SOMO35 (top right), AOT40 for vegetation (bottom left) and AOT40 for forests (bottom right)

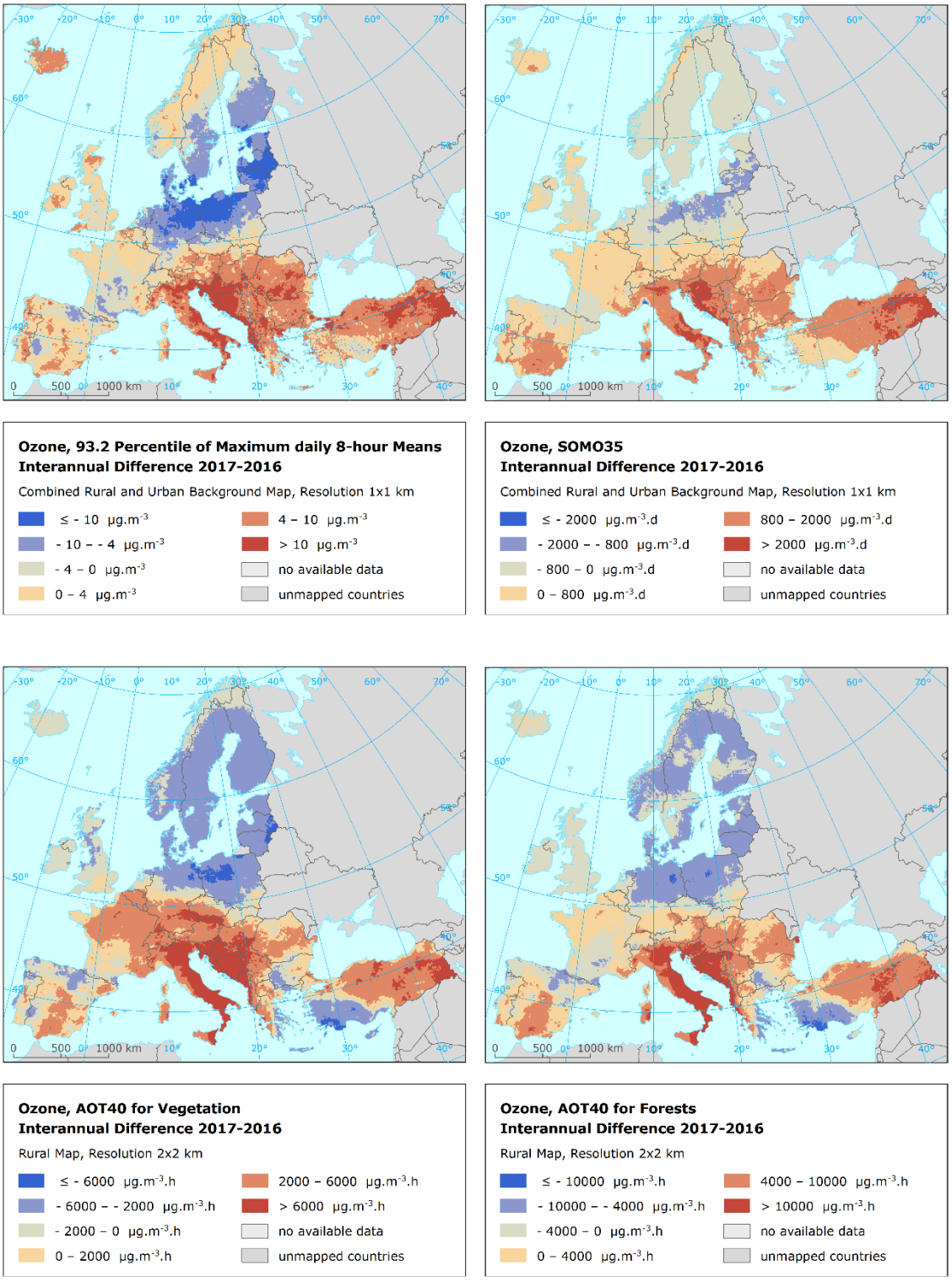

In the Map 4.3, the inter-annual difference for both the health related ozone indicators (i.e. for 93.2 percentile of maximum daily 8-hour means and SOMO35) and the vegetation related ozone indicators (i.e. for AOT40 for vegetation and AOT40 for forests) are presented. In all the maps, red areas show an increase of ozone concentrations, while blue areas show a decrease.

Most of the south-eastern Europe and Italy show a quite high increase for 93.2 percentile of maximum daily 8-hour means from 2016 to 2017. Contrary to that, one can see a steep decline in Baltic countries, Poland, Denmark, north Germany, and south of Finland and Sweden.

The difference pattern for SOMO35 is quite similar to that of the percentile indicator, however, the extremes are less elevated or prominent. Decreases are observed in Baltic countries, northern Poland and northern Germany, while increases can be seen in the most of Italy, in Balkan countries, in Turkey and in southern Spain.

In the case of both AOT40 indicators, decreases are observed in Baltic countries, Denmark, Sweden, Finland, central and northern Poland, north Germany, and south-western Turkey, while increases can be seen in Balkan countries, Italy, and most of Turkey.

Population exposure

Table A4.3 provides the inter-annual difference of the population-weighted concentrations between 2016 and 2017 for ozone health related indicators, for individual countries and for Europe as a whole.

Table A4.3 Population-weighted concentration in 2016 and 2017 and its difference between 2016 and 2017 for ozone indicators 93.2 percentile of 8-h daily maximums (left) and SOMO35 (right).

Country		Population-weighted conc. [µg.m^{-3}] / [µg.m^{-3}.d]					
		93.2 perc. of 8-h d.			SOMO35		
		2016	2017	'17 - '16	2016	2017	'17 - '16
Albania	AL	107.7	116.9	9.2	5475	6898	1423
Andorra	AD	109.2	111.2	1.9	4423	5182	758
Austria	AT	111.8	117.3	5.5	4522	5311	789
Belgium	BE	100.2	102.6	2.4	2203	2553	350
Bosnia-Herzegovina	BA	105.2	122.1	16.9	4409	6967	2558
Bulgaria	BG	98.7	102.2	3.5	3347	3938	591
Croatia	HR	109.5	123.2	13.7	4996	7110	2114
Cyprus	CY	105.0	103.7	-1.3	5612	6029	417
Czechia	CZ	114.7	112.0	-2.6	4353	4307	-46
Denmark	DK	95.3	87.2	-8.1	2293	1711	-582
Estonia	EE	92.6	84.8	-7.8	1949	1462	-487
Finland	FI	88.8	83.0	-5.8	1510	1153	-358
France	FR	104.8	104.4	-0.3	3420	3809	389
Germany	DE	110.7	105.3	-5.5	3368	3182	-185
Greece	GR	115.8	103.7	-12.1	6871	4858	-2013
Hungary	HU	106.2	114.8	8.6	3952	5010	1057
Iceland	IS	78.3	80.4	2.1	499	782	283
Ireland	IE	84.4	87.0	2.6	1323	1418	95
Italy	IT	122.1	129.2	7.0	6058	7405	1347
Latvia	LV	99.0	87.4	-11.7	2773	1557	-1216
Liechtenstein	LI	117.3	119.9	2.6	4945	5045	100
Lithuania	LT	98.1	84.5	-13.6	2456	1417	-1039
*) under the UN Security Council Resolution 1244/99							

Country		Population-weighted conc. [µg.m^{-3}] / [µg.m^{-3}.d]					
		93.2 perc. of 8-h d.			SOMO35		
		2016	2017	'17 - '16	2016	2017	'17 - '16
Luxembourg	LU	99.6	104.4	4.8	2211	3001	790
Malta	MT	106.5	104.3	-2.2	5985	6174	189
Monaco	MC	120.2	120.2	0.1	7186	8223	1037
Montenegro	ME	106	118	12.1	5269	6787	1518
Netherlands	NL	100.9	96.3	-4.6	2428	2281	-148
North Macedonia	MK	95.2	102.6	7.4	4434	4248	-186
Norway	NO	84.0	86.6	2.6	1502	1448	-53
Poland	PL	109.2	103.2	-6.0	3699	3111	-588
Portugal	PT	107.0	105.8	-1.2	4074	3914	-160
Romania	RO	90.4	102.6	12.2	2485	3885	1400
San Marino	SM	118.0	128.1	10.1	5667	7192	1525
Serbia (incl. Kosovo*)	RS	96.9	102.3	5.3	3755	4418	663
Slovakia	SK	109.0	113.5	4.5	4232	4861	628
Slovenia	SI	111.9	125.5	13.6	5007	7035	2028
Spain	ES	109.7	110.9	1.2	5212	5600	388
Sweden	SE	90.7	86.1	-4.6	1819	1641	-178
Switzerland	CH	117.3	117.1	-0.2	4842	5281	440
Turkey	TR	102.7	100.8	-1.9	4673	4864	192
United Kingdom	UK	84.1	84.5	0.5	1168	1218	50
Total		**104.5**	**104.5**	**-0.1**	**3745**	**4006**	**261**
Total without Turkey		**104.8**	**105.0**	**0.2**	**3619**	**3890**	**271**
EU-28		**105.0**	**104.8**	**-0.2**	**3598**	**3838**	**240**

In 2017 the overall population-weighted concentration for ozone indicator 93.2 percentile of maximum daily 8-hour means for whole of Europe was 105 µg·m^{-3}, i.e. of about 0.1 µg·m^{-3} less than in 2016. The highest increases are shown in Bosnia & Herzegovina, Croatia and Slovenia, while the steepest decreases in Lithuania, Greece and Latvia.

In the case of SOMO35, the average European-wide population-weighted concentration for 2017 is estimated at about 4000 µg·m^{-3}·d, which is of about 260 µg·m^{-3}·d more than in 2016. The highest increases and the steepest decreases took place in the same countries as for 93.2 percentile of daily 8-hour maximums.

Vegetation exposure

Table A4.4 provides the inter-annual difference of the agricultural-weighted concentrations for AOT40 for vegetation and the forest-weighted concentrations for AOT40 for forests between 2016 and 2017.

In 2017, the agricultural-weighted concentration of vegetation-related AOT40 shows an increase of cc. 730 $\mu g \cdot m^{-3} \cdot h$ compared to 2016, while the forest-weighted concentration of forest-related AOT40 shows a decrease of about 450 $\mu g \cdot m^{-3} \cdot h$ compared to 2016. The highest increases are seen in Bosna & Herzegovina and Croatia, while the steepest decreases in all three Baltic countries, Finland and Poland.

Table A4.4 Agricultural weighted (left) and forest-weighted (right) concentration in 2016 and 2017 and its difference between 2016 and 2017 for ozone indicators AOT40 for vegetation (left) and AOT40 for forests (right).

Country		Agricult.-weighted conc. AOT40 for veg. [µg.m^{-3}.h]			Forest-weighted conc. AOT40 for for. [µg.m^{-3}.h]		
		2016	2017	'17 - '16	2016	2017	'17 - '16
Albania	AL	19923	25124	5201	38763	47859	9095
Austria	AT	15086	20335	5250	28224	31018	2794
Belgium	BE	6728	10386	3659	15301	16037	736
Bosnia-Herzegovina	BA	11732	21525	9794	25520	38578	13058
Bulgaria	BG	11006	10597	-409	29709	29179	-530
Croatia	HR	13737	22092	8355	26764	39708	12944
Cyprus	CY	21704	17882	-3822	43831	40798	-3032
Czechia	CZ	14158	16596	2438	26610	26009	-601
Denmark	DK	6252	2270	-3981	9799	5352	-4447
Estonia	EE	5236	984	-4252	7076	2578	-4498
Finland	FI	4585	348	-4237	4888	739	-4149
France	FR	7386	9548	2162	21858	21858	0
Germany	DE	10650	10505	-145	22086	18783	-3304
Greece	GR	22763	22758	-5	43901	43556	-345
Hungary	HU	11927	16143	4217	24543	30569	6026
Iceland	IS	32	5	-27	4	43	39
Ireland	IE	2331	875	-1456	3561	2347	-1214
Italy	IT	21620	28686	7066	39860	50584	10724
Latvia	LV	6047	911	-5136	8410	2881	-5530
Liechtenstein	LI	15168	20195	5028	31769	34140	2372
Lithuania	LT	7019	1673	-5346	10661	4868	-5793
Luxembourg	LU	7679	12078	4399	15960	16978	1018
Malta	MT	21344	22151	807	42542	47202	4660
Monaco	MC	24531			38471	27768	-10703
Montenegro	ME	15161	22879	7718	31868	43070	11203
Netherlands	NL	6472	6069	-403	12647	10717	-1930
North Macedonia	MK	18701	19633	932	39663	42646	2983
Norway	NO	3645	957	-2687	5235	1942	-3294
Poland	PL	12180	8077	-4104	20242	14954	-5288
Portugal	PT	10141	9647	-493	21598	22628	1029
Romania	RO	6847	8569	1723	17098	21389	4291
San Marino	SM	18841	28942	10100	31897	46837	14940
Serbia (incl. Kosovo*)	RS	12542	17943	5401	29436	34714	5278
Slovakia	SK	13276	14085	810	24212	24458	245
Slovenia	SI	16251	23687	7435	30110	40259	10148
Spain	ES	15845	16541	696	28396	28317	-79
Sweden	SE	5761	2096	-3664	6300	2043	-4257
Switzerland	CH	14255	19075	4819	29953	31268	1315
Turkey	TR		18400	18400		30301	30301
United Kingdom	UK	3435	2476	-958	4784	3430	-1354
Total			**12670**			**17717**	**17717**
Total without Turkey		**10942**	**11676**	**734**	**17573**	**17126**	**-447**
EU-28		**10872**	**11468**	**597**	**17714**	**16628**	**-1086**

*) under the UN Security Council Resolution 1244/99

A4.4 NO_2 and NO_x

Air concentrations

Map A4.4 presents the inter-annual difference between 2016 and 2017 for NO_2 and NO_x annual averages. Red areas show an increase of concentration in 2017, while blue areas show a decrease.

For NO2, the steepest decreases are shown in some parts of United Kingdom, Sweden, Denmark and Germany. The highest increases are seen in some parts of the Balkans and northern Italy.

In the case of NO_x, the steepest decreases are seen in some parts of Scandinavia, United Kingdom and border areas of Germany and France. The highest increases can be seen in southern Spain, central and south Turkey and south-east Balkan. In this context, note the lack of stations in the south-east Balkan.

Map A4.4 Difference concentrations between 2016 and 2017 for NO_2 annual average (left) and NO_x annual average (right)

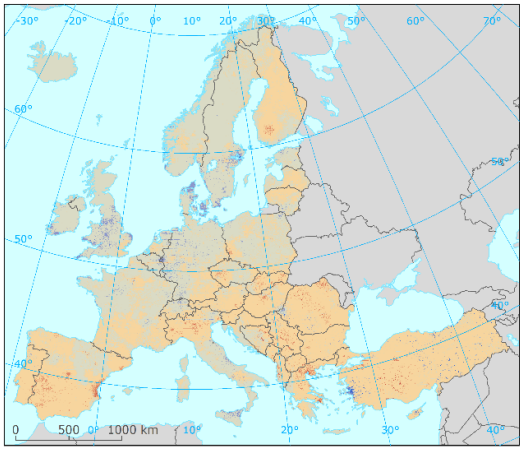

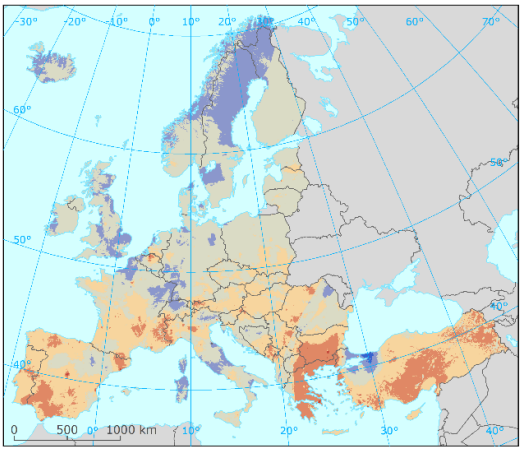

Nitrogen Dioxide (NO_2), Annual Average
Interannual Difference 2017-2016
Combined Rural and Urban Background Map, Resolution 1x1 km

- ≤ - 5 µg.m^{-3}
- - 5 – - 2 µg.m^{-3}
- - 2 – 0 µg.m^{-3}
- 0 – 2 µg.m^{-3}
- 2 – 5 µg.m^{-3}
- > 5 µg.m^{-3}
- no available data
- unmapped countries

Nitrogen Oxides (NO_x), Annual Average
Interannual Difference 2017-2016
Combined Rural and Urban Background Map, Resolution 1x1 km

- ≤ - 10 µg.m^{-3}
- - 10 – - 4 µg.m^{-3}
- - 4 – 0 µg.m^{-3}
- 0 – 4 µg.m^{-3}
- 4 – 10 µg.m^{-3}
- > 10 µg.m^{-3}
- no available data
- unmapped countries

Population exposure

Table A4.5 provides the inter-annual difference between 2016 and 2017 for NO_2 annual average. In 2017 the overall population-weighted concentration for NO_2 annual average for whole of Europe was 19.2 µg·m^{-3}, i.e. slightly less than in 2016. The steepest decreases are shown in Cyprus, Sweden, Norway and the United Kingdom, while the highest increases in Greece, Albania and Bosnia & Herzegovina .

Table A4.5 Population-weighted concentration in 2016 and 2017 and its difference between 2016 and 2017 for NO_2 annual average

Country		Pop.-weighted conc. [µg.m^{-3}]			Country		Pop.-weighted conc. [µg.m^{-3}]			Country		Pop.-weighted conc. [µg.m^{-3}]		
		2016	2017	'17 - '16			2016	2017	'17 - '16			2016	2017	'17 - '16
Albania	AL	13.7	16.9	3.1	Hungary	HU	16.6	17.8	1.2	Portugal	PT	15.3	16.2	0.9
Andorra	AD	18.2	20.5	2.3	Iceland	IS	10.1	10.2	0.2	Romania	RO	17.6	18.8	1.2
Austria	AT	18.9	18.9	0.0	Ireland	IE	11.0	9.3	-1.7	San Marino	SM	16.3	14.5	-1.9
Belgium	BE	21.7	20.9	-0.8	Italy	IT	22.1	22.1	0.0	Serbia (incl. Kosovo*)	RS	18.4	19.6	1.2
Bosnia-Herzegovina	BA	13.2	15.7	2.5	Latvia	LV	12.0	11.1	-0.8	Slovakia	SK	13.5	14.7	1.2
Bulgaria	BG	18.8	19.2	0.4	Liechtenstein	LI	17.8	18.2	0.4	Slovenia	SI	15.4	16.2	0.8
Croatia	HR	15.2	15.6	0.4	Lithuania	LT	11.7	10.8	-0.9	Spain	ES	20.0	21.6	1.6
Cyprus	CY	24.0	19.6	-4.4	Luxembourg	LU	20.7	19.5	-1.2	Sweden	SE	10.7	7.7	-2.9
Czechia	CZ	15.2	15.2	0.0	Malta	MT	14.9	16.0	1.1	Switzerland	CH	19.7	18.8	-0.9
Denmark	DK	10.4	8.8	-1.6	Monaco	MC	26.8	26.8	-0.1	Turkey	TR	26.9	25.3	-1.6
Estonia	EE	7.8	6.3	-1.6	Montenegro	ME	11.9	13.5	1.6	United Kingdom	UK	21.8	19.8	-2.0
Finland	FI	8.0	7.6	-0.4	Netherlands	NL	20.5	20.2	-0.3	**Total**		**19.6**	**19.2**	**-0.4**
France	FR	17.3	16.9	-0.4	North Macedonia	MK	17.4	19.8	2.4	**Total without Turkey**		**18.6**	**18.4**	**-0.2**
Germany	DE	20.2	19.4	-0.8	Norway	NO	12.4	10.4	-2.0	**EU-28**		**18.7**	**18.5**	**-0.3**
Greece	GR	19.6	23.6	3.9	Poland	PL	15.2	14.9	-0.3					

*) under the UN Security Council Resolution 1244/99

Annex 5 – Concentration maps including station points

Throughout the report, the concentration maps presented do not include station points. The reason is to better visualise the health related indicators with their distinct concentration levels at the more fragmented and smaller urban areas in predominant rural areas.

As presented in Annex 3, the kriging interpolation methodology somewhat smooths the concentration field. Therefore, it is valuable to present in this Annex 5 the indicator maps *including* the concentration values resulting from the measurement data at the station points. These points provide important additional visual information on the smoothing effect caused by the interpolation. For instance, maps A5.1 and A5.2 present PM_{10} indicators annual average and 90.4 percentile of daily means and include the stations points used in the interpolation. They correspond to Maps 2.1 and 2.2 of the main report, which do not have station points. Table A5.1 provides an overview on the maps of the main report and the corresponding maps including stations point values as presented in this annex.

Both the rural and the urban/suburban background stations are included in the maps of the health related indicators, while the rural stations only are shown in the maps of vegetation related indicators. For $PM_{2.5}$ and NO_x, only the stations with relevant measured data (i.e. not the pseudo stations) are presented.

Table A5.1 Overview of maps presented in this Annex 5 and their relation with the maps presented in the main report

Air pollutant	Indicator	Map including station points	Map without station points
PM_{10}	Annual average	A5.1	2.1
	90.4 percentile of daily means	A5.2	2.2
$PM_{2.5}$	Annual average	A5.3	3.1
Ozone	93.2 percentile of maximum daily 8-hour means	A5.4	4.1
	SOMO35	A5.5	4.2
	SOMO10	A5.6	4.3
	AOT40 for vegetation ([a])	A5.7	4.4
	AOT40 for forests ([a])	A5.8	4.5
NO_2	Annual average	A5.9	5.1
NO_x	Annual average ([a])	A5.10	5.2

([a]) Rural map, applicable for rural areas only.

Map A5.1 Concentration map of PM_{10} annual average including station points, 2017

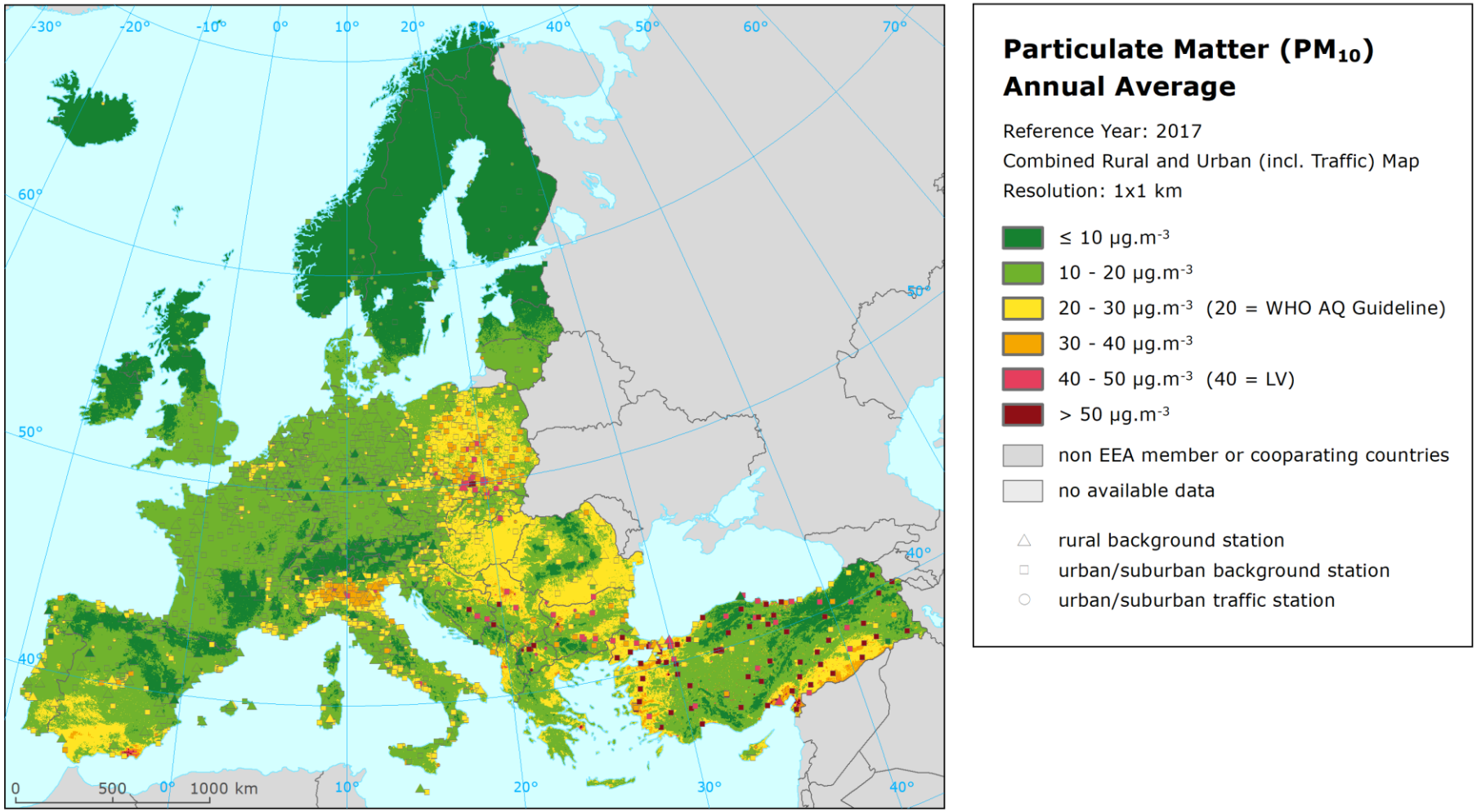

Map A5.2 Concentration map of PM_{10} indicator 90.4 percentile of daily means including station points, 2017

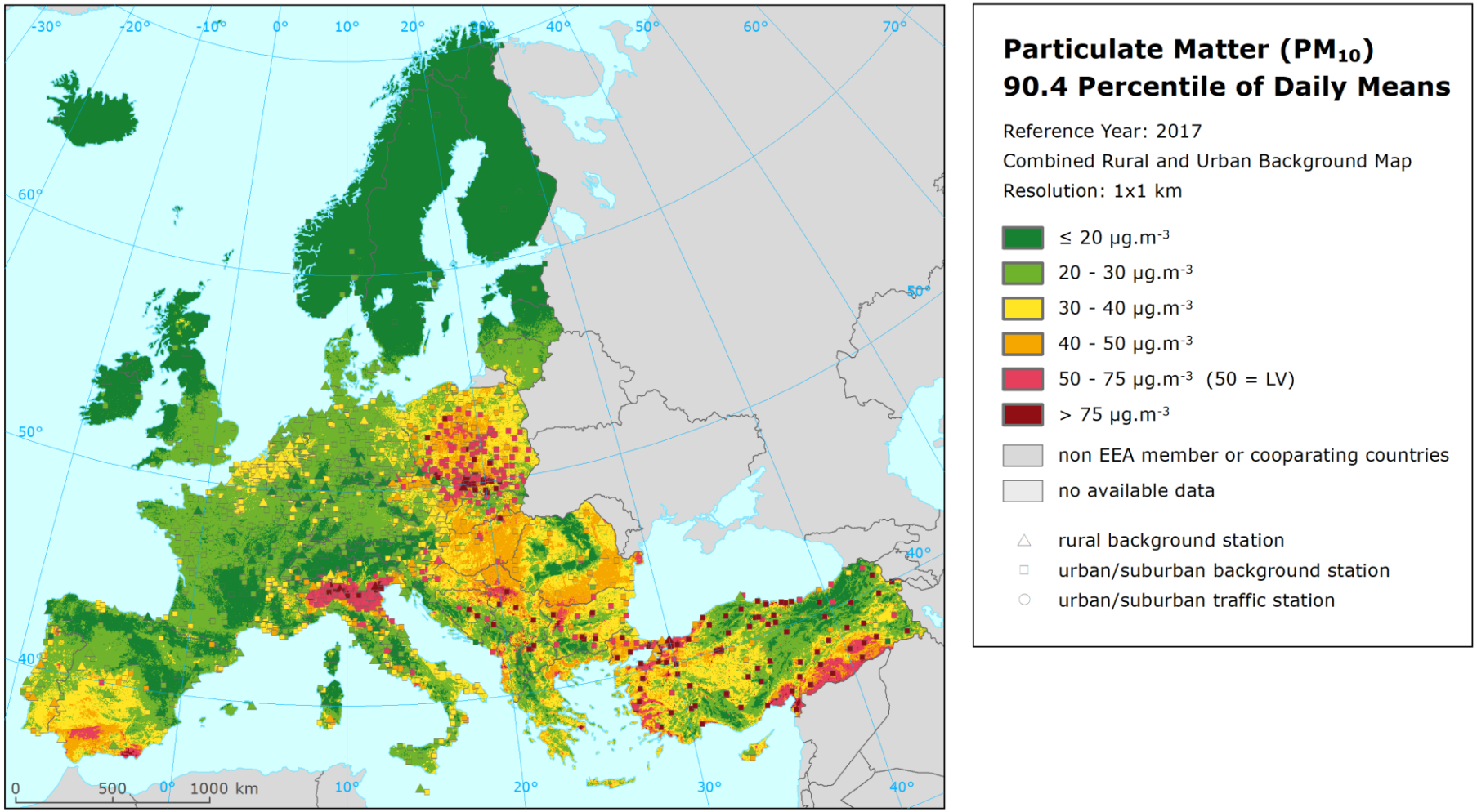

Map A5.3 Concentration map of $PM_{2.5}$ annual average including station points, 2017

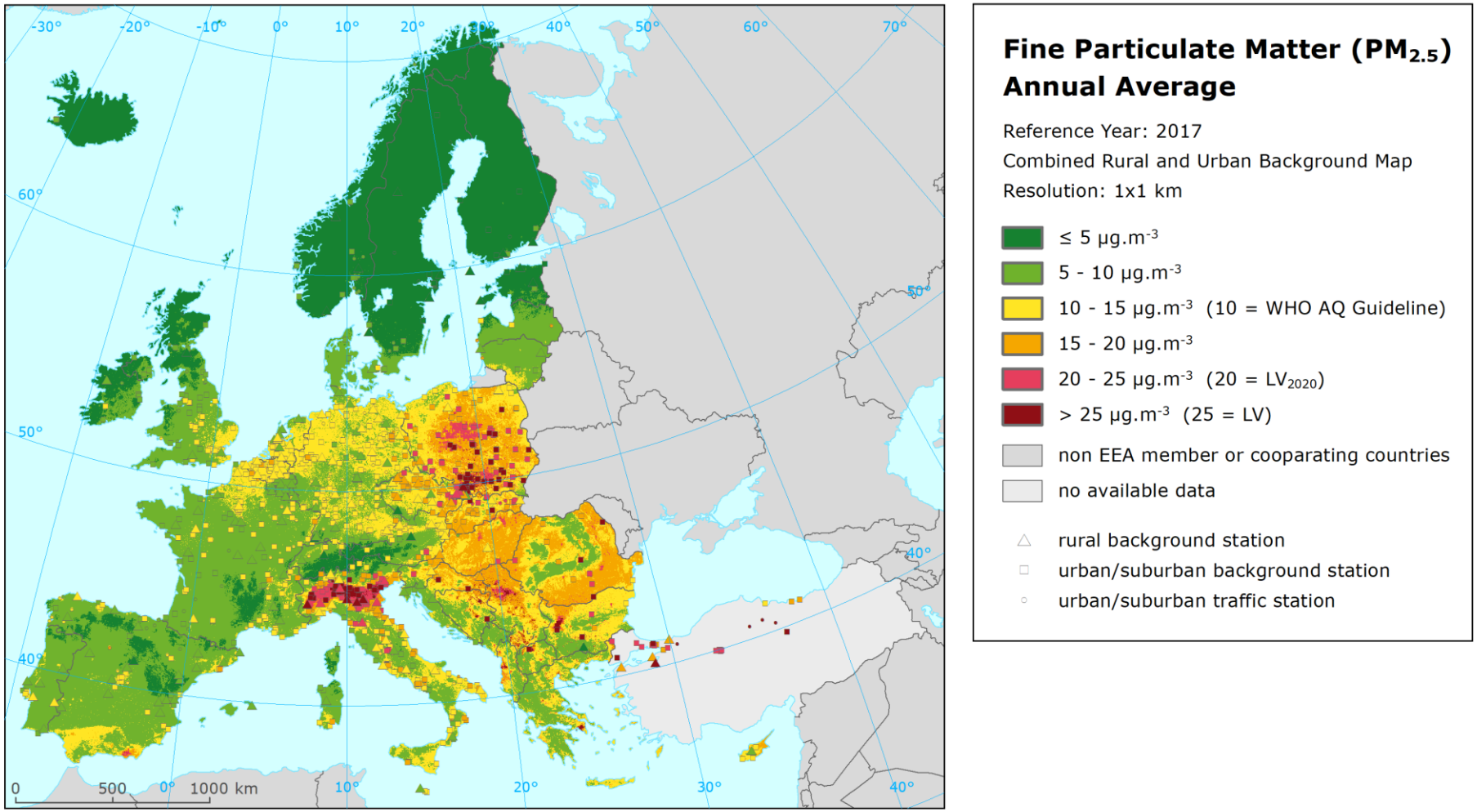

Map A5.4 Concentration map of ozone indicator 93.2 percentile of maximum daily 8-hour means including station points, 2017

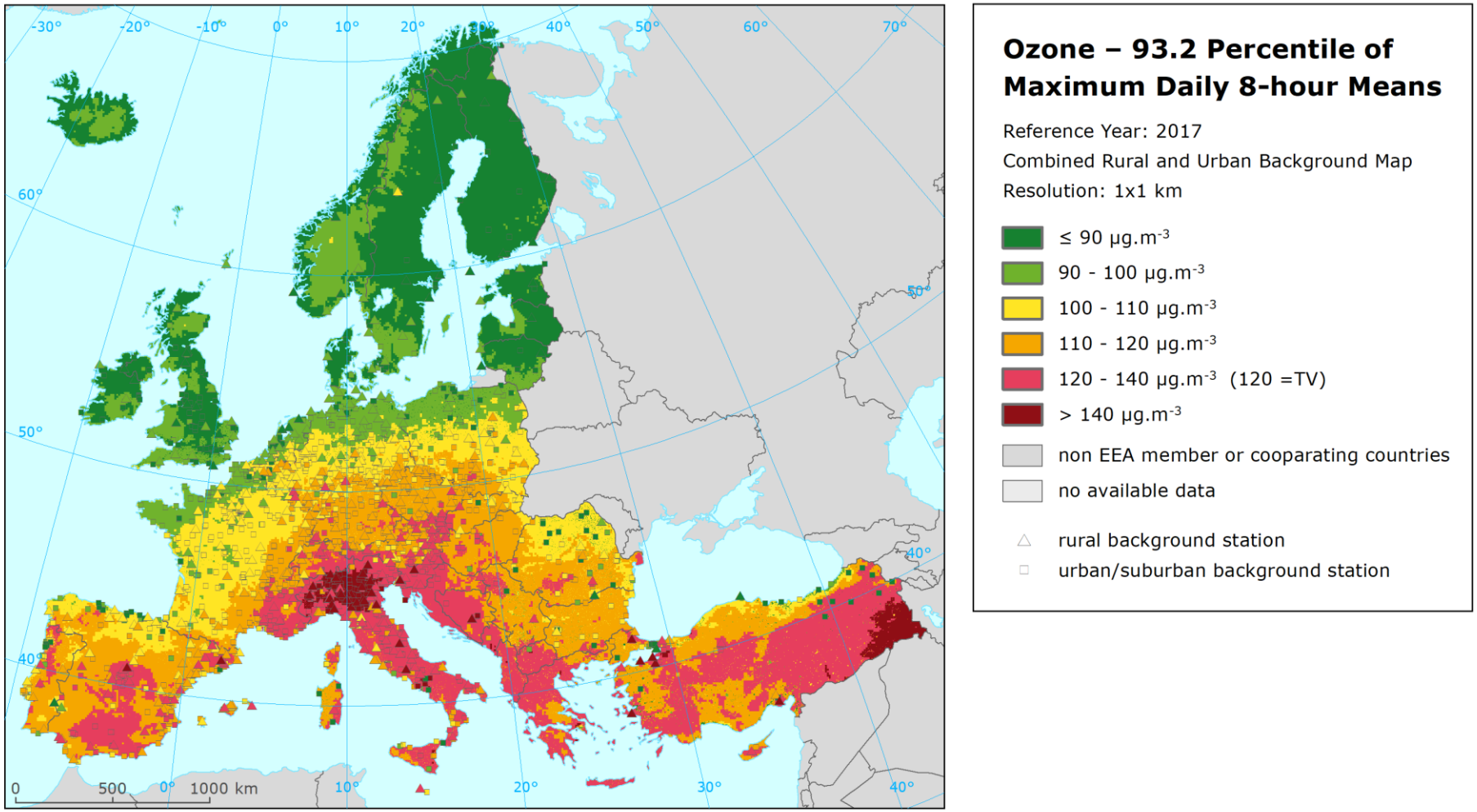

Map A5.5 Concentration map of ozone indicator SOMO35 including station points, 2017

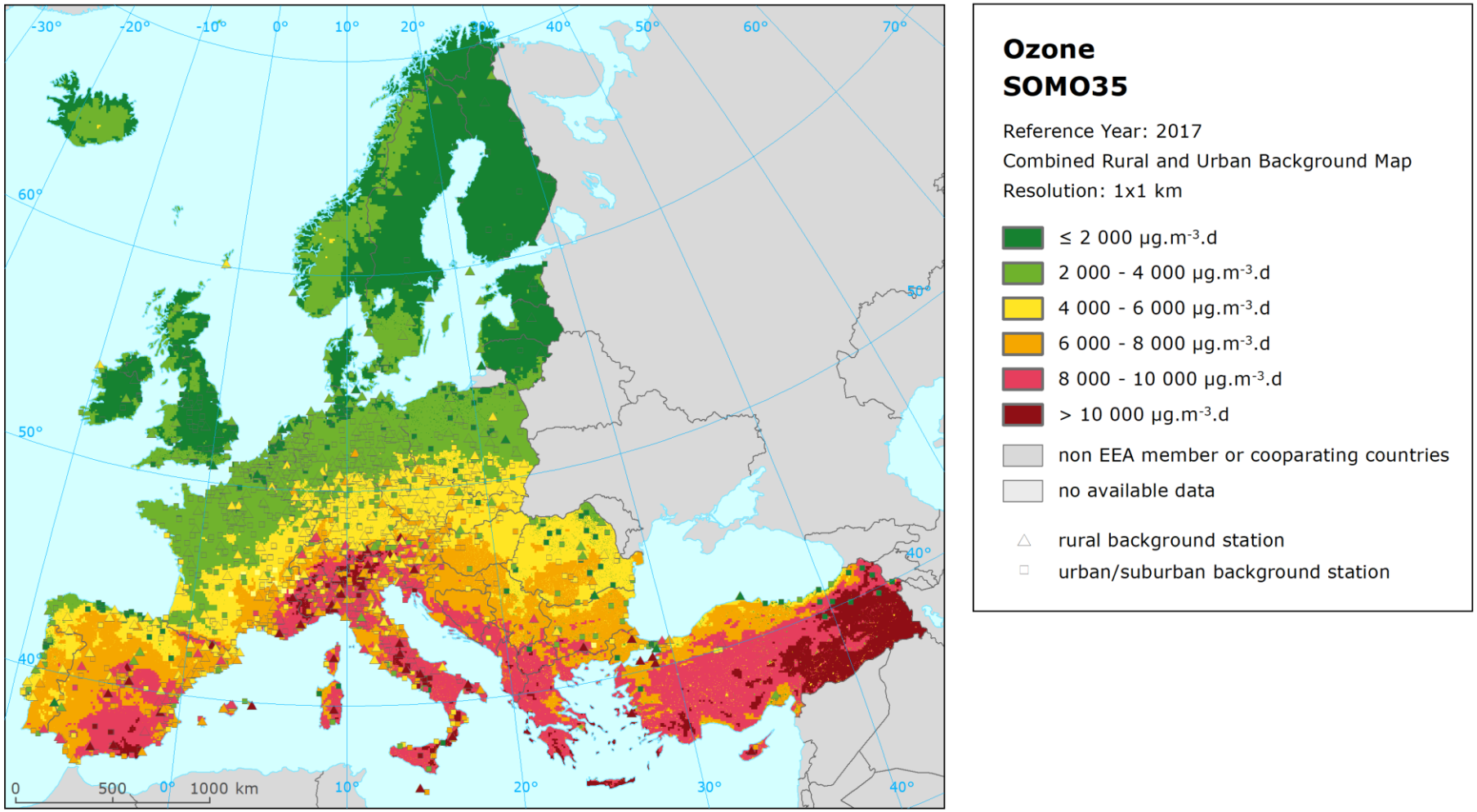

Map A5.6 Concentration map of ozone indicator SOMO10 including station points, 2017

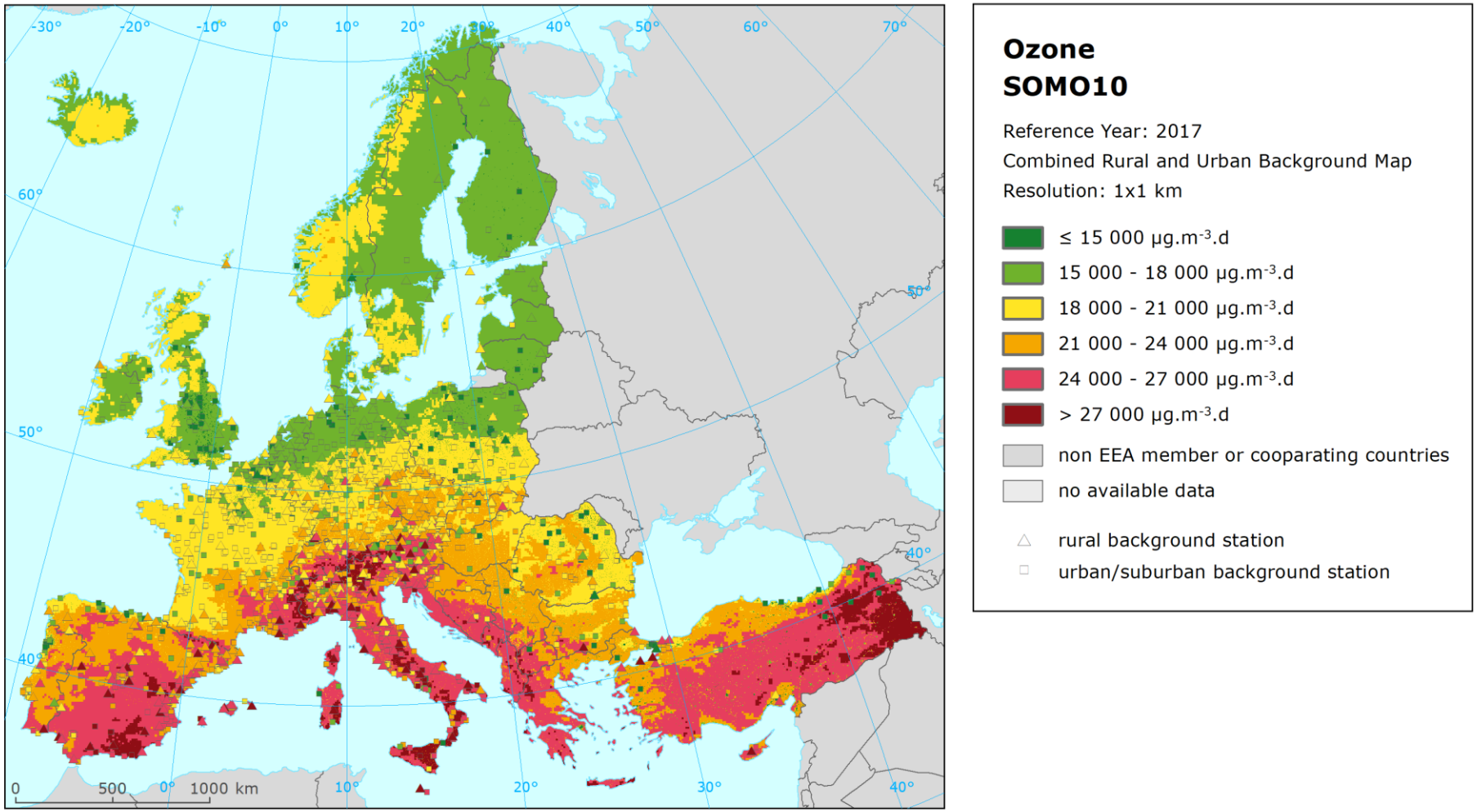

Map A5.7 Concentration map of ozone indicator AOT40 for vegetation including station points, rural air quality, 2017

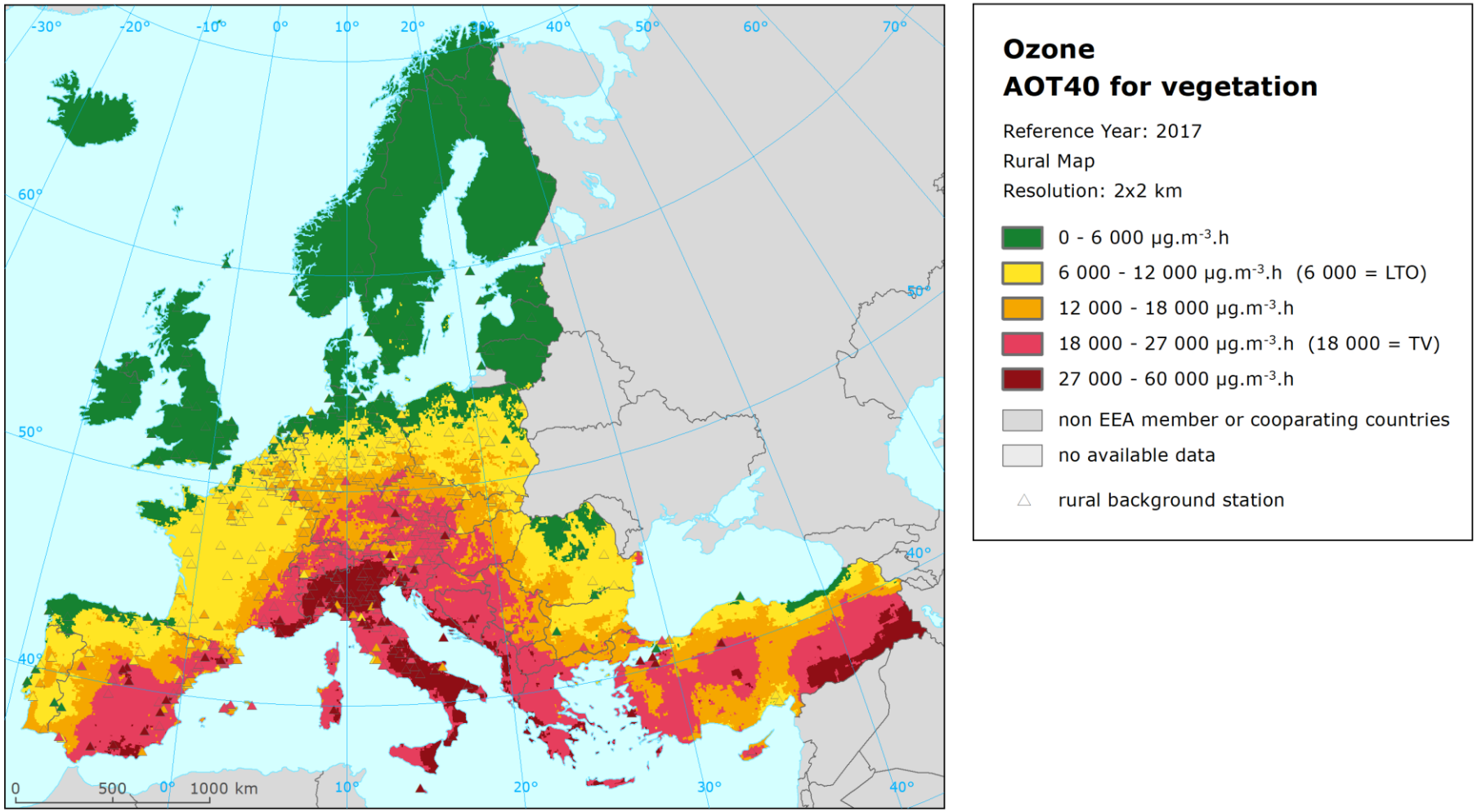

Map A5.8 Concentration map of ozone indicator AOT40 for forests including station points, rural air quality, 2017

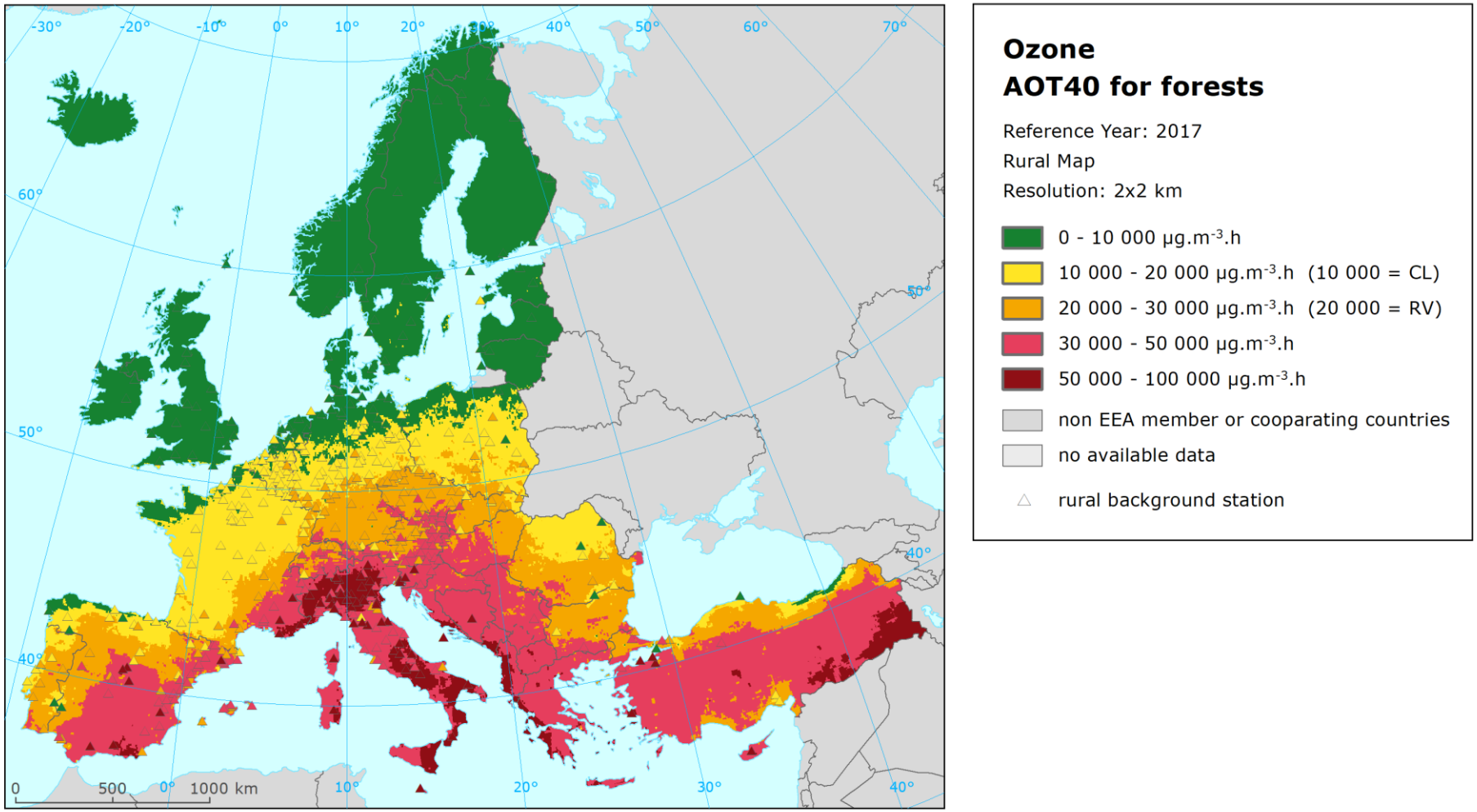

Map A5.9 Concentration map of NO_2 annual average including station points, 2017

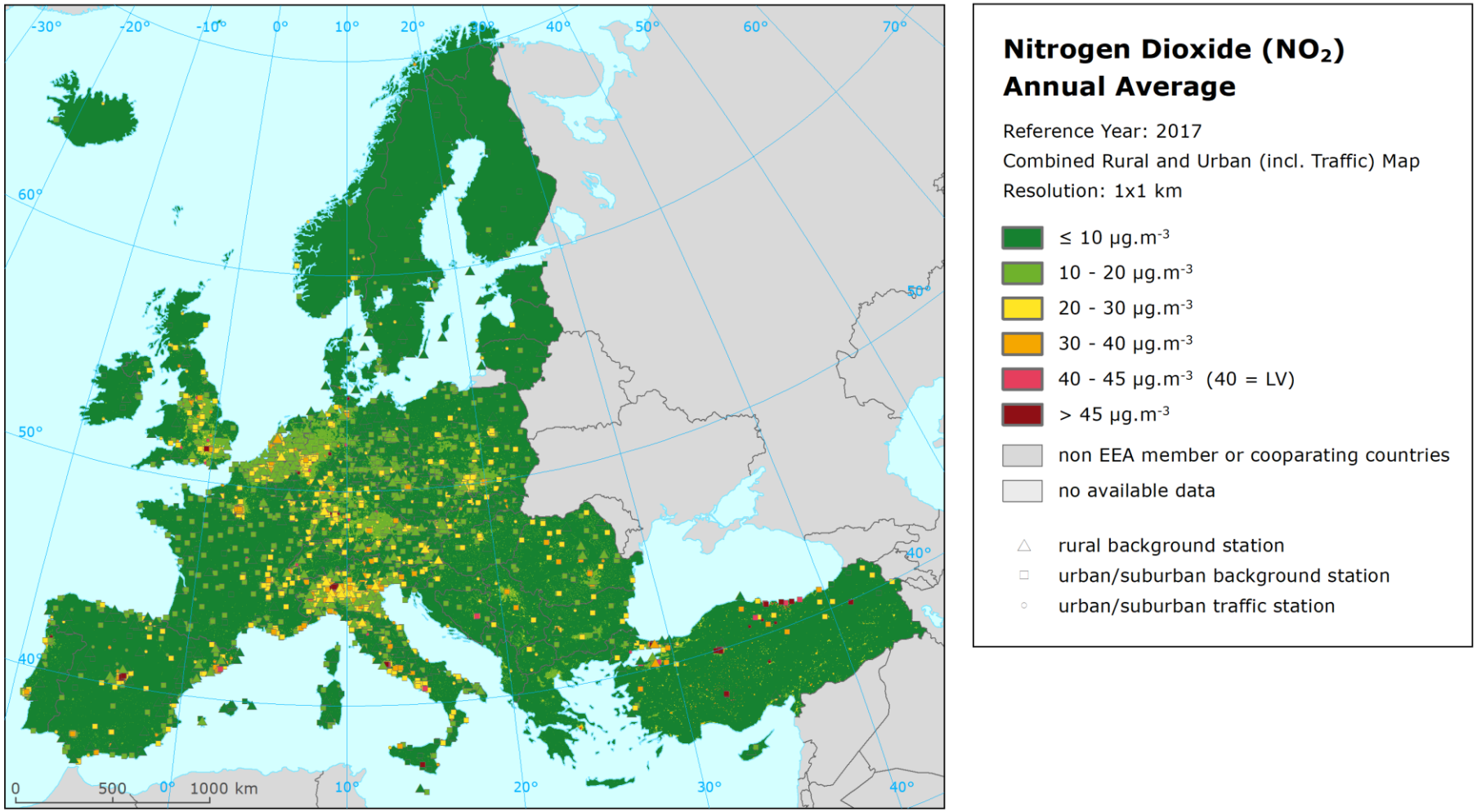

Map A5.10 Concentration map of NO_x annual average including station points, rural air quality, 2017

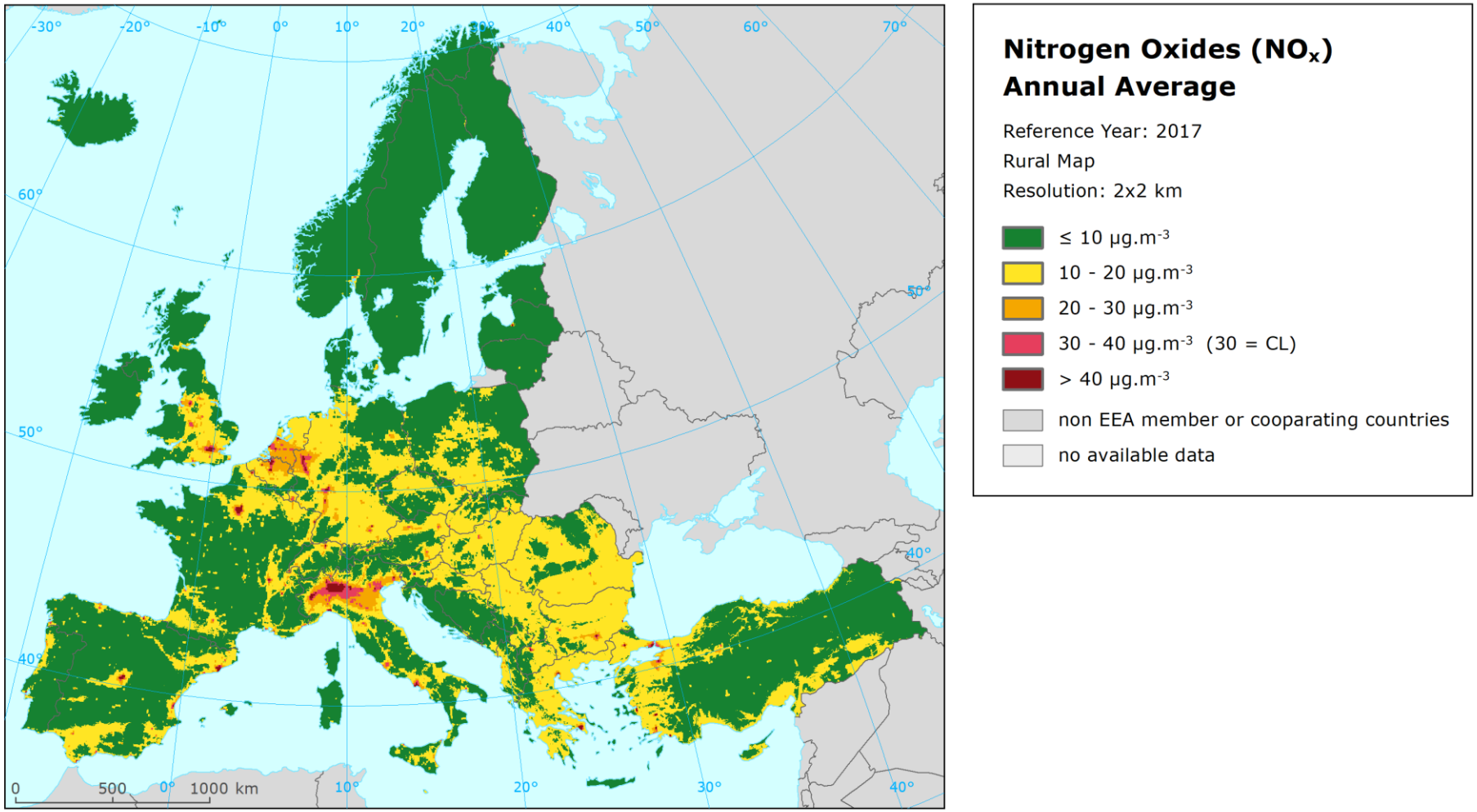

European Topic Centre on Air pollution,
transport, noise and industrial pollution
c/o NILU – Norwegian Institute for Air Research
P.O. Box 100, NO-2027 Kjeller, Norway
Tel.: +47 63 89 80 00
Email: etc.atni@nilu.no
Web : https://www.eionet.europa.eu/etcs/etc-atni

The European Topic Centre on Air pollution, transport, noise and industrial pollution (ETC/ATNI) is a consortium of European institutes under a framework partnership contract to the European Environment Agency.

European Environment Agency
European Topic Centre on Air pollution,
transport, noise and industrial pollution